SLOW CRACK PROPAGATION IN GLASS

by

G.W. Weidmann, BA MSc MInstP

A thesis submitted to the University of Keele
for the Degree of Doctor of Philosophy

Department of Physics
University of Keele
Keele, Staffordshire

now at

Department of Mechanical Engineering
Imperial College of Science and Technology
London SW7

January 1973

ABSTRACT

Slow crack propagation in glass is examined in a variety of environments using the double-torsion technique. The results are interpreted in terms of a limited plasticity fracture criterion and the time dependence of the yield stress.

SYNOPSIS

Although many people still think of glass as a perfectly brittle material*, there has been growing evidence in recent years, that some form of irrecoverable energy-absorbing process must take place at the tips of cracks in glass. In this thesis measurements of slow crack propagation in glass in different environments, using specimens loaded in double torsion, are described, and an attempt is made to account for the experimental observations using a theory based on a limited plasticity fracture criterion and previous results for the variation of yield stress with time obtained from indentation hardness measurements.

After an introductory chapter devoted to an account of the strength of materials and to reasons why observed strengths fall short of those theoretically calculated, the phenomenology of glass strength is reviewed in Chapter 1. The importance of studies of crack propagation in developing a comprehensive explanation of the observed phenomena is emphasized. Following this, Chapter 2 contains an outline of the development of fracture mechanics and details the derivation of the parameters used later to characterise crack propagation in glass. The experimental apparatus and technique, its calibration and the measurements are described in Chapter 3, and a preliminary discussion of the results and their comparison with previous work are given in Chapter 4. This is followed in Chapter 5 by an account of some observations of apparent crack healing in glass, in which it is suggested that the available data could be explained by the condensation of environmental water vapour in cracks in glass. In

* see e.g. TRELOAR, L.R.G. (1971) Plast. Polym. 39 29
BOYD, G.M. (1972) Engng Fracture Mech. 4 459

Chapter 6, the final chapter, after an examination of possible energy-absorbing processes in fracture, the relationship between the indentation hardness and yield stress of glass is discussed. Theoretical expressions for the crack speed, based on a limited plasticity fracture criterion and the variation of yield stress with time, are developed, and their correlation with the experimental results is explored. It is concluded that such a correlation is possible if reasonable assumptions are made, but further experimental data are required before the proposed mechanism of slow crack propagation can be confirmed.

ACKNOWLEDGEMENTS

I would like to express my gratitude to Dr. D.G. Holloway for so ably supervising this work and for acting as a constant source of stimulus and encouragement. I would also like to thank

Mr. W. Brearley	for his advice and suggestions on technical matters
Mr. F. Rowerth and Messrs. G. Dudley, E. Greasley, G. Marsh and M. Wallace	for their ready provision of technical and workshop facilities
Mr. O.A. Egesel	for his very able preparation of the drawings
Miss M.A. Russell	for the care and skill with which she typed this thesis
and my wife, Lynne	for enduring grass-widowhood so often for the sake of this work.

CONTENTS

CONTENTS (continued)

LIST OF FIGURES

LIST OF FIGURES (continued)

LIST OF FIGURES (continued)

INTRODUCTION

STRENGTH OF MATERIALS

Considerations of the strength of materials have been important since man first started using materials in load-bearing situations. Although the Egyptian, Greek, Roman and other early cultures must have developed empirical rules to enable them to erect their pyramids, temples and bridges, it was not until Leonardo da Vinci (1452-1519) and Galileo Galilei (1564-1642) that the foundations of the scientific study of the strength of materials were laid. Da Vinci, with his tensile tests on iron wires, made the first recorded experimental determination of a material's strength, whilst the beginnings of stress analysis appeared in Galileo's "Two New Sciences" (1638) in which it was also noted that solids resisted loads by virtue of their cohesion. With the development of the subject has come the recognition that real, bulk solids fail at stress levels well below the theoretical strengths calculated for ideal solids whose cohesion is controlled solely by the nature and disposition of the bonding between atoms.

The notion that the strength of a solid is the maximum stress that it will withstand without separation, or fracture, occurring, is not necessarily a very helpful one. A ductile solid may be considered to have failed at the onset of permanent deformation though it might still exhibit considerable resistance to fracture. A material can exhibit different modes of failure depending on the stress system applied and, in some cases, on the dimensions of the stressed member. The resistance to fracture in tension of a macroscopically brittle material, where failure is by propagation

of a crack, is controlled by the state of the surface rather than by that of the bulk of the material. The definition of a unique strength parameter to cover all types of solid and all modes of failure is not a straightforward task. Considerable progress has been made in defining the brittle tensile fracture behaviour of materials in terms of the resistance offered to the propagation of a crack under prescribed conditions. This resistance is variously characterised by the specific fracture surface energy, γ, the critical strain energy release rate per unit length of crack front, G_c, or the critical crack tip stress intensity factor, K_c. More recently, the J-parameter has been introduced, which allows larger scale plastic effects at the tip of a propagating crack to be taken into account, and which is equal to G when there is no plasticity.

In this introductory chapter, the atomic basis of the strength of materials together with some of the estimates of theoretical strength will be reviewed briefly, with particular reference to glass. The sources of weakness encountered in real materials will then be discussed. With this background the experimental work of this thesis and its interpretation will be introduced by a chapter devoted to previous work on the failure of glass, and one on the criteria and mechanics of fracture.

1.1 Bonding in Solids and Strength

The cohesion of a solid is due to the attractive forces between its constituent atoms or molecules. These arise out of electrical interactions between them and, in turn, play a major role in determining the structure of the solid. The interactions may be classified as ionic, covalent or metallic bonds between atoms with

unfilled electronic shells, and van der Waals and hydrogen bonds between molecules or atoms with closed shells. Table i.1 shows typical binding energies for various types of solid (1 kJ $mole^{-1}$ ≡ 0.239 kcal $mole^{-1}$ ≡ 1.04 x 10^{-2} eV per atom or molecule).

Table i.1

Binding energies of solids

Type of Bonding	Binding energy kJ $mole^{-1}$
Hydrogen bonding	~ 20
van der Waals	10 - 50
Metallic (no partially filled d-shells)	95 - 480
Metallic (transition metals)	380 - 960
Covalent	750 - 1450
Ionic (monovalent)	480 - 770
Ionic (divalent)	960 - 1750

The ionic bond, in which the force of attraction is the coulombic interaction between oppositely charged ions, is non-directional due to its spherical symmetry. An ion will be surrounded by as many oppositely charged ions as can be accommodated geometrically - a close-packed structure - provided that overall electrical neutrality is preserved. The final structure is determined by the relative sizes of the ions, which also govern their polarisability, and their valence. Solids containing ions of similar sizes, such as NaCl or AgF, are more completely ionic than those in which a mismatch in ionic size with consequent polarisation introduces an element of covalent character to the bond. This occurs, for example, in AgI where I^- is almost twice the size of Ag^+ and the bonding is predominantly covalent.

Covalent bonds result from the sharing between atoms of electrons. The manner in which this occurs depends on the way in which the electronic quantum states of the atoms combine to give molecular quantum states. If these are of lower energy than the corresponding atomic states they become bonding states. Since there can only be a limited number of bonding states between atoms and since each can contain a maximum of only two electrons, the covalent bond can become saturated. It is also often a directional bond depending on the distribution in space of the bonding states. Whilst ionic solids are generally crystalline this is not always true for those which are covalently bonded, particularly solids such as thermoplastics, which consist of saturated covalently bonded molecules held together by the much weaker van der Waals forces. The number of electrons available for bonding controls the structure of covalent solids. An atom with N electrons in a partly filled outer shell can bond with only 8-N neighbours by sharing electrons. Thus the halogens (N=7) join up in pairs, and van der Waals forces hold these diatomic molecules together in the solid. Some forms of sulphur and selenium (N=6) exhibit long chain structures. For N=5, as in arsenic, layer structures can be formed, the layers being held together by van der Waals forces. The limit is reached when N=4, where the entire solid can consist of a single covalently bonded molecule in which each atom is bonded to four neighbours by tetrahedrally directed bonds. This type of structure is exemplified by diamond.

In metals the bonding electrons are not localised but are free to move through the array of positive ions. There is a greater number of bonding states than there are electrons to fill them and

these states differ very little in energy. The metallic bond is essentially a non-directional covalent bond which cannot be saturated and thus restrictions on the position, number and type of adjoining atoms are removed. This allows close-packing of atoms and the simple crystal structures found in metals, and also leads to the ability of metals to form alloys.

Van der Waals forces, which are important in solids whose constituent atoms or molecules are saturated, arise out of a combination of the interaction of permanent dipoles, the interaction between a permanent dipole and a dipole induced by it in another molecule, and the interaction between a fluctuating dipole and the fluctuating dipole induced by it in a neighbouring atom or molecule. The hydrogen bond, which is important in the structure of proteins and of ice, is an interaction between the intense electrostatic field associated with the proton and the electronegative elements of small atomic volume such as N, O or F. The bond may be considered as either a special case of van der Waals forces or as an essentially ionic bond.

As will be seen from the next section, a high theoretical tensile strength, σ_t, can be related to high values of Young's modulus and surface energy, and to a small interatomic spacing. In addition, particularly for crystalline materials, a high value of theoretical shear strength, τ_t, is required to prevent failure by shear at low stresses. Ionic crystals, in general, have lower values of σ_t than covalently bound solids and metals due to the possibility of electrically neutral planes acting as low energy cleavage planes. Metals, however, have low values of τ_t/σ_t due to the ease with which slip can occur along close-packed planes.

High values of τ_t are associated with high values of the shear modulus, and this is to be found in solids with strongly directional bonds. Thus, theoretically, the highest strengths are expected in materials with covalent or highly polarised ionic bonds. In addition, small atoms and short bond lengths are required to produce a high density of bonds and, hence, a high modulus. Finally, to ensure a three-dimensional network of bonds with no planes of weakness, the covalence per atom should be high.

These characteristics mean that in theory the strongest solids will have low densities, since the atoms are small and directional bonding precludes close-packed structures. They will also have high melting points since these are related to the high modulus values through the binding energy. Elements such as boron, carbon, silicon and beryllium have these properties and are found to have high strengths as do their compounds, either with each other or with nitrogen or oxygen. Nature, for once, appears to be on the side of the engineer in giving him high strength to weight ratios and high melting points in the strongest materials.

1.2 Theoretical Strength

In principle the theoretical strength of a material could be rigorously calculated by the methods of quantum mechanics. This would require a complete description of the mutual interactions of the atoms, their response to an applied stress and their dynamics. Even if sufficiently detailed knowledge of the system were available the complexity of such a calculation would be enormous. Thus, in practice, calculations of theoretical strengths have involved varying degrees of approximation.

Some of the calculations, not necessarily the earliest ones, are based on very simple ideas. POLANYI (1921) assumed that the macroscopic deformation in tension followed Hooke's law up to fracture and equated the increase in surface energy to the release of strain energy stored in a layer whose thickness equalled the interatomic spacing, β. This produced a value for the theoretical strength, σ_t, of a material of

$$\sigma_t = (4ET/\beta)^{\frac{1}{2}} \qquad (i.1)$$

where E is Young's modulus and T is the surface energy. OROWAN (1955) employed similar arguments but considered from the point of view of an atomic force-separation law which was assumed to be Hookean. The strain energy term now included a contribution from the atomic interaction at higher separations than that corresponding to σ_t. This produced an expression

$$\sigma_t = (2ET/\beta)^{\frac{1}{2}} \qquad (i.2)$$

Using typical values for glass of E = 70 GN m^{-2}, T = 0.5 J m^{-2} and $\beta = 1.6 \times 10^{-10}$ m gives σ_t = 21 GN m^{-2}, or 0.30 E. CONDON (1954) based his calculations on the argument that when two surfaces part on fracture, the attractive forces between them fall from σ_t to zero in a distance of the order β. If this fall is assumed to be linear then the work done per unit area against these forces is $\frac{1}{2}\sigma_t\beta$ which equals the energy acquired by the surfaces on fracture. Hence

$$\sigma_t = 4T/\beta \qquad (i.3)$$

Substituting the same values as above leads to σ_t = 8.0 GN m^{-2}.

OROWAN (1934, 1945-6) also put forward a different approach in which the atomic force-displacement curve was more realistically assumed to be sinusoidal in form. Taking the initial deformation to be Hookean allowed the modulus of the material to be included in the calculation. Equating the work done in separating a pair of adjacent atomic planes to 2T per unit area gave

$$\sigma_t = (ET/\beta)^{\frac{1}{2}} \qquad (i.4)$$

For glass this yields σ_t = 14 GN m^{-2}, or 0.20 E.

Although these are all order of magnitude calculations they have the great attraction of being equally applicable to all materials. The actual values obtained depend as much on the values chosen for T and β as they do on the particular assumptions made. For glass estimates of T range from 0.54 J m^{-2}, obtained from extrapolation to room temperature of high temperature values (GRIFFITH, 1920) to 1.75 J m^{-2} estimated from the heat of vaporisation of silica (CHARLES, 1961). It is interesting to compare these with the lowest value of fracture surface energy, 0.34 J m^{-2}, obtained from measurements on very slowly moving cracks in glass (LINGER, 1967). Similarly with the value of β, the atomic spacing; some authors have used 3.5 x 10^{-10} m obtained by dividing the molar volume by Avogadro's number and taking the cube root (e.g. CONDON, 1954; ZIJLSTRA, 1961) whilst others have taken the Si-O bond length of 1.6 x 10^{-10} m (e.g. CHARLES, 1961). Thus estimates of σ_t can differ by a factor of about four depending on the values of T and of β which are used in addition to the further factor of four introduced by the different approaches outlined above.

Various authors have attempted more precise calculations of the

theoretical strength of materials based on more accurate models of atomic bonding. MACMILLAN (1972) has presented a recent review of this work. Most success has been achieved with ionic and van der Waals solids in which the details of the interatomic forces are best understood. However, there have been two calculations of the strength of glass derived from properties of the atomic structure.

NÁRAY-SZABÓ and LADIK (1960) calculated the coulombic binding energy, D_e, for the pseudo-diatomic molecule SiO_3-O as the difference in formation energies of an SiO_4 ion and an SiO_3 group. By assuming a Morse function for the potential of the molecule they could calculate the force in the Si-O bond at the point of inflexion where bond breakage occurs. Multiplying this force by an estimate of the number of bridging oxygen ions per unit cross-section gives a theoretical strength of 24.2 GN m^{-2}, or 0.35 E.

DEMISHEV and BARTENEV (1966a, b) predicted the temperature dependence of the theoretical strength of soda-lime silica glass under triaxial stress. They also used a Morse function for the potential, which had the form $U = - A/r^m + B/r^n$, and expressed the temperature variation of U in terms of the experimentally measured variations with temperature of the coefficient of thermal expansion and the velocity of sound in the material. This gave a room temperature value of the theoretical strength of 6.42 GN m^{-2}* or approximately 0.1 E.

Two further estimates were provided by HILLIG (1962) and MARSH (1963b). Hillig observed an increase of Young's modulus of vitreous silica with increasing stress: the modulus was still rising at stresses around E/5. He suggested that it was more

---

* MACMILLAN (1969 and 1972) quotes Demishev and Bartenev as obtaining a value ten times higher than this, and seems in error.

appropriate to use the value of the modulus of quartz, towards which the measured moduli were tending, in the calculation of the theoretical strength. This gives σ_t = 24 GN m^{-2}. Marsh arrived at almost the same figure. He showed both theoretically and experimentally that the terminal fracture velocity in glasses varies as $(\sigma_Y/d)^{\frac{1}{2}}$ where σ_Y is the flow stress and d is the density. When the flow stress reaches σ_t, the velocity reaches its theoretical maximum, thus the extrapolated flow stress at the theoretical terminal fracture velocity gives a measure of σ_t.

To summarise; the best available estimates of the theoretical strength of a material such as glass still produce a 4 x spread in values, though for van der Waals crystals such as argon or ionic crystals such as NaCl, where more refined calculations are possible, there is better agreement between different authors. A reasonable order of magnitude estimate for the theoretical strength of materials is E/10.

1.3 Sources of Weakness in Solids

Real bulk materials do not achieve strengths which are even close to the theoretical strength, i.e. about E/10. Typically bulk glass fails at approximately E/1000 and a strong steel at E/100. This occurs because real solids, except under very special circumstances, contain imperfections which can play a major role in determining their properties. These imperfections may be inherent, such as local density variations in amorphous materials or fluctuations due to thermal lattice vibrations, they may be "grown-in" irregularities in crystalline structures such as vacancies, dislocations or impurities, or they can arise out of preparation and

handling causing surface damage. Surface damage is the main reason for the relative weakness of brittle materials, whilst the presence of glissile dislocations is the chief cause of the failure of ductile materials at relatively low stresses.

The effect of a crack in the surface of a material is to enhance the local stress at the crack tip. For a plate in tension containing a through-the-thickness edge crack, the applied stress, σ_a, is increased near the crack tip to

$$\sigma = 2\sigma_a (c/\rho)^{\frac{1}{2}} \qquad (i.5)$$

where c is the length of the crack and ρ is the radius of its tip (INGLIS, 1913). For a brittle material, in which little or no plastic deformation occurs, relatively low applied stresses are needed for the crack to propagate. In a ductile material, where plastic yielding can blunt the crack tip, higher applied stresses are needed to rupture the solid. Many materials which are ductile under simple tensile loading can fail in a brittle manner under complex stress such as in the presence of a notch. The severity of a prexisting flaw in some materials can be diminished by environmental attack. Thus a corrosive agent which normally acts to reduce the strength of a material can actually strengthen a given specimen of it by rendering its surface flaws more innocuous.

In metals and certain ionic crystals the mechanism of plastic flow is well established as being due to dislocation movement. In covalently bonded materials the situation is by no means clear. It has been demonstrated by means of indentation experiments on crystalline carbon, silicon and germanium that dislocation movement is associated with plastic deformation at temperatures higher than

about one half of the absolute melting point (JOHNSON, 1966). Below these temperatures and for the amorphous covalently bonded materials such as glass, densification has been proposed by ERNSBERGER (1968) to explain the microplastic effects associated with scratches and indentations. Both Ernsberger and PETER (1970) emphasize that it is difficult to conceive that volume-conserving plastic flow can take place in materials whose structures do not permit glissile dislocations. However, NORTHWOOD and PORTER (1970) demonstrated that such flow could be produced in germanium at room temperature, and GILMAN (1968a, b) pointed out that, even in non-crystalline materials, shear events will tend to be correlated at a local level. For a sufficiently high correlation the dislocation line concept may be retained in such materials by allowing the magnitudes and directions of the Burgers vectors to fluctuate about mean values. Densification, in any case, cannot occur under tensile stresses such as those at the tip of a propagating crack (although, a priori, the converse of densification cannot be ruled out). There is a need to invoke some irrecoverable energy absorption process such as plastic flow in this situation to account for the large discrepancy between fracture surface energy and thermodynamic surface energy in a material like glass (e.g. LINGER and HOLLOWAY, 1968). In this thesis an attempt is made to develop a theory based on a limited plastic flow criterion of fracture to account for observations of the crack propagation behaviour in glass.

CHAPTER 1

THE FAILURE OF GLASS

1.1 Introduction

This chapter will be devoted to a review of previous work on the failure of glass. It is not intended to present an exhaustive survey, but rather to sketch out the main lines of the development of the subject. As a link with the previous section, the structure of glass is discussed first. This is followed by considerations of the strength and static fatigue of glass and the need for more detailed understanding of the fracture process and the effects of environment on it. Finally, measurements of the fracture energy are reviewed, and in the light of these and some early observations of stress dependent crack growth in glass, the need for more accurate data on the latter is discussed.

1.2 The Structure of Glass

Many substances, both organic and inorganic, can be prepared in the glassy state, usually by supercooling from the liquid, but the discussion here will be confined to glass based on silica, SiO_2.

Glassy materials are characterised by the fact that, although they have the properties of the solid state, such as hardness and strength, their amorphous structure is more akin to that of liquids. Both structural studies and the extended melting range indicate an absence of long range order. Figures 1.1(a) and 1.1(b) show the radial distribution curves determined by X-ray diffraction of water and vitreous silica (redrawn from DANFORD and LEVY, 1962, and

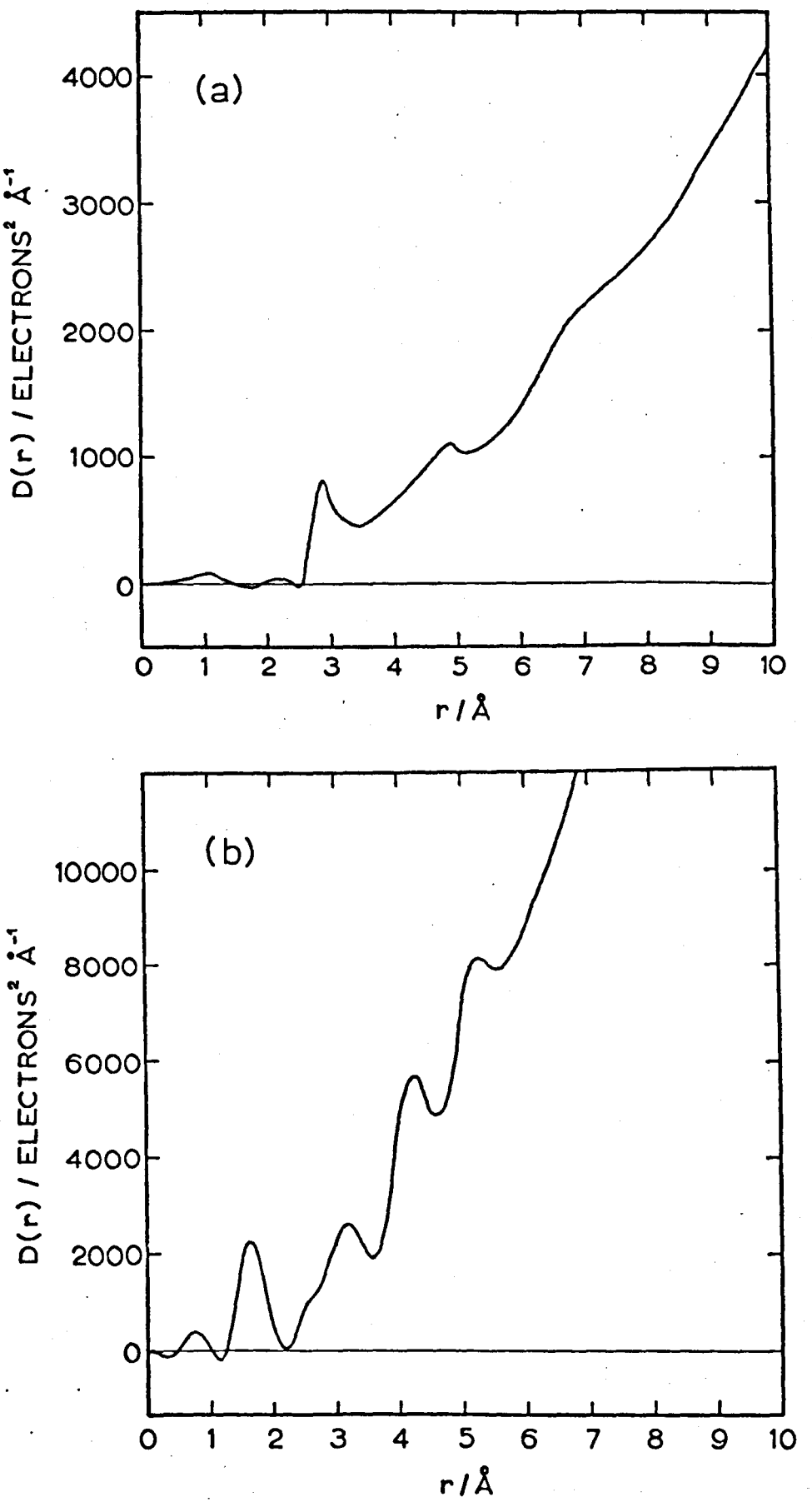

Figure 1.1 Radial density distribution, D(r), of electrons
(a) in water (after DANFORD and LEVY, 1962)
(b) in vitreous silica (after WARREN, 1937)

WARREN, 1937, respectively) from which it can be seen that the lack of order at distances greater than about 7Å (7×10^{-10} m) is common to both. There are, however, indications of short range order. Supporting evidence comes from the fact that the width of the infra-red absorption peak identified with Si-O-Si bond stretching vibrations is much the same in vitreous silica as it is in two crystalline forms of silica, quartz and cristobalite (SIMON, 1960).

The basic unit in crystalline silica is the SiO_4 tetrahedron in which a central silicon atom is partially covalently bound to four symmetrically disposed oxygen atoms. It is generally accepted that these tetrahedra remain the basic unit in the glassy state but that the sizes and planes of the angles between the tetrahedra are randomized sufficiently to give the structure its lack of long range periodicity. Controversy has centred on the precise extent of this randomness. In one of the earliest systematic X-ray investigations of glasses, RANDALL, ROOKSBY and COOPER (1930) suggested that glasses were aggregates of extremely small crystals, or crystallites, whose average size was estimated to be of the order of 10-100Å in vitreous silica. Such a structure, however, might be expected to produce low angle X-ray scattering and this was not detected by WARREN (1937). ZACHARIASEN (1932) proposed that the structure consisted of an extended random network of tetrahedra lacking periodicity or symmetry, and this theory was strongly supported by WARREN (1933, 1937) and his co-workers on the basis of their X-ray work. A two-dimensional representation of such a network is shown in figure 1.2 where the presence of cationic network modifiers (Na^+ and Ca^{2+} in soda-lime silica glass) compensates the excess negative charge of the non-bridging oxygen ions.

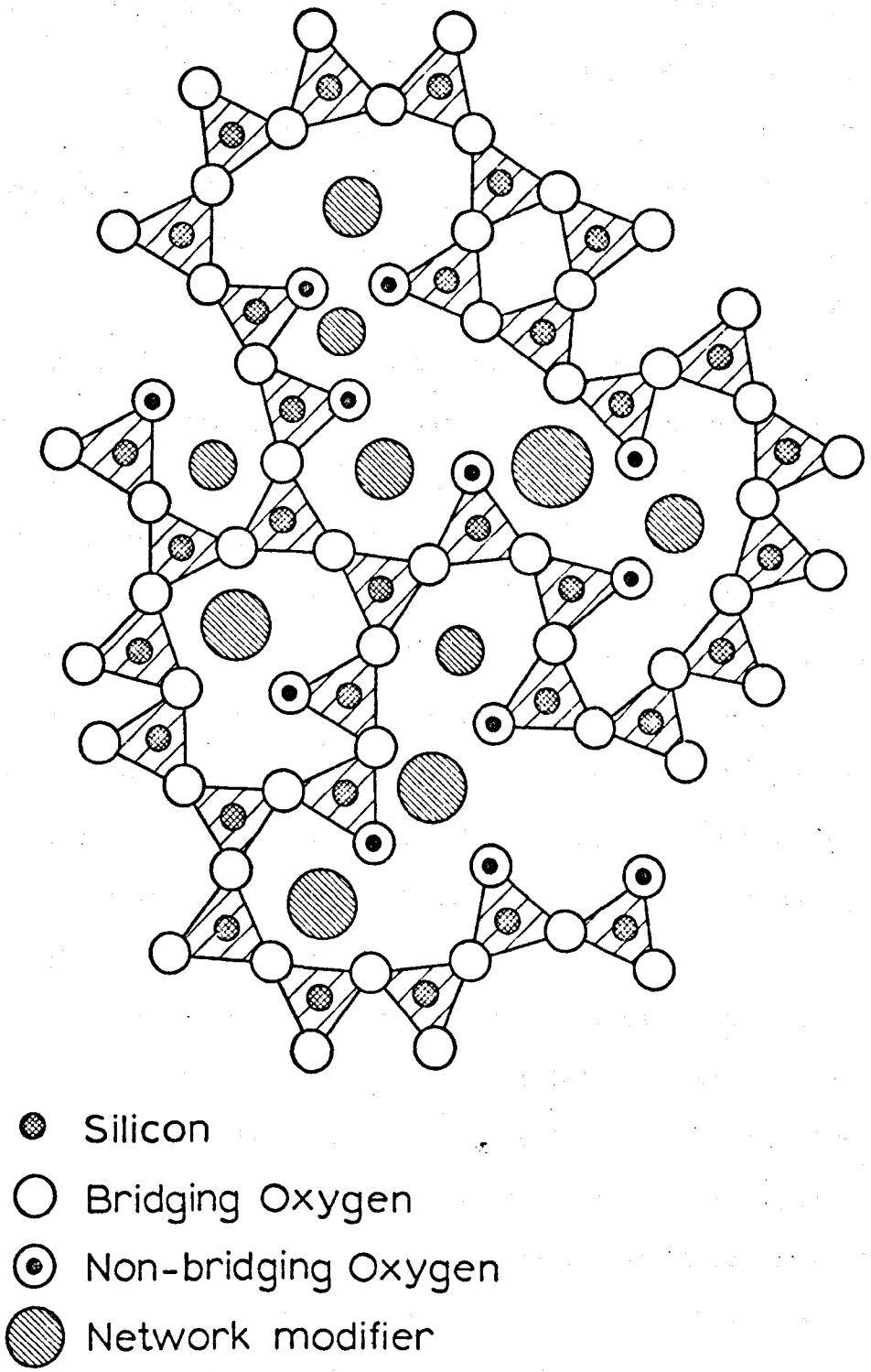

Figure 1.2 Two-dimensional representation of Zachariasen random network model of glass structure (after HOLLAND, 1964)

VALENKOV and PORAI-KOSHITZ (1936) criticized this structural picture of glass on the grounds that a necessary consequence of it was that the transition from the glassy to the crystalline state would have to be a sharp one. This conflicted with the results of their investigations into the devitrification process which showed that the transition occurred gradually at a constant temperature. They put forward an alternative theory in which the glass was considered to be made up of small paracrystalline regions in which the order was relatively high, separated by regions of lesser order. A similar structure was proposed by ZARZYCKI and MEZARD (1962) on the basis of a direct electron microscope study of glass. In this, fibres of vitreous silica and germania, and of soda-lime silica glass were drawn inside the column of the electron microscope to avoid any atmospheric contamination. They concluded that their observations of structural elements approximately 100Å in size could best be explained in terms of paracrystalline domains of this size being set in a paracrystalline 'superlattice'.

In the range 10-20 mole per cent of metal oxide there is an abrupt variation in such properties as partial molar volume, viscosity and thermal expansion which the above theories on glass structure do not account for. MACKENZIE (1960) has reviewed some of the structural theories put forward which might be compatible with this composition dependence. He himself puts forward a composite of these which involves different structural units at different compositions. These range from the Zachariasen random network below 10 mole per cent, through discrete ions such as $Si_6O_{15}^{6-}$ and $Si_8O_{20}^{8-}$ between 10 and 20 mole per cent, to 'islets' of vitreous silica with discrete ions in the form of rings, sheets and chains up to 40 mole per cent.

As might be appreciated from this brief survey the actual structure of glass has not been established with any certainty. The regions of greatest interest, which are those below about 100Å in size where some higher degree of ordering, falling short of fully crystalline, might be expected, are still largely inaccessible to experimental observation. However, it seems clear that the structure must be in some way dependent on composition, in particular on the proportion of metal oxide. This is reinforced by infra-red studies (SIMON, 1960) in which the width of the Si-O-Si absorption peak is found to increase markedly with increasing percentage of Na_2O. These structural differences provide a context in which the greater strength of vitreous silica compared to that of soda-lime silica glass may be set.

1.3 The Strength of Glass

It has been noted earlier that glass fails through the propagation of a crack which is almost invariably initiated at the surface of the glass. It was GRIFFITH (1920, 1924) who recognised the importance of stress concentrating flaws as fracture initiation sites, and the drastic effect these had in reducing the strength of a brittle material. Griffith's work was pioneering in several respects. It marked the beginning of a quantitative approach to the mechanics of fracture, it put forward what is essentially a thermodynamic criterion for fracture, it established the possibility of making flaw-free, high strength materials, and it demonstrated the apparent effect of specimen size on the breaking strength of glass.

In essence, Griffith claimed that it was possible to predict the breaking strengths of glass articles containing cracks of known lengths without performing fracture tests. Using a solution due to INGLIS (1913) for the stress around an elliptical crack in an infinite two-dimensional sheet (see equation (i.5)), GRIFFITH (1920) obtained an expression relating the applied stress at failure, σ_b, to the crack half-length, c, Young's modulus, E, Poisson's ratio, ν, and the surface energy of the material, T. This was

$$\sigma_b = (2ET/\pi\nu c)^{\frac{1}{2}} \qquad (1.1)$$

The surface energy, T, was obtained by extrapolation to room temperature of high temperature values. Values of σ_b from equation (1.1) for different values of c were found to be in good agreement with the results of fracture tests on glass vessels which were pre-cracked, annealed and then tested.

GRIFFITH (1924) modified the above expression for σ_b to

$$\sigma_b = (2ET/\pi c)^{\frac{1}{2}} \qquad (1.2)$$

Although it is not clear how Griffith performed this correction, it is now accepted that the later version is the correct one (see e.g. SNEDDON, 1961; HAYES, 1970). Equation (1.2) approximately halves the predicted values of σ_b compared with those from equation (1.1), destroying the previous agreement between theory and experiment. Griffith, therefore, performed a further series of tests, which are described in the later paper. In these tests, the annealing treatment of the pre-cracked vessels was altered until agreement was achieved between the measured breaking stresses and those predicted by equation (1.2). This procedure of altering the experiment

until it agrees with the theory would seem to beg the question of whether the theory can be used to predict the experiment. It is also worth noting that Griffith's value of T is approximately one-tenth of the fracture surface energy, γ, of glass measured by later investigators (e.g. LINGER, 1967; WIEDERHORN, 1969). If, rather than T, γ is more correctly used in equation (1.2), σ_b is increased by about a factor of three. This gives approximately double the maximum value of σ_b found by Griffith when he investigated the effect of different annealing treatments.

GRIFFITH (1920) also showed that strength levels of up to 0.1 E could be achieved on freshly drawn fibres of the same glass (a potash-alumino silicate), irrespective of diameter. However, these strengths decreased with time after preparation, the larger the fibre diameter the greater the decrease in strength.

Griffith postulated that the strength-impairing flaws in glass were microcracks in the glass surface, although there was no direct evidence for their existence. Several investigators have attempted to confirm the presence of these 'Griffith cracks' mostly by decoration or ion-exchange methods. ANDRADE and TSIEN (1937) established that patterns of cracks could be brought out on the surface of glass by deposition of sodium vapour onto it. They found that the number of cracks depended on the age of the specimen, and they claimed that the cracks could not have arisen from mechanical damage, but must have developed spontaneously. GORDON, MARSH and PARRATT (1959), using a similar technique, found a correlation between the mechanical weakness of glass samples and the incidence of revealed surface cracks. They inferred that the patterns obtained corresponded to pre-existing crack systems which, they concluded, originated either

through abrasion or localised surface devitrification. ERNSBERGER (1960) criticized the sodium vapour method of revealing surface flaws on the grounds that the patterns of cracks produced were largely artefacts of the method, even though the patterns may have been nucleated by pre-existing cracks. Instead, he used a lithium ion-exchange treatment to induce tensile stresses in the glass surface and thus enlarge any cracks already present. He came to the same conclusion as Gordon et al, namely that the patterns produced arose either from pre-existing mechanical damage or from fine-scale devitrification. HOLLOWAY (1959) found that, for glass fibres drawn at low temperatures, and in the absence of mechanical damage, the chief strength-impairing flaws were "point" defects on the surface. It was shown that fracture originated from these points. The defects were thought to arise from the dissolution of contaminating particles into the glass, forming small regions of different composition which produced local stress concentrations on cooling.

Much of the discussion following Griffith's work centred on whether or not the postulated 'Griffith flaws' were intrinsic to the glass. If they were intrinsic then the size of the flaw would be limited by the size of the specimen. Thus there should be an intrinsic size effect. The results, however, of OTTO (1955), THOMAS (1960), PROCTOR (1961) and HILLIG (1961), amongst others, demonstrated that there is no size effect in pristine glass. The same high strength levels were achieved in glass specimens whose diameters ranged from about 5 μm to 8 mm.

In soda-lime silica glass the highest strengths consistently shown are about E/20, whilst for vitreous silica these are about E/5.

HILLIG (1962) has suggested that the discrepancy between these values and the estimates of theoretical strengths could be explained for soda-lime glass by the presence of intrinsic flaws arising out of the amorphous structure, and for vitreous silica by the observed increase in modulus with strain. MALLINDER and PROCTOR (1964) measured the modulus as a function of strain for both types of glass. They found that, whilst the modulus of vitreous silica increased with increasing strain, that of soda-lime silica glass decreased. Thus, if Hillig's explanation were correct for vitreous silica, a similar explanation could also be used for soda-lime silica glass without the need to invoke the presence of intrinsic flaws.

MARSH (1963b) put forward an alternative suggestion: that otherwise flaw-free glasses fail at their yield stress, and it is this, rather than the theoretical strength, which determines the maximum achievable tensile strengths. He showed that, for a variety of glasses, the flow stresses at different times and temperatures, taken from indentation hardness measurements, were the same as the fracture stresses under similar conditions. The fact that failure in glass appears totally brittle is explained as being due to the very limited scale of the plasticity. On the basis of the flow stress values it can be estimated that a plastic zone size of about 10^{-8} m and a plastic extension of about 5×10^{-10} m would be sufficient to account for the fracture surface energies measured in glass.

Marsh also attempted to correlate the 'fatigue-free' or liquid nitrogen fracture stress with the corresponding indentation hardness flow stress. To measure the liquid nitrogen fracture stress he used a method in which a soda-lime silica glass fibre was bent into an elastica whose diameter was reduced until failure occurred. The result he obtained, about 0.15 E, was much higher than the values

anyone else had obtained, but corresponded exactly to his measured liquid nitrogen flow stress. In his calculation, however, Marsh used HILLIG's (1962) data for the increase in modulus of fused silica with increasing strain. Using the results of MALLINDER and PROCTOR (1964), for the decrease in modulus of soda-lime glass with increasing strain, in Marsh's calculation, a rather unbelievable fracture stress of 0.65 E is obtained (E is in all cases the initial modulus). He also used Hillig's data in the flow stress calculation. Substituting instead the modulus variation found by Mallinder and Proctor, reduces the value of flow stress by about one-half, bringing it into better agreement with the fracture stresses found by other investigators. Thus, whatever the error in Marsh's fracture measurements his flow stress data are still consistent with his hypothesis.

1.4 Static Fatigue in Glass

Static fatigue is the decrease of strength of a material with time under constant load. Although the phenomenon is displayed to varying degrees by many materials, it has probably been more extensively investigated in glass than in any other material.

GRENET (1899) was one of the earliest investigators to note that the time to failure of glass decreased with increasing load. MILLIGAN (1929) found that both the breaking strength and the time to failure of glass were affected by the environment, in particular by water. The existence of a limiting stress, or static fatigue limit, below which breakage would not occur, irrespective of time under load was shown by McCORMICK (1936) and HOLLAND and TURNER (1940).

BAKER and PRESTON (1946) demonstrated that delayed failure could be recognised in times as short as 10 ms, whilst the effects on the rate of static fatigue of temperature and of prior outgassing and baking were shown by VONNEGUT and GLATHART (1946) and GURNEY and PEARSON (1949) respectively. Theories on static fatigue were put forward by OROWAN (1944), who considered that the reduction of strength was due to the reduction of surface energy by gaseous absorption on crack surfaces, and by MURGATROYD (1944), who postulated that delayed failure was caused by viscous flow processes.

Although these early investigations had demonstrated most of the factors affecting static fatigue behaviour in glass, the information was not available in a systematic form. In particular, the effects of the nature and size of surface flaws and of the surrounding atmosphere needed clarifying.

CHARLES (1958a) investigated the water vapour corrosion of soda-lime silica glass at temperatures above 150°C. He showed that glasses of the same composition but lower density corroded more quickly than those of higher density. By assuming the validity of extrapolating his observed dependence of corrosion rate on temperature to room temperature, and by considering that the glass structure under triaxial stress was equivalent to that of the lower density, he proposed a mechanism of differential flaw growth by water vapour corrosion under stress to account for the static fatigue of glass. In a subsequent paper (CHARLES, 1958b) static fatigue tests on abraded soda-lime glass rods in saturated water vapour at temperatures between -170°C and 242°C were described. In addition to finding a correlation between the static fatigue behaviour and the macroscopic corrosion results obtained previously, Charles also inferred that it was the alkali content which was responsible for

the static fatigue of most inorganic glasses since there was a correlation between the temperature dependence of the failure process and that of the self-diffusion of sodium ions in bulk glass. Both this theory of Charles and the more refined one of CHARLES and HILLIG (1961) fall short of providing a complete theory for static fatigue. The increased corrosion of glass under stress has not, to the author's knowledge, been demonstrated, and this forms a corner-stone of their proposed mechanism for flaw growth. In addition, as MOULD and SOUTHWICK (1959b) have pointed out, the theory does not predict the observed relationship between the instantaneous breaking strength and a reduced time parameter which Mould and Southwick used to characterise static fatigue.

Probably the most complete investigation of the static fatigue of abraded glass was that reported by MOULD (1960, 1961) and MOULD and SOUTHWICK (1959a, b). In their work, the sizes and shapes of the abrasions, the preconditioning of the specimens and the test atmospheres were all carefully controlled and systematically varied. By plotting their results in the form of σ/σ_N vs. $t/t_{0.5}$, where σ was the breaking stress at time t, σ_N was the breaking stress in liquid nitrogen (in which no fatigue was observed) and $t_{0.5}$ was the time at which $\sigma = 0.5\ \sigma_N$, they showed that the results for all abrasive treatments fell on a single curve, the universal fatigue curve, for a given preconditioning treatment (MOULD and SOUTHWICK, 1959b). This is shown in figure 1.3. In the same paper they compared the predictions of the static fatigue theories of MURGATROYD (1944), GLATHART and PRESTON (1946), STUART and ANDERSON (1953), ELLIOTT (1958) and CHARLES (1958a, b) with the universal fatigue curve and with their observed relation between $t_{0.5}$ and $1/\sigma_N^2$. They concluded that none of

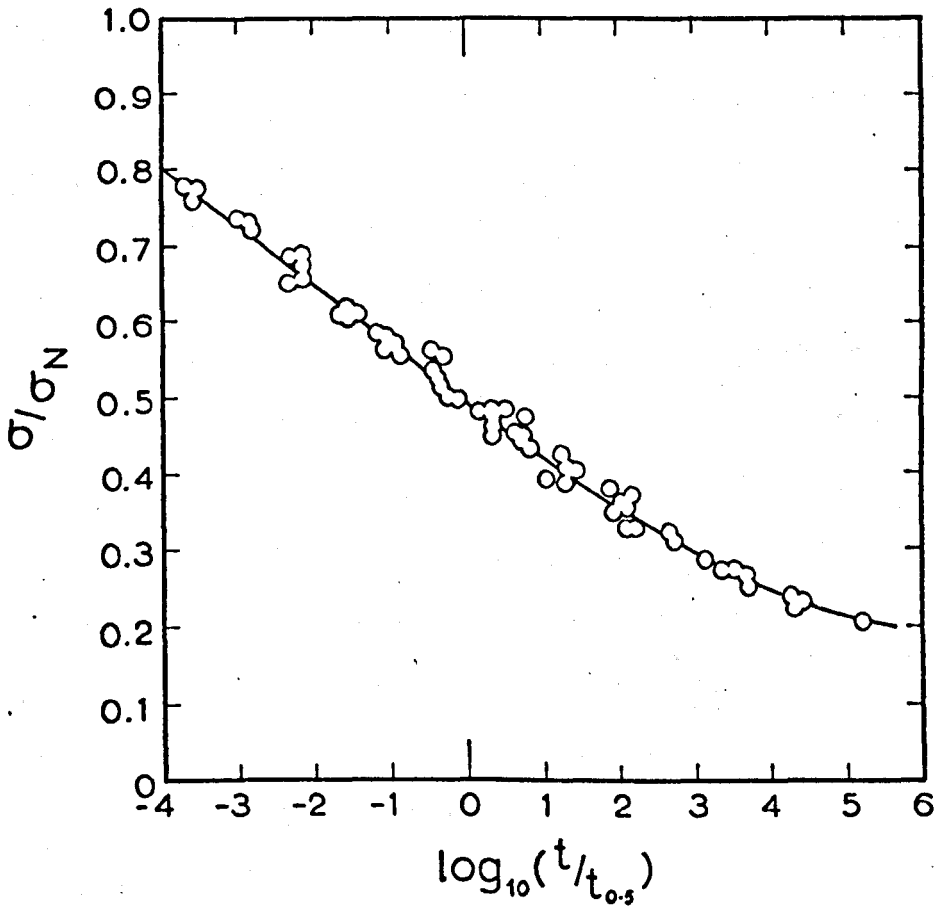

Figure 1.3 Universal fatigue curve for abraded glass (MOULD and SOUTHWICK, 1959b)

these theories provided a complete and adequate explanation of the results.

Their work was extended by investigations into the effect of various aging treatments on the strength and static fatigue of freshly abraded specimens (MOULD, 1960) and into the effect of different environments on the static fatigue behaviour (MOULD, 1961). It was found that baking in vacuo of freshly abraded specimens drastically decreased the static fatigue rate in distilled water and at the same time increased the instantaneous strength. Aging in water and water vapour also increased the instantaneous strength by up to 60% depending on humidity but did not affect the static fatigue rate. The studies on the effect of different environments showed that liquid water is the most effective agent for promoting a high rate of static fatigue and very dry air is the least effective. Mould concluded that the presence of ions or molecules other than water was relatively unimportant except in reducing the concentration of water and its availability at the crack tip.

These investigations by Mould and Southwick, and those of Charles, were conducted on abraded soda-lime silica glass specimens. PROCTOR, WHITNEY and JOHNSON (1967), in the course of a comprehensive study of the properties of high strength fused silica, found that their static fatigue results did not fall on the universal fatigue curve of Mould and Southwick. They were not certain whether this reflected a composition dependence of static fatigue rate, or whether the enormous difference in size of the stressed region between abraded and high strength specimens affected diffusion rates. RITTER (1969) originally reported that the static fatigue rate was the same in high-strength and low-strength specimens of soda-lime

silica glass and that this differs significantly from that found for an alumino-borosilicate glass (RITTER, 1970). However, in a more recent paper the opposite was reported (RITTER and SHERBURNE, 1971), namely that the static fatigue rate for acid-etched soda-lime silica agreed with those of high strength fused silica and aluminosilicate glasses, and differed significantly from that of abraded soda-lime silica glass. It is apparent that more work is necessary before any definite conclusions can be drawn on the effects of composition and of surface condition on static fatigue.

A further point of interest is whether or not static fatigue occurs in glass at the temperature of liquid nitrogen. Most investigators have reported no static fatigue occurring at this temperature. Both PROCTOR et al (1967), working with fused silica, and KROPSCHOT and MIKESELL (1957), working with a borosilicate glass, found that delayed failure occurred in liquid nitrogen although static fatigue (i.e. an experimentally significant decrease in failure stress with time) could not be detected. Experiments reported later in this thesis demonstrate that stress dependent crack growth in soda-lime silica glass takes place in liquid nitrogen. If this is the case, then static fatigue would also be expected to occur, although, since the crack speed rises very sharply with increased stress, very long times would be needed to detect the static fatigue.

Although the stress corrosion theory of CHARLES (1958a) and CHARLES and HILLIG (1961) is accepted as a valid explanation of static fatigue in glass by many workers in the field, it suffers from a number of weaknesses, two of which have been mentioned above. MARSH (1964b) has detailed some further shortcomings of the theory, amongst which are: that the theory cannot account for static fatigue

in flaw-free specimens, since it is concerned with differential flaw growth, and that the dynamics of the stress corrosion process requires a crack of practically constant length which is in conflict with SHAND's (1961) conclusion that there is steady crack growth during the fatigue life. It has been mentioned earlier that MARSH (1963a, b, 1964a, b) found a correlation between the fracture stresses of "flaw-free" glass at different times and temperatures, and the flow stresses calculated from indentation hardness measurements. He maintained that a complete explanation of the fracture properties of glass was possible in terms of the time- and environment-dependent flow stress theory, including those aspects of static fatigue behaviour which the stress corrosion theory fails to explain. The detailed interpretation of static fatigue in terms of plastic flow was referred to a future paper. This, unfortunately, has never been published. One of the objects of this thesis is to attempt to relate the stress dependence of crack growth in glass in different environments to static fatigue using a theory based on the time dependence of the flow stress.

1.5 The Fracture Energy of Glass

The use of the tensile breaking stress of an ordinary sample of glass as a measure of its strength provides more a reflection of the nature and severity of the flaws on its surface than a measure of any fundamental property of the glass. Both the tensile strength and the static fatigue experiments demonstrate that the ability of ordinary glass to support an applied stress reflects the resistance which it offers to the propagation of pre-existing cracks. Hence a

direct measurement of the work necessary to propagate a crack through a glass specimen should provide a measure of a strength parameter which is a more fundamental property of the material than the tensile breaking stress.

BERDENNIKOV (1933, 1934) was probably the earliest to perform this kind of measurement on glass. Using precracked soda-lime silica glass microscope slides in tension, he determined the stress required to initiate further crack growth in different environments. From this he calculated the fracture energy at initiation. As WIEDERHORN (1966a) has pointed out, Berdennikov used an incorrect strain energy term in his calculation. The corrected values of fracture energy range from 0.97 J m^{-2} in water to 4.06 J m^{-2} in a vacuum.

A different technique was used by ROESLER (1956) and CULF (1957). A cylindrical, flat-ended die was used to produce a conically shaped crack in glass. With a constant applied load, the fracture was stable in that the rate of crack growth decreased with time. From a knowledge of the crack dimensions and the applied load the fracture energy could be calculated using an approximate analysis derived by Roesler. Both Roesler and Culf took their measurements at the arbitarily chosen time of 15 minutes after the application of load. Roesler was interested in obtaining a value for the fracture energy at the approach to equilibrium since this should then correspond to the thermodynamic surface energy invoked by GRIFFITH (1920) with which he wished to compare it. He found that equilibrium was apparently attained only after several days under load, at which time the fracture energy was about 2.0 J m^{-2} in air compared to the very short time value of 10 J m^{-2}. He concluded that the failure to achieve an equilibrium crack position coupled with the high value

of fracture energy compared to the surface energy must be due either to elastic hysteresis or to viscosity in the glass. Culf, using the same technique, obtained 15 minute values of fracture energy of soda-lime silica glass in different liquid and gaseous environments. She explained the lowering of the fracture energy from its maximum value of 7.8 J m^{-2} in carbon dioxide to its minimum of 2.9 J m^{-2} in water in terms of the effect of surface adsorption, and obtained an approximate correlation between the fracture energies and the heats of wetting of the liquid environments in contact with silica gel.

A technique for the direct measurement of the work done during crack propagation was developed by NAKAYAMA (1964, 1965) and CLARKE, TATTERSALL and TAPPIN (1966). This was applied to glass by Nakayama and by DAVIDGE and TAPPIN (1968). The technique consisted of loading a specially notched specimen in three-point bending at a constant rate of deflection. From the area under the load-time curve, or the load-deflection curve, and the specimen dimensions, the work done per unit area, or fracture energy, was calculated. By using a hard machine, to reduce the strain energy stored in the machine, and a shaped notch, to reduce the stress required to initiate fracture, the total strain energy stored in the system at the moment of initiation could be made less than total energy required to fracture the specimen. In this way the fracture could be controlled, since further external work was required before the specimen failed completely. As a reproducible and convenient means of measuring the strength of a material, the technique suffers from a number of drawbacks. It is assumed that all the measured external work goes into the creation of two new surfaces. This ignores the possibility of imparting kinetic energy to the fracture fragments (although the

use of the shaped notch and the hard machine should minimise such a contribution) and also the possibility of multiple cracking. Further, only a single measurement is made on each specimen and the scatter is high. Finally, Davidge and Tappin found that their values of fracture energy depended on the depth of the initial notch, or, alternatively, since their specimens all had the same cross-section, on the area fractured. There is too great a scatter in Nakayama's results to say whether a similar dependence was obtained.

Probably the most successful technique used for measuring fracture energies in glass using controlled crack growth has been the double-cantilever cleavage technique. Following the use of the cleavage technique to measure the fracture energy of mica (OBREIMOFF, 1930) and of crystals (GILMAN, 1960), where natural cleavage planes controlled the direction of crack propagation, the technique was applied to isotropic polymeric materials by BENBOW and ROESLER (1957) and BERRY (1963). Benbow and Roesler applied longitudinal compressive stresses to control the crack direction, but this had an unknown effect on the stresses at the crack tip. Berry cut shallow grooves along the centre-lines of the front and back surfaces, and these successfully contained the crack. LINGER (1967) and, independently, WIEDERHORN (1966a, b) have used Berry's configuration to measure the fracture energy of glass.

The soda-lime silica glass microscope slides which Wiederhorn used in his tests were subjected either to constant loads or to constant rates of deflection. The crack length was measured as a function of time to provide the crack velocity, and the fracture energy was calculated at the onset of very fast fracture. In the double-cantilever mode of crack propagation it can be shown

(GILLIS and GILMAN, 1964) that, unless the crack length, L, is greater than about five times the specimen half-width, w, corrections are needed to equations for the fracture energy derived from simple beam theory. The two main corrections are for the effects of shear and of end-rotation, the latter corresponding to strain energy stored beyond the tip of the crack. Wiederhorn used an equation derived by WESTWOOD and HITCH (1963) which included a correction for shear, but not for end-rotation. GRIFFITHS (1968) has shown that for specimens such as Wiederhorn used, with $5w > L > 1.5w$, this can introduce errors of up to 50%.

If the double-cantilever specimen is held at constant deflection, rather than having a constant load or constant rate of deflection applied, the crack propagation is stable in that the crack speed decreases with increasing crack length. This method was used by LINGER (1967) who was able to obtain several measurements on any one specimen. The necessity of correcting for the effects of shear and end-rotation was avoided by ensuring that $L > 5w$. A knowledge of either the crack length, or the applied load, or both, at the initiation of rapid fracture accompanying an increase in the deflection allowed the fracture energy to be calculated. Experiments were performed in a variety of environments and on both Pyrex and soda-lime silica glass. The results of his work together with those of other investigators are summarised in table 1.1.

In a later paper, WIEDERHORN (1969) presented further results on the fracture energies of glasses of different composition at different temperatures in dry, inert environments. The experimental technique was exactly the same as the one used previously, but the fracture energies were calculated from an equation derived by

Environment	BERDENNIKOV (1933, 1934) (corrected) tension	CULF (1957) 15 min cone crack	NAKAYAMA (1964, 1965) work to fracture	DAVIDGE and TAPPIN (1968) work to fracture	WIEDERHORN (1966a, b) cleavage	LINGER (1967) cleavage	WIEDERHORN (1969) cleavage
air (20°C, 50% rh)		4.0	3.4 → 10.0	5.0 → 6.8	2.6	4.5	
dry nitrogen (g) (20°C)		7.6			2.8	3.8	3.85
water (20°C)	0.97	2.9				3.0	
liquid nitrogen (-196°C)					3.2	4.1	4.6
vacuum (20°C)	4.1				4.1	5.2	
dry inert liquid (typical) (20°C)	3.2	6.7				4.2	

Table 1.1 Values of fracture energy of soda-lime silica glass in J m^{-2}. Apart from those of CULF (1957) all represent experimentally determined values at the initiation of fast fracture.

WIEDERHORN, SHORB and MOSES (1968). The equation was shown to be derivable both from the analysis of GILLIS and GILMAN (1964), which was based on corrections to simple beam theory, and from the numerical stress analysis, or boundary collocation results of SRAWLEY and GROSS (1967). Wiederhorn found that the fracture energy, in general, increased with decreasing temperature and with increasing Young's modulus. Under similar conditions, the results of WIEDERHORN (1969) and LINGER (1967) are in good agreement as is shown in table 1.1. It is worth noting that in all cases the values of fracture energy are approximately an order of magnitude greater than the estimated surface energy.

1.6 Propagation of Cracks in Glass

In an ideally brittle, elastic material, crack propagation is controlled essentially by the First Law of Thermodynamics. The implications of this are that the energy required to fracture such a material is equal to the surface energy of the two new surfaces, that for each increment of strain there is a corresponding equilibrium crack position, and that the process of crack propagation can be a reversible one, provided that the fracture surfaces are not modified by, for example, interactions with the environment.

It has already been noted in the previous section that the fracture energy of glass at variously defined initiation points is much higher than estimates of the surface energy. It has also been noted that if cracks in glass do attain equilibrium this takes place at a lower value of fracture energy and after some considerable time. LINGER (1967) followed the progress of a crack in glass for over a

year in a double-cantilever beam specimen held at constant deflection. After this time the crack was still moving and the fracture energy was estimated to be 0.34 J m^{-2}. Thus, it is apparent that glass is not an ideal brittle material, and that a more detailed examination of the crack propagation behaviour in different environments and as a function of stress is required in order to understand the fracture process. (The possibility of the fracture process in glass being a reversible one is discussed in a later chapter).

One of the earliest reports that the rate of crack growth in glass depended on the applied stress was that of MURGATROYD (1942). Cracks were propagated both by applying thermal stresses to glass containers and by loading plate glass in the double-cantilever cleavage mode (through what was literally a string and sealing wax arrangement). Observed velocities ranged from 10^{-6} m s^{-1} to 10^{-4} m s^{-1} depending on the level of applied stress, though no figures were given for the stresses.

SHAND (1961) attempted to correlate static fatigue behaviour with stress-dependent crack growth in glass. A semi-empirical method was developed for estimating crack velocities from curves of stress versus time-to-failure. It is, however, difficult to see how Shand actually used the method. His analysis predicts an inverse dependence between the failure time, t, and the square of the applied stress, σ. The curves which he constructs for different values of initial crack depth, a, are sigmoidal in shape when plotted as log σ vs. log t instead of straight lines. The analytical relationship between a and t does not correspond to the one plotted, and of the experimental results quoted from SHAND (1954), which are used to scale the log σ vs. log t plot from experiments with cracks of known sizes, only one

actually appears in that paper. Thus it is difficult to comment on the significance of the transformation of this data into curves showing the fracture energy as a function of crack speed.

There is, therefore, a need for actual measurements of the variation of crack propagation rates with applied load in different environments to achieve a better understanding of the factors controlling the fracture process in glass. At the time that the work described in this thesis was started (1967) there was virtually no information available in the literature on this topic. Since then, several pieces of work have been published, not all of which contained satisfactory results (these other works are considered, together with the results of this work, in Chapter 4). It was, thus, still considered worthwhile to continue with the measurements to be described in Chapters 3 and 4, especially as the procedures adopted differed significantly from those used by the other investigators.

CHAPTER 2

FRACTURE CRITERIA AND FRACTURE MECHANICS

2.1 Introduction

In this chapter, as in the previous one, the intention is not to present an exhaustive survey. Rather it is to trace the development of the analytical study of fracture, and to show how the parameters used in this thesis to characterise the fracture of glass are derived.

The work of da Vinci and of Galileo has already been mentioned in the Introduction. Da Vinci* found that the strength of the iron wire he tested increased with decreasing length, a not surprising result considering the quality of wire available at that time. Galileo stated, on the other hand, that the strength of a member in tension should depend only upon the area and not on the length. Mariotte (1620-1684) proposed that fracture occurs when the fractional elongation exceeds a certain limit. Coulomb (1736-1806), in attempting to account for the oblique fracture in compression of stone cylinders, put forward a critical shear stress failure criterion (this became known as the Coulomb-Mohr theory after Mohr suggested a method of representing this criterion geometrically). These and subsequent criteria may, in general, be categorized as criteria of strain, of stress, or of energy, and criteria in each of these categories have been proposed within the context of fracture mechanics.

Fracture mechanics has developed enormously since the Second World War, spurred on by the dramatic, and often catastrophic, brittle

---

* TIMOSHENKO (1953) gives an account of these early works

failures of large metal structures such as ships, storage vessels and aircraft. Much of this development has centred around the problem of explaining the fracture behaviour of metals, a problem complicated by the dependence of the transition from ductile to brittle failure on temperature, strain rate and dimensions. However, in that the analyses assume linear elasticity and limited plasticity, they are equally applicable to materials such as glass.

2.2 The Griffith Criterion

The work of GRIFFITH (1920, 1924) has already been discussed in Chapter 1 in connection with the strength of glass. His work, however, has a more general relevance. Griffith postulated that the determining factor in the fracture process was that the surface energy of the two new surfaces formed when a crack extended must be less than the elastic energy lost by the body containing the crack plus that lost by the loading system. This then established an energy balance of the form

$$\partial U/\partial A \geq \partial T/\partial A \qquad (2.1)$$

as a criterion for fracture (U is the elastic energy, T is the surface energy, and A is the area of crack surface). This energy balance is essentially a statement of the First Law of Thermodynamics, and as such applies strictly only to processes close to equilibrium. Also, through use of the thermodynamic surface energy, T, the criterion is a both necessary and sufficient condition only for the fracture of ideal, perfectly brittle materials. For all other materials, the criterion provides a minimum necessary condition.

IRWIN (1947) and, independently, OROWAN (1948-9) suggested that

Griffith's theory could be modified so that a limited amount of plastic behaviour could be taken into account. The modification involved replacing the surface energy, T, by the total energy absorbed in propagating the crack, γ. Then

$$\gamma = T + \gamma_p \qquad (2.2)$$

where γ_p represents the energy of plastic distortion absorbed in the fracture process. OROWAN (1955) noted that, particularly in metals, γ_p was about three orders of magnitude greater than T, and the latter could thus be neglected. It was argued by both Irwin and Orowan that, provided the plastic distortion was confined to a region whose dimensions were small compared to the crack length and specimen dimensions, this would not significantly affect the stored strain energy in the body calculated on the assumption of purely elastic behaviour. Thus, for an elliptical crack of length 2c in an infinite sheet, the tensile stress, σ_b, at failure given by equation (1.2) is modified to

$$\sigma_b = (2E\gamma/\pi c)^{\frac{1}{2}} \qquad (2.3)$$

2.3 Strain Energy Release Rate

IRWIN and KIES (1952, 1954) took the modified Griffith theory further. They suggested that the value of the strain energy release rate ("rate" referring to the derivative with respect to crack area) that equalled the energy absorbed on crack extension might provide an improved failure criterion. If the process of crack extension was independent of the loading or specimen geometries, then crack

extension would occur at a critical value of the strain energy release rate. This critical value could be regarded as a material property, and could be determined experimentally. For an elastic material, the stored strain energy, U, is given by

$$U = F^2C/2 \tag{2.4}$$

where F is the applied load and C is the specimen compliance. Differentiating this with respect to crack area gives the strain energy release rate

$$\left(\frac{\partial U}{\partial A}\right)_F = \frac{F^2}{2} \cdot \frac{\partial C}{\partial A} \tag{2.5}$$

Thus, evaluating $\partial C/\partial A$, by measuring the compliance of a specimen at different crack lengths, allows the critical strain energy release rate to be determined from a fracture test on a similar specimen through measurements of the fracture load, F. This compliance calibration method is quite general and can be applied to complicated specimen geometries.

By analogy with the concept of the force on a dislocation line, IRWIN (1956, 1957) suggested that the strain energy release rate could be regarded as the force per unit length of crack front tending to cause extension of the crack. This force, denoted by G (after Griffith) would have the critical value G_c when the crack starts to propagate. Since G_c is given by the derivative of strain energy with respect to projected crack area, it is equal to twice γ, which is the fracture energy per unit area of fracture surface.

Materials whose elastic or plastic properties are time-dependent may not have well-defined, constant values of G_c or γ. A crack in a specimen of such a material, in a constant load, tensile test, will

show an initial period of slow growth, followed by fast fracture (the division into these two regimes of crack growth is conventional, and does not necessarily imply that the crack length as a function of time shows an abrupt change). It has been noted in the previous chapter that glass behaves in this way, and so also do many metals and plastics.

2.4 Stress Intensity Factor

The concept of the strain energy release rate as a crack driving force was extended by IRWIN (1956, 1957) who demonstrated that G could be associated with the elastic stress distribution close to the crack tip. Using stress function solutions due to WESTERGAARD (1939), and a similar approach to that of SNEDDON (1946), Irwin obtained an expression of the form

$$\sigma_{ij} = K_X (2\pi r)^{-\frac{1}{2}} g_{ij} (\theta) \qquad (2.6)$$

for the stresses, σ_{ij}, near the tip of a planar crack in an infinite body (figure 2.1). Here r and θ are polar coordinates whose origin is at the crack tip and the subscript X (X = I, II, III) denotes which of three fundamental modes of relative crack face motion is under consideration. In principle, any relative motion of the crack faces can be expressed as a combination of these three fundamental modes which are illustrated in figure 2.2. The opening mode, or mode I, consists of separation of the crack faces in the direction perpendicular to the plane of the crack. The sliding mode, or mode II, is a relative shear motion of the crack faces perpendicular to the leading edge of the crack, and the tearing mode, or mode III, is

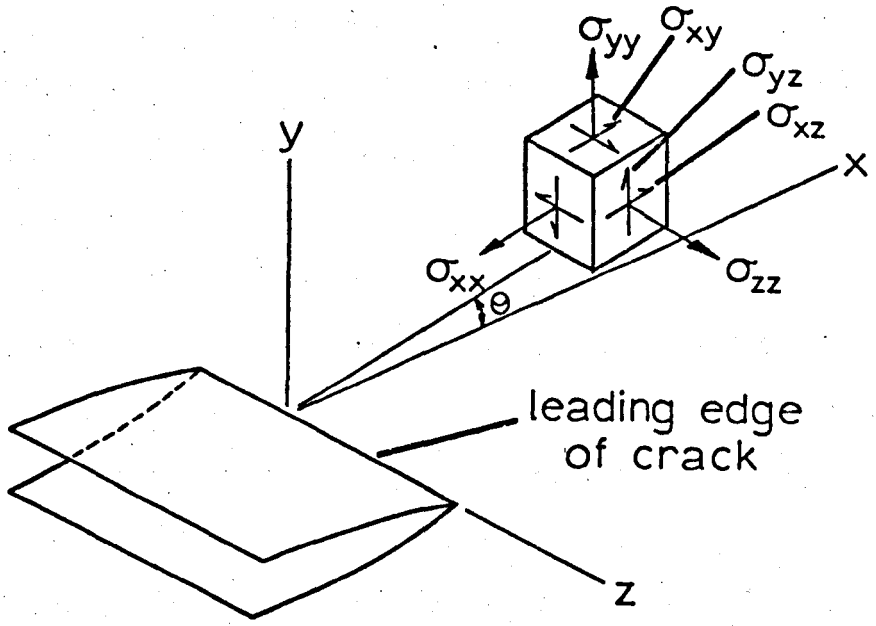

Figure 2.1 Coordinate system at crack tip

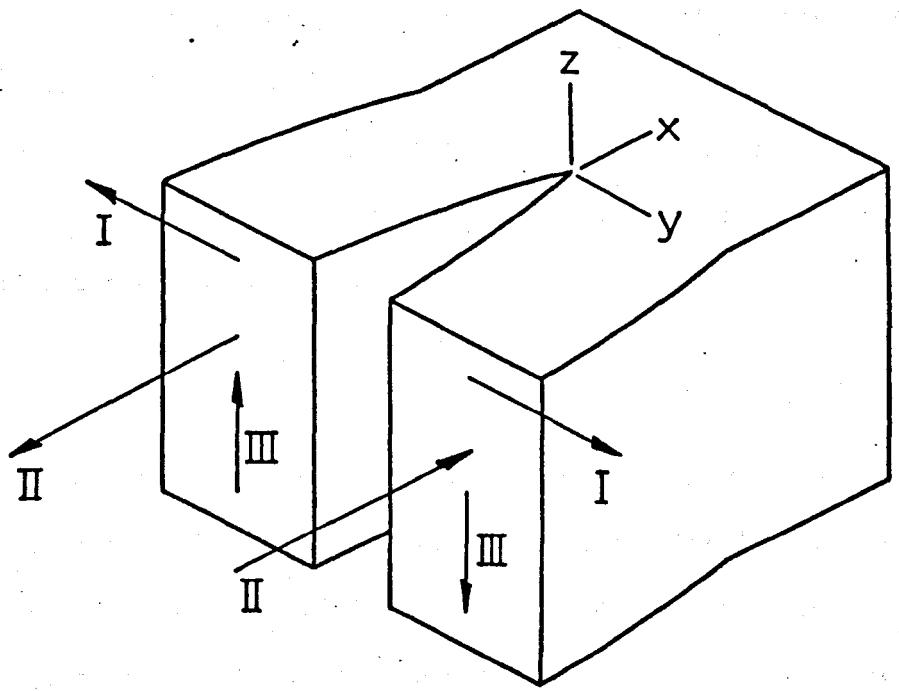

Figure 2.2 The fundamental modes of relative crack face motion

a relative shear motion parallel to the leading edge. The function $g_{ij}(\theta)$ is one whose form depends on the particular stress component, σ_{ij}, and mode, X, but is independent of the loading and specimen geometry.

Thus K, which is the same for all σ_{ij} in a given mode, is the only parameter which relates the elastic stress field in the neighbourhood of the crack tip to the loading and geometry of the system. K is known as the stress intensity factor, and is defined by the condition that the appropriate stress component, σ_{ij}, ahead of the crack in the crack plane, for which $g_{ij}(\theta) = 1$, when $\theta = 0$, is given by

$$(\sigma_{ij})_{\theta=0} = K(2\pi r)^{-\frac{1}{2}} \qquad (2.7)$$

For mode I, which is the mode of most relevance to practical studies of crack propagation, $(\sigma_{ij})_{\theta=0}$ refers to σ_{yy}, the tensile stress across the crack plane.

By applying virtual work arguments, in terms of the stresses which would be necessary to close an existing crack, IRWIN (1956) showed that K was related to G by

$$K^2 = EG \qquad (2.8)$$

Thus, if the attainment of a critical strain energy release rate, or crack driving force, G_c, provides a valid criterion for the fracture of a given material, this is the equivalent, in an elastic material, to the attainment of a critical value of stress close to the crack tip.

It should be noted that, in common with the bulk of fracture mechanics, this analysis is essentially confined to two-dimensional

situations so that the mathematics remain tractable. For practical purposes this involves one of two simplifying assumptions. It is either assumed that the material is in the form of a thin sheet so that stresses are uniform in the plane of the sheet and there are no stresses perpendicular to this plane. This is known as plane stress. Alternatively, very thick bodies are assumed to be in a state of plane strain, in which the strains are uniform in the plane of the body and there are no strains in the direction of its thickness. Equation (2.8) applies strictly for plane stress, and for plane strain is modified to

$$K^2 = EG/(1-\nu^2) \qquad (2.9)$$

in which the modulus, E, is replaced by an effective modulus $E/(1-\nu^2)$. For a given applied stress, K (plane stress) is equal to K (plane strain). In general, however, K_c (plane stress) is higher than K_c (plane strain), and fracture tests are designed to ensure plane strain conditions which provide a lower bound to the resistance of a material to crack propagation.

In general, materials do not display perfectly elastic fracture behaviour and, as with any proposed fracture criterion, the existence of a critical K or G at fracture must be verified experimentally in different specimen geometries for a given material before K_c or G_c can be taken as a valid fracture criterion for this material. Once this has been demonstrated, K_c or G_c may be considered as material properties whose relationship to the applied K or G is analogous to that between the yield stress and the applied stress.

Expressions for K have been determined for a large number of loading and specimen geometries (SRAWLEY and BROWN, 1964; PARIS and SIH, 1964) usually by numerical stress analysis procedures. For a

crack in an infinite plate under tension, K is given by

$$K_I^2 = \pi\sigma^2 c \qquad (2.10)$$

for an applied stress, σ, and crack length, 2c. In general, a correction is needed when considering a finite specimen to allow for bending stresses or the presence of a free edge, and equation (2.10) is modified to

$$K_I^2 = Y^2\sigma^2 c \qquad (2.11)$$

where Y^2 is known as the finite plate correction factor, values of which have been determined for different configurations and crack length to specimen width ratios (e.g. PARIS and SIH, 1964).

The expression for the stress concentration, equation (2.7), in the same way as that of INGLIS (1913), equation (i.5), leads to a stress singularity at the crack tip. This is a feature common to all analyses based on continuum mechanics, whether they be purely elastic or elastic-plastic (see e.g. HAYES, 1970), and reflects the inapplicability of a continuum model when considering distances from the crack tip which are comparable to the sizes of discrete structural units of the material. In general, this difficulty is circumvented, for a material which has limited plasticity associated with the fracture process, through consideration of the plastic zone. It is argued that, providing the plasticity is limited, the distribution of stress is not affected at points away from the immediate region of the crack tip and that the strain energy will not differ appreciably from that derived for the elastic case. For a simple elastic-perfectly plastic material the stress within the plastic zone can be assumed to be constant and equal to the yield stress, and a characteristic

dimension is derived (depending on the particular model employed) which defines the interface between plastic and elastic behaviour. Thus the stress singularity is "removed" from the elastic problem by imposing the assumption of constant stress in the plastic zone.

2.5 Plastic Zones

IRWIN (1960) suggested that the elastic stress field distribution around a crack with an associated plastic zone would be the same as that around a crack in an ideal elastic material, if the length of the elastic crack was $c' = c + r_p$ where c was the actual crack length and r_p was evaluated by substituting the yield stress, σ_Y, for σ_{ij} in equation (2.7) and putting $r = r_p$. Then

$$r_p \approx \frac{1}{2\pi} \cdot \frac{K_I^2}{\sigma_Y^2} \qquad (2.12)$$

and r_p defines an effective plastic zone size. The plastic zone may be modelled by one which is circular in cross-section as shown in figure 2.3, in which the effect of the transition from plane strain conditions in the interior of the material to plane stress at the surface can be seen. Under plane stress conditions materials can fail in shear, as opposed to cleavage failure under plane strain. The amount of plasticity associated with crack growth determines the minimum allowable specimen thickness for plane strain failure, since the larger the plastic zone, the greater will be the thickness of the surface layer subjected to plane stress conditions. For plane strain in a specimen of thickness, w, the condition is

$$w \gg r_p = \frac{1}{2\pi} \cdot \frac{K_I^2}{\sigma_Y^2} \qquad (2.13)$$

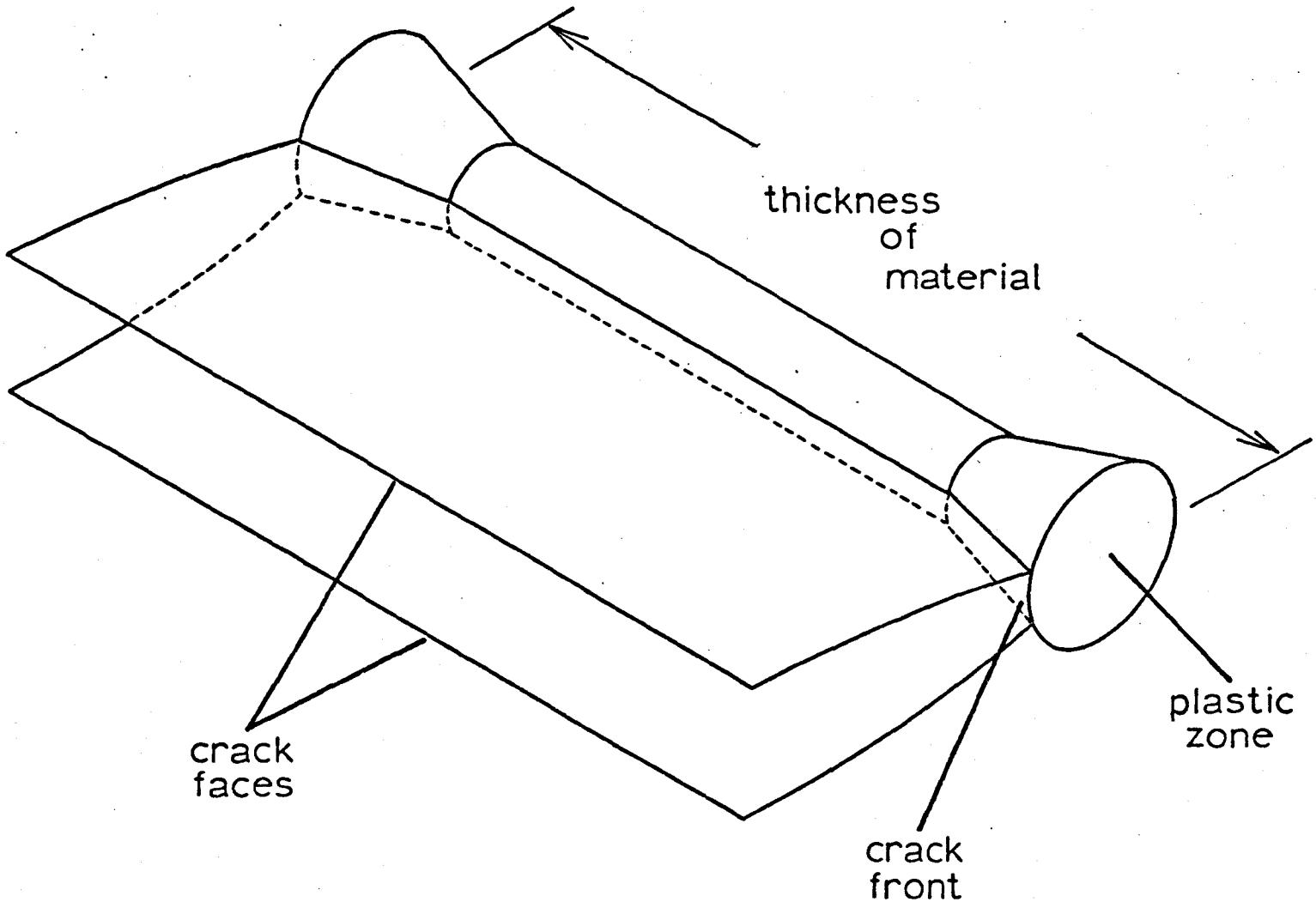

Figure 2.3 Model of plastic zone at crack tip

For a material such as glass, for which $r_p \sim 10^{-8}$ m, equation (2.13) places no effective restriction on the thickness of macroscopic specimens. For materials such as metals and thermoplastics, some of which have large values of r_p, equation (2.13) must be borne in mind when designing fracture tests.

Independently, DUGDALE (1960) and BILBY, COTTRELL and SWINDEN (1963) proposed similar, one-dimensional models for the plasticity at a crack tip. The length of the plastic zone is fixed by the postulate that there shall be no stress singularity at the end of the plastic zone (within the plastic zone the stress is equal to the yield stress). This gives a relationship between the crack length, 2c, and the plastic zone length, r_p,

$$\frac{r_p}{c + r_p} = 2 \sin^2 \left(\frac{\pi}{4} \cdot \frac{\sigma}{\sigma_Y}\right) \qquad (2.14)$$

for an applied stress, σ. If $r_p \ll c$, then

$$r_p = \frac{\pi^2}{8} \cdot \frac{\sigma^2 c}{\sigma_Y^2} \qquad (2.15)$$

Since the Dugdale model is based on a crack in an infinite sheet in tension, σ^2 from equation (2.10) can be substituted into equation (2.15) yielding

$$r_p = \frac{\pi}{8} \cdot \frac{K_I^2}{\sigma_Y^2} \qquad (2.16)$$

which is comparable to the result obtained by IRWIN (1960), equation (2.12).

In a crack with a plastic zone at the crack tip, the crack faces are displaced from each other due to the plasticity. This displacement is termed the crack opening displacement, or COD, and WELLS (1963)

proposed that a critical COD might form a simple, fracture criterion. Measurement of the actual COD, α, at the crack tip was not necessary, since the displacement at a point remote from the tip could be related to that at the tip through the geometry and elastic properties of the specimen. BURDEKIN and STONE (1966), using a Dugdale model, showed that the crack opening displacement, α, was related to the stress intensity factor, K_I, for an elastic-perfectly plastic material, by

$$K_I^2 = E\sigma_Y\alpha \qquad (2.17)$$

or

$$G_I = \sigma_Y\alpha \qquad (2.18)$$

It is not absolutely necessary for these models of the plasticity associated with growing cracks to provide shapes or sizes of plastic zones that correspond to physical reality. Their chief value is that they allow the plasticity to be characterised by parameters with the dimensions of length which may be related to the stresses applied remotely at the boundaries of the specimen. (This is analogous to associating an effective mass with an electron, or a positive hole, when considering electronic processes in solids). The parameters thus defined can be used to give possible alternative fracture criteria. Since, in general, real materials exhibit neither linear elastic nor perfectly plastic behaviour, G_{Ic}, K_{Ic} and α_c no longer necessarily provide alternative statements of the same fracture criterion. Neither do they necessarily remain constant during fracture. However, even though they may in many cases lack the generality of a constant fracture criterion, these parameters can still be usefully employed to characterise fracture behaviour.

CHAPTER 3

EXPERIMENTAL: APPARATUS AND MEASUREMENTS

3.1 Introduction

The need for data on the variation of crack speed with applied stress in glass in different environments was discussed at the end of Chapter 1. The experimental work to be described in this chapter was undertaken with the objective of satisfying this need.

Initial experiments were performed on double-cantilever beam specimens with the apparatus developed by LINGER (1967) in this laboratory. Serious difficulties were encountered, however, in achieving consistent results with this system. Since, in air, crack speeds in glass increase by about ten orders of magnitude when the load on the specimen is doubled, very small variations in the applied load are sufficient to produce appreciable changes in the crack speed. Such small variations in load were thought to arise from misalignments in the system used for loading and supporting the specimen, and this was extensively modified in an effort to overcome the problem. In the form which produced the most reproducible results the specimen was supported horizontally by low-friction supports, and was loaded in a horizontal plane through flexible chain links. The flexible links prevented any bending or twisting stresses being imposed on the specimen, but their use meant that the weight of the specimen had to be independently supported so that the plane of loading remained horizontal. This, in turn, meant that testing in liquid environments was inconvenient.

A completely different system of propagating cracks in glass was therefore adopted for the main work of this thesis. This was

based on the double-torsion configuration introduced by OUTWATER and GERRY (1966, 1967). One of the chief advantages of using this method of loading was that constant crack velocities were obtained with constant applied loads. In addition, with the modified apparatus which is described later the specimen was vertical. This made immersion in liquid environments a straightforward matter.

In this chapter, the mechanics of double-torsion are analysed and this is followed by descriptions of the apparatus and of the experiments which were performed. These include calibration measurements, determination of the moduli of glass and the measurement of crack propagation characteristics in different environments.

3.2 Mechanics of Double-Torsion

The mechanics of double-torsion are developed in this section from strain energy considerations, assuming linear, isotropic elasticity. A further assumption is that each half of a cracked specimen can be modelled by a rectangular beam whose length equals the crack length and to one end of which a torque is applied, the other end remaining fixed. Deviations from this simple model which can occur in practice will be considered later.

With reference to figure 3.1, which depicts a specimen under double-torsion loading, and taking the loading points of the left-hand arm of the specimen as fixed, the incremental work, dW, done by the applied torque, M, to increase the angular deflection, θ, of the right-hand arm of the specimen by an increment, $d\theta$, is

$$dW = M\,d\theta \qquad (3.1)$$

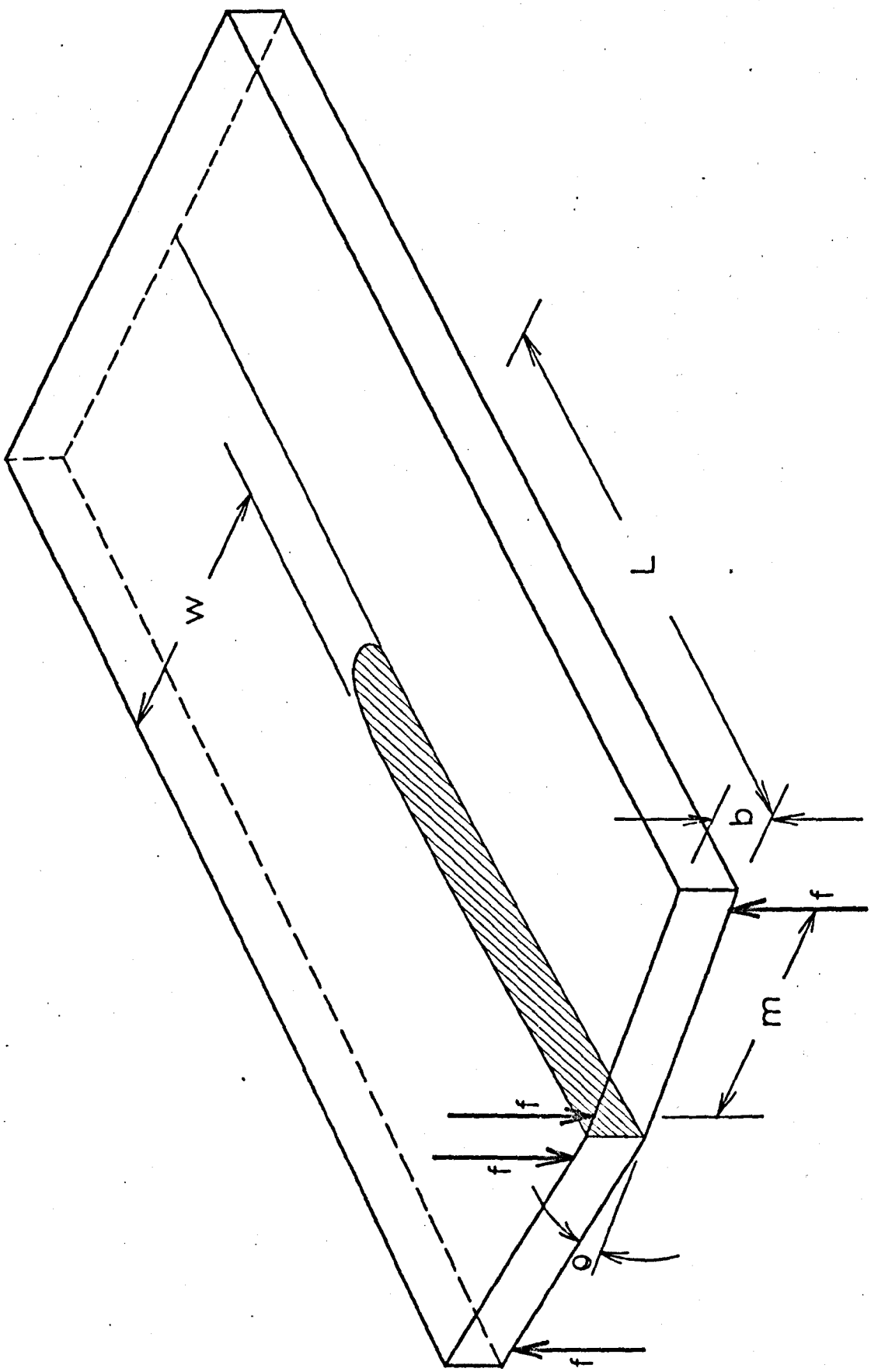

Figure 3.1 Diagrammatic representation of double-torsion specimen

where M = fm, f is the force at each loading point and m is the distance between the two loading points on one arm of the specimen. The compliance, C, of the specimen may be defined by

$$C = \theta/M = \theta/fm \tag{3.2}$$

Thus

$$\theta = f m C \tag{3.3}$$

and

$$d\theta = m C \, df \tag{3.4}$$

Hence

$$dW = f m^2 C \, df \tag{3.5}$$

and the total work done on the specimen in producing a deflection θ is

$$W = f^2 m^2 C/2 \tag{3.6}$$

which is equal to the stored strain energy, U, in the specimen. The strain energy release rate, G_{Ic}, is defined by

$$G_{Ic} = (\partial U/\partial A)_f \tag{3.7}$$

where A = bL, b is the specimen thickness and L is the crack length. Thus

$$G_{Ic} = \frac{f^2 m^2}{2b} \left(\frac{\partial C}{\partial L}\right)_f \tag{3.8}$$

which corresponds to the equation developed by IRWIN and KIES (1954).

From elasticity theory (TIMOSHENKO and GOODIER, 1970) M is given, for one arm of the specimen, by

$$M = \frac{1}{3} \mu \frac{\theta}{2} \frac{b^3 w}{L} (1-0.63\ b/w) \tag{3.9}$$

where μ is the shear modulus of the material and w is the half-width

of the specimen. This expression is accurate to better than one per cent for $w > 2b$ (Timoshenko and Goodier, op cit). From equations (3.2) and (3.9)

$$C = \frac{6L}{\mu\, b^3 w\, (1-0.63\ b/w)} \qquad (3.10)$$

Hence

$$G_{Ic} = \frac{3\, f^2\, m^2}{\mu\, b^4 w\, (1-0.63\ b/w)} \qquad (3.11)$$

which, as can be seen, is independent of the crack length, L.

G_{Ic} can also be expressed in terms of the angular deflection, θ, of the specimen. Using equations (3.3) and (3.10) and substituting in equation (3.11) gives

$$G_{Ic} = \frac{\mu\, \theta^2\, b^2 w\, (1-0.63\ b/w)}{12L^2} \qquad (3.12)$$

From equation (3.9) it can be seen that, for a constant applied torque, θ is proportional to L, so in equation (3.12) G_{Ic} is constant for a constant applied load. For convenience, the values of G_{Ic} given by equations (3.11) and (3.12) are denoted by G_c (f) and G_c (θ) respectively, and the subscript I is omitted hereafter.

In practice there are several possible reasons for deviations from the simple theory developed above. Probably the most important of these is the fact that the crack front is not perpendicular to the direction of crack propagation. Instead, its cross-section is like that depicted in figure 3.2, with the crack approaching the "compressive" surface of the specimen asymptotically, eventually breaking through. Some preliminary experiments revealed that the distance between the crack tip at the "tensile" surface and that at the "compressive" surface apparently depended on the specimen compliance. The distance was considerably shorter in poly(methyl methacrylate)

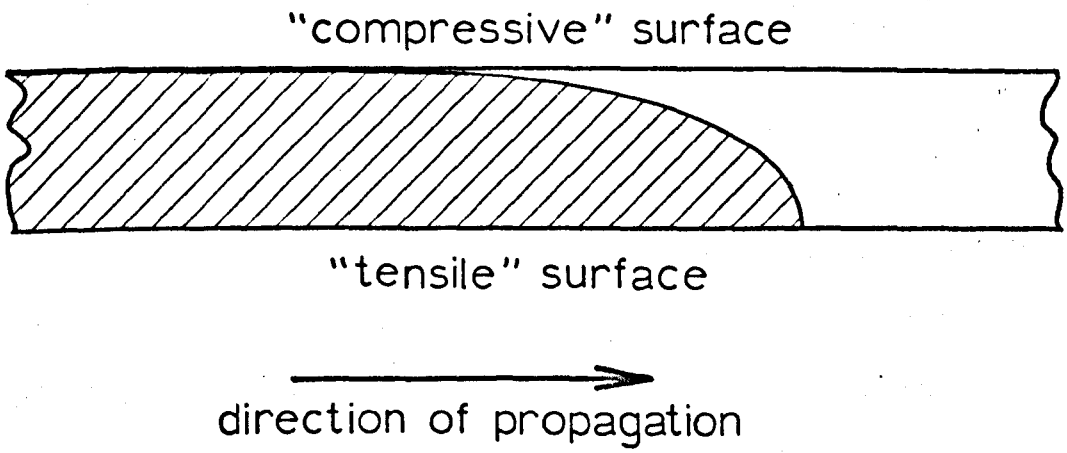

Figure 3.2 Illustration of shape of crack front

("Perspex") than in glass of the same thickness, and it increased with increasing specimen thickness. Once the crack had completely broken through the thickness of the specimen, the crack tips at the two surfaces moved by equal amounts when the crack extended. This suggested that the shape of the crack front was not changing with increasing crack length. The rate of change of compliance with crack length should be independent of the shape of the crack front, provided that the latter does not change with crack length. Thus, although the compliance of a cracked double-torsion specimen is expected to differ from that predicted by the simple theory, the shape of the crack front should not affect the calculated value of G_{Ic} in the region where that shape remains constant.

There are two further effects which, in principle, might be expected to affect the calculated value of G_{Ic}. One of these is end-rotation, or deformation of the specimen beyond the tip of the crack. The effect of this is to allow the storage of strain energy ahead of the crack tip and thus give the specimen a higher compliance than it would have if the ends of the two halves of the specimen were rigidly fixed. The other possible effect is hindered rotation of the two arms of the specimen due either to the presence of the web of unbroken material or to contact between the opposite faces of the fully cracked material. An attempt to isolate these effects and to estimate their magnitude was made in the compliance calibration experiments to be described later. The results indicated that significant errors would be introduced by neglecting these effects and relying on the simple theory.

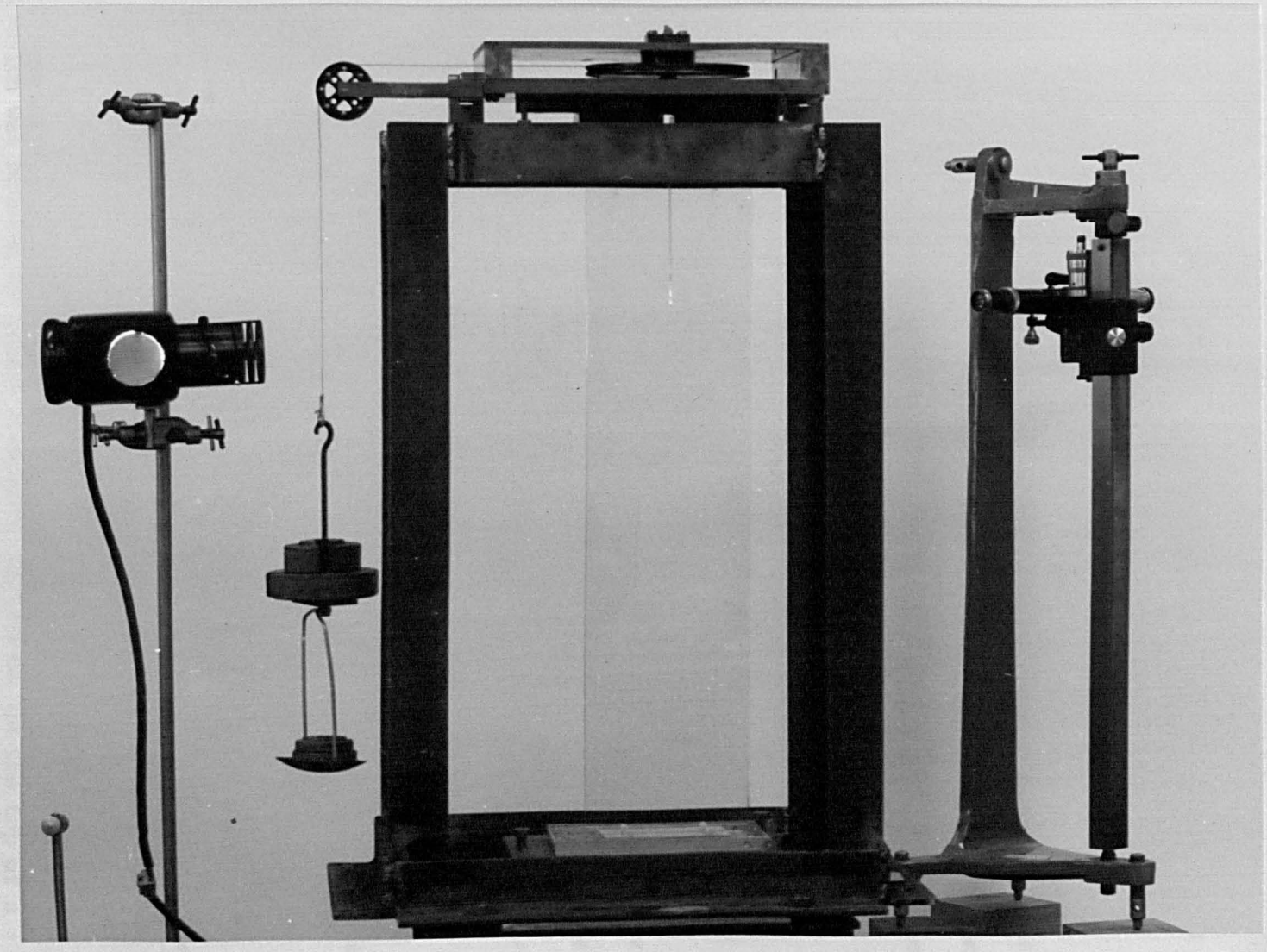

Figure 3.3 General view of the double-torsion apparatus

3.3 Double-Torsion Apparatus

Some preliminary trials were conducted with a direct dead-weight loading double-torsion apparatus based on that described by OUTWATER and GERRY (1966) and KIES and CLARK (1969). It was found difficult to control the direction of crack propagation with this apparatus, the large loads required were awkward to handle, and problems were encountered in starting the crack without catastrophic failure occurring. Because of these difficulties, and also because the apparatus, in which the specimen was horizontal, was inconvenient for conducting tests in liquid environments, it was decided to construct an improved form of the apparatus which would take the above factors into account. The design was based on that of an existing four-point bend machine and two versions were built. The first, which incorporated the original machine, proved suitable for testing the thinner specimens, whilst the second, which had a higher load capacity, was used mainly for tests on the thickest specimens.

A general view of the improved double-torsion apparatus is shown in figure 3.3 and its mode of action is illustrated diagrammatically in figure 3.4. The rotation of the pulley [1] under the action of the force F causes the pins [2], which are rigidly linked to the pulley, to exert a torque on the right-hand side of the specimen [4]. This torque induces an equal and opposite torque through the fixed pins [3]. The 155 mm diameter pulley (112 mm in the earlier machine) was enclosed in an open-sided rigid steel box which was mounted on hinges and levelling screws on the top of a frame constructed of steel angle. Figure 3.5 shows details of the top of the apparatus, hinged open. The pairs of pins [2] and [3] were mounted on carriages so that the common centre-lines of each

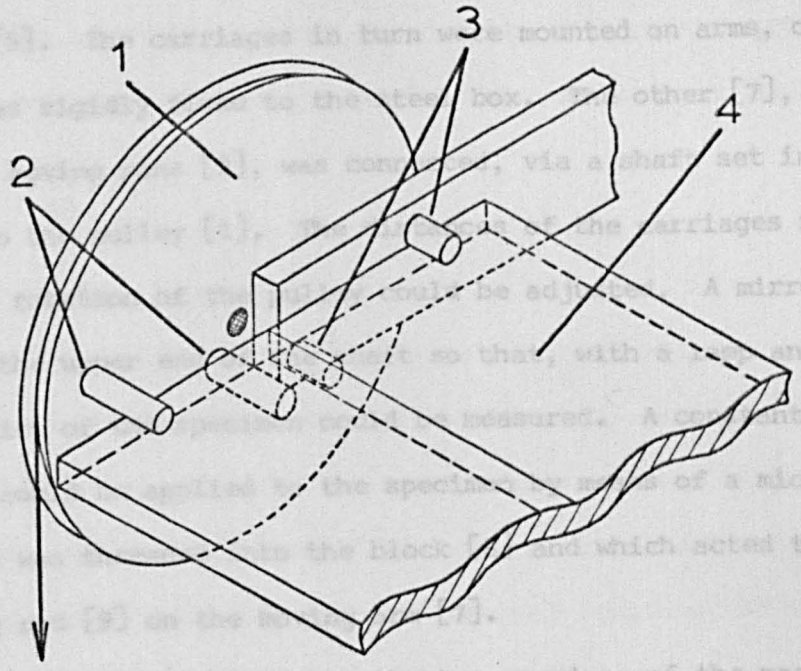

Figure 3.4 Illustration of mode of action of apparatus

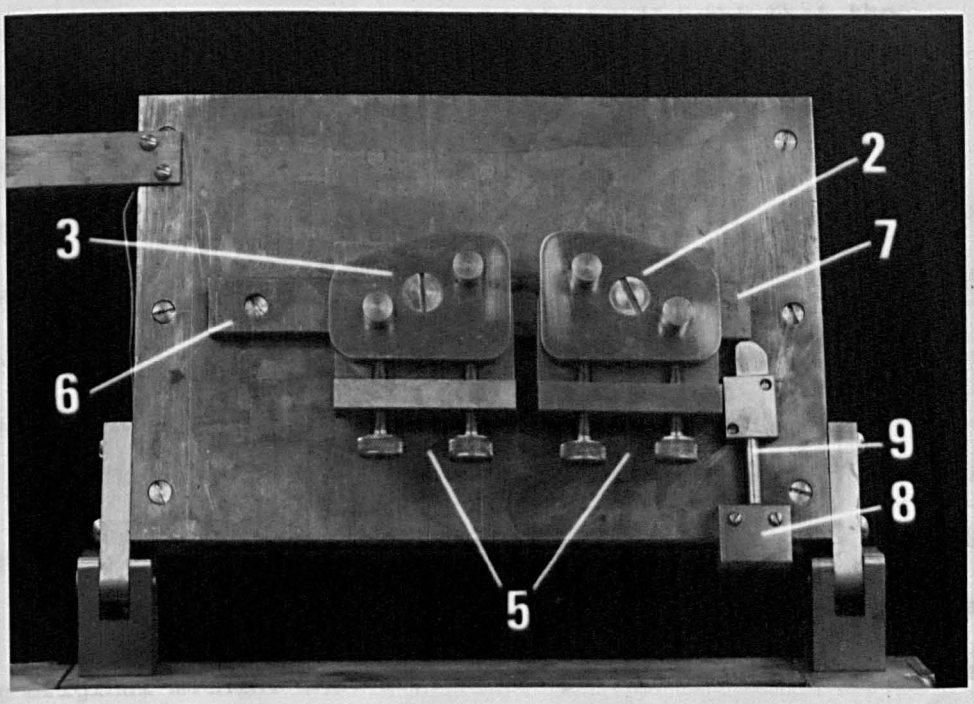

Figure 3.5 View of top of apparatus

pair of pins could each be rotated through small angles by means of the screws [5]. The carriages in turn were mounted on arms, one of which [6] was rigidly fixed to the steel box. The other [7], which carried the moving pins [2], was connected, via a shaft set in roller bearings, to the pulley [1]. The distances of the carriages from the axis of rotation of the pulley could be adjusted. A mirror was mounted on the upper end of the shaft so that, with a lamp and scale, the deflection of the specimen could be measured. A constant deflection could be applied to the specimen by means of a micrometer screw which was threaded into the block [8] and which acted through the sliding rod [9] on the moving arm [7].

The main difference between the two versions of the machine was that the later one was more strongly constructed, with larger sections being used throughout. This was done since satisfactory results were only obtained from the earlier machine when testing 3 mm and 4 mm glass. With 6 mm glass the cracks would always run off to the same side of the specimen under test. Although the problem was not exhaustively analysed, it was thought that the compliance of either the loading pins (whose diameter was 3.2 mm) or some other part of the loading system in the original machine was comparable to that of the 6 mm glass. Excessive deflections in the machine could then produce an asymmetric stress distribution in the specimen. Whether or not this was the case, the problem did not recur in the later machine.

Friction in both machines was approximately 1 per cent of the lowest loads used in the crack propagation tests. This estimate is based on the minimum loads required to cause movement of the pulleys. In the original machine this load was 7 gf (0.069 N) whilst in the

later machine it was 12 gf (0.118 N). The individual weights used in loading were accurate to about 1 per cent, so that the maximum error in G from uncertainties in the load was about 4 per cent.

3.4 Double-Torsion Specimens

Double-torsion specimens were prepared from both 3 mm and 6 mm Float glass and from 32 oz (4 mm approx.) sheet glass. The compositions of these glasses, as quoted by the manufacturer, Messrs. Pilkington Brothers Ltd., are shown in table 3.1. The material was purchased from a local supplier already cut to a nominal length of 30 in (750 mm) and to nominal widths of 5 in (125 mm), 6 in (150 mm), 7 in (175 mm) and 8 in (200 mm).

Table 3.1

Compositions of Float and sheet glass

	Float % weight	Sheet % weight
SiO_2	72.7	72.6
CaO	9.3	8.2
Na_2O	13.0	13.0
MgO	3.1	3.9
Al_2O_3	1.0	1.3
Fe_2O_3	0.1	0.1
K_2O	0.6	0.7
SO_3	0.2	0.2

The main practical problem encountered with the double-torsion technique was that of inducing the crack to remain in the mid-plane

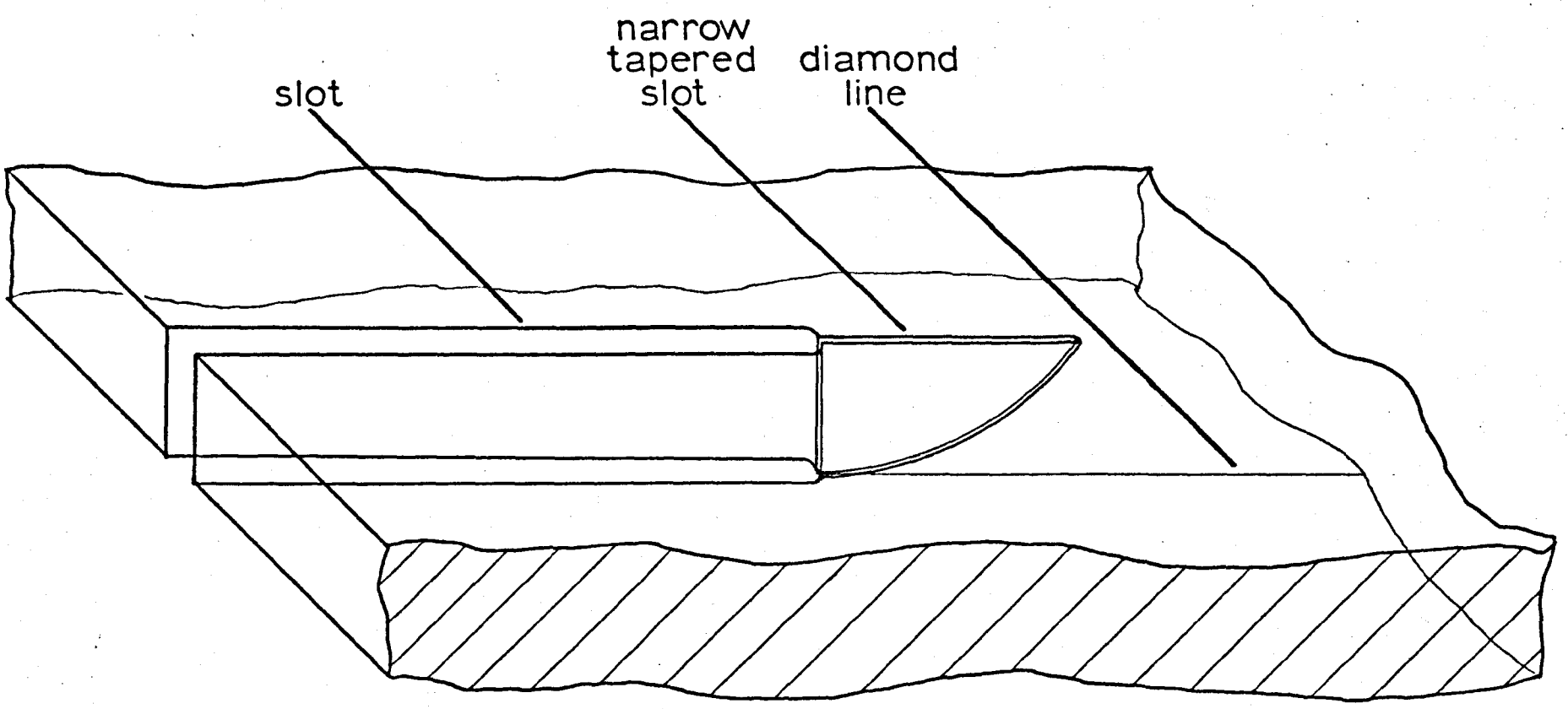

Figure 3.6 Detail of system of slots in prepared specimen

of the specimen during propagation. This required both symmetrical crack initiation and a means of constraining the direction once the crack was initiated. The latter was achieved by scribing a diamond line along the centre-line of one surface of the specimen. Considerable care had to be taken with the scribing operation to avoid generating subsidiary cracks at right-angles to the line of the main diamond fissure (ORD, 1957). Such subsidiary cracks would provide local resistance to crack propagation (COOK and GORDON, 1964) and, if sufficiently severe, could have a serious effect on the test results. After much trial (and much error!) it was found that the most satisfactory method of initiating a crack was from the end of a central slot some 100-150 mm long, which terminated in a narrow, tapered cut running into a previously scribed diamond line (figure 3.6).

To prepare a specimen for test, an as-bought plate was slotted along its centre-line to the required length with a diamond-impregnated wheel. The plate was then annealed in an air oven at 535^{o}C for several hours and cooled to room temperature at approximately 1^{o}C min^{-1}. Preliminary experiments had shown that annealing helped to reduce scatter in the results. After annealing, the diamond line was scribed along the length of the specimen on its centre-line and the narrow taper was cut. The specimen was then inserted in the machine and was aligned symmetrically with respect to the loading pins, (figure 3.7). These in turn had previously been positioned symmetrically about the axis of rotation of the pulley. The pins were then adjusted until they were just in contact with the specimen. The specimen was supported from below by two glass rods cemented to a plate of glass which rested on a dispersed layer of ballotini (figure 3.8). The tray containing the ballotini rested in turn on

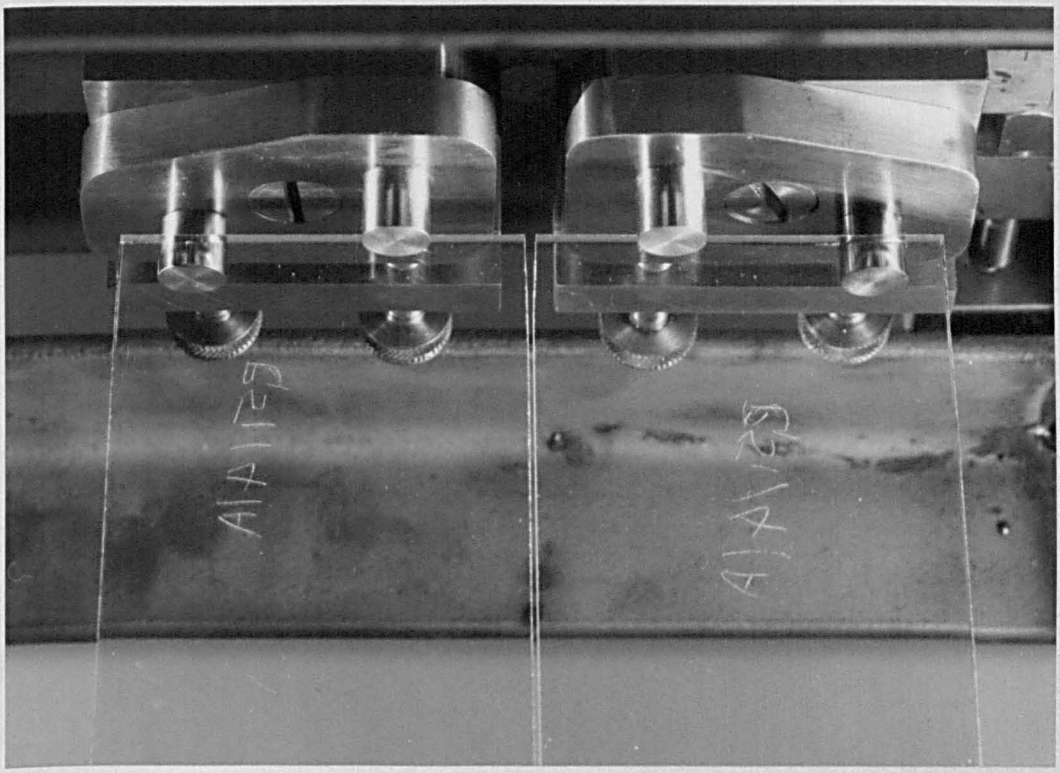

Figure 3.7 Specimen mounted in apparatus, showing loading pins

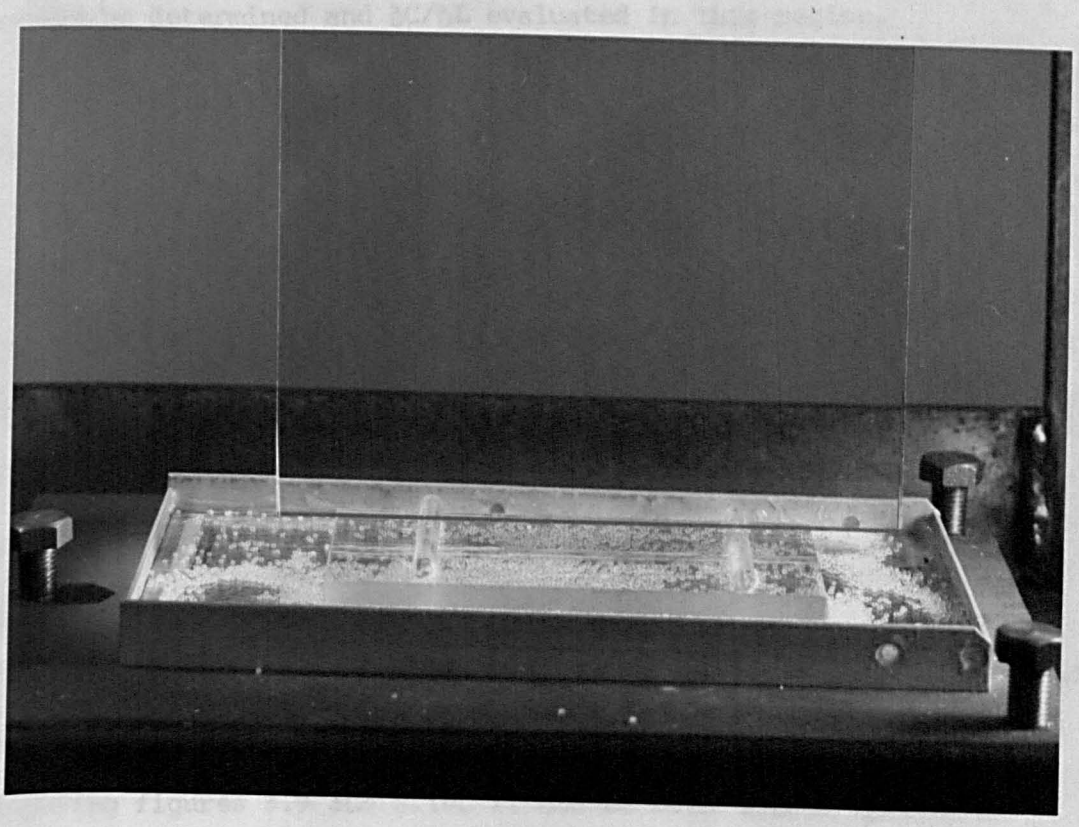

Figure 3.8 Specimen mounted in apparatus, showing ballotini support system

a platform whose height and tilt could be adjusted. A deflection was applied to the specimen by means of the micrometer screw acting on the moving arm of the machine. The deflection was slowly increased until a crack had started and had run about 20 mm along the diamond line into the unnotched glass. The specimen was then ready for test.

3.5 Calibration Measurements

Two methods of calibrating the double-torsion test were used. One was to measure the crack velocity, at constant load, over the whole length of the specimen. From this, the variation of crack driving force with crack length could be ascertained. The other method was to measure the compliance, C, of specimens as a function of crack length, L, so that the region of linear variation of C with L could be determined and $\partial C/\partial L$ evaluated in this region.

The crack velocity measurements were performed on both 6 mm Float and 32 oz sheet glass specimens. The specimens were prepared as described in the previous section and loads were chosen to give crack speeds in the region of 10^{-4} m s^{-1} for convenience of measurement. Figure 3.9 shows the resulting crack velocity vs. crack length characteristics from which it can be seen that the region of constant velocity is of far greater extent in the thinner glass, ranging from 180 mm to 570 mm compared with the 300 mm to 500 mm in the 6 mm glass. The variation of the thickness, b, with crack length of the 32 oz sheet glass specimen is shown in figure 3.10. Being proportional to b^{-4}, G is very sensitive to variations in b. Comparing figures 3.9 and 3.10, it can be seen that a systematic increase in b of about one half per cent leads to a decrease in crack

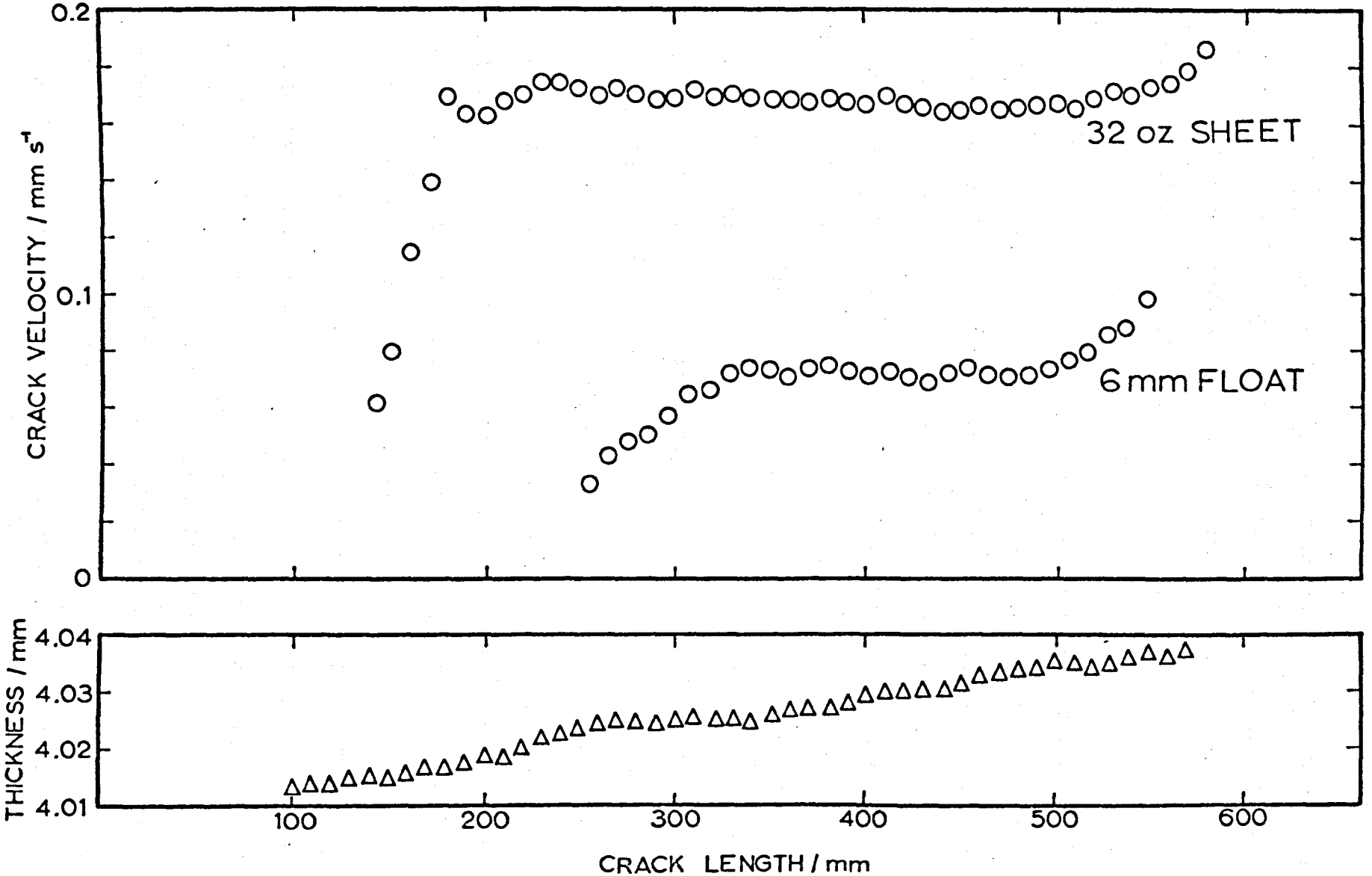

Figure 3.9 Variation of crack velocity with crack length at constant load

Figure 3.10 Variation of thickness with crack length in 32 oz sheet glass

speed of about 5 per cent. In an environment, or in a region where the crack speed was a more rapidly varying function of G_c, changes in the thickness would have a more drastic effect. No such systematic variations in thickness were found with either the 3 mm or the 6 mm Float glass; any random fluctuations in thickness were much smaller.

The compliance calibration measurements performed several functions. The regions of constant $\partial C/\partial L$ could be compared with the regions of constant crack velocity found in the previous tests. The experimental variation of compliance with crack length could be compared with that predicted theoretically. The measurements could be used to check the value of the shear modulus, μ. Finally, by comparing the variation of C with L for slotted and for notched specimens, estimates of the contributions of the effects not included in the simple theory could be made.

Slotted specimens were prepared from 6 mm Float glass and cracked specimens from 6 mm Float glass and from 32 oz sheet glass. The compliances at different values of slot or crack lengths were calculated from measurements of the variation of deflection with applied load. Care had to be taken, when selecting loads for the cracked specimens, to ensure that these did not cause appreciable propagation of the crack. The results are shown in figure 3.11 together with the lines calculated from equation (3.10). The regions of linear variation of compliance with crack length correspond closely to the regions of constant crack speed. The slope, in the linear region, for the slotted specimens is the same as that of the theoretical line for the 6 mm glass, whilst the slope for the cracked specimens is about 10 per cent lower. With the 32 oz sheet glass specimen the

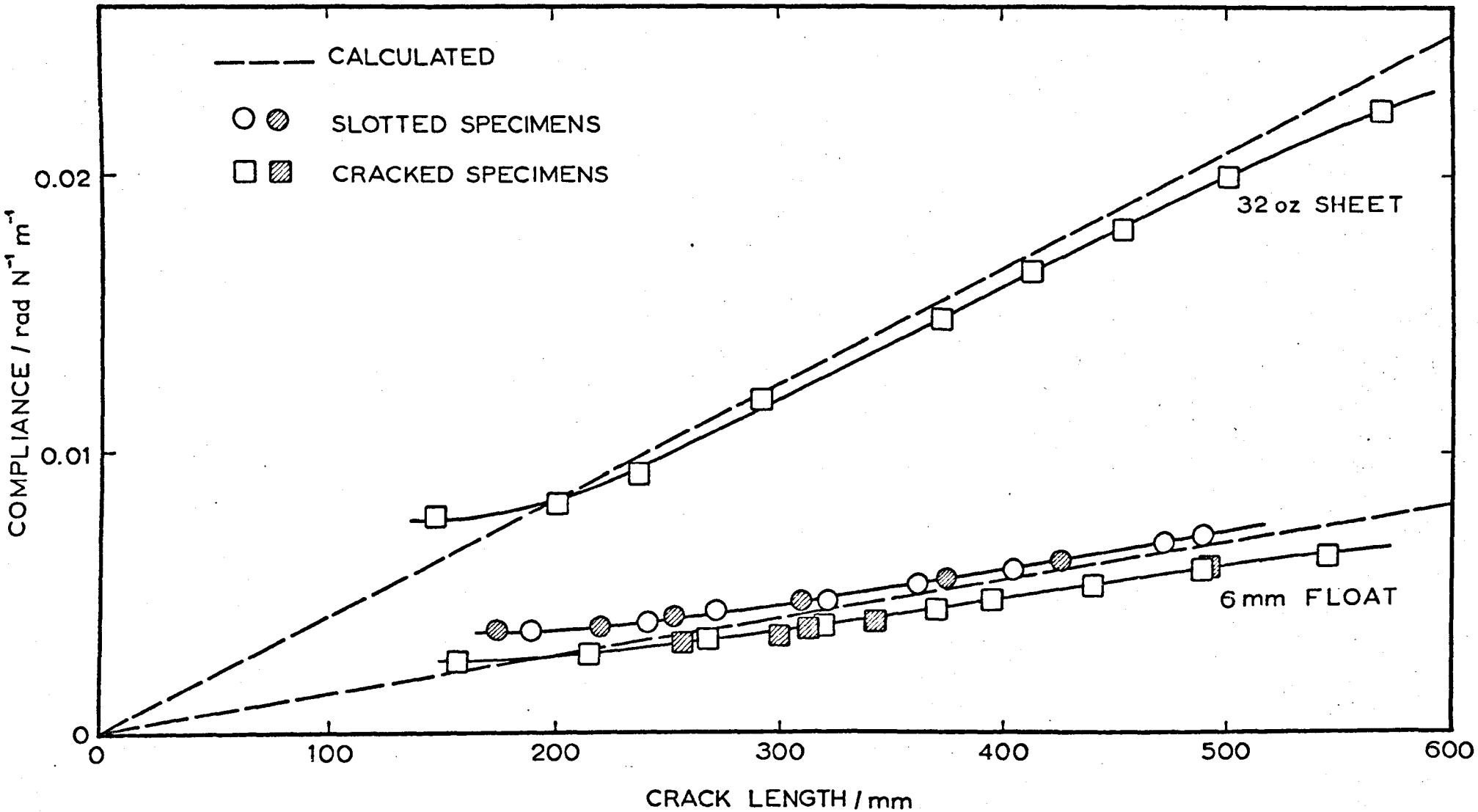

Figure 3.11 Calculated and measured values of compliance as a function of crack length in both slotted and cracked specimens

difference between the slope of the theoretical line and that determined experimentally is about 5 per cent.

As was anticipated, the compliance of a slotted specimen is higher than that of a cracked specimen of the same thickness. Comparing the results for the slotted specimen with the theoretical line, it would appear that the effect of end-rotation is to increase the compliance, as expected, but by a constant amount independent of slot length in the region of constant $\partial C/\partial L$. On the other hand, the results for the cracked specimen indicate that the effect either of end-rotation or of hindered rotation (or a combination of the two) is a function of crack length. If it can be assumed that end-rotation effects are the same in slotted and in cracked specimens, then the difference in slopes between the two sets of results can be ascribed to a crack length dependent hindered rotation effect, the magnitude of which is dependent on the specimen thickness.

The value of shear modulus, μ, used in the calculation of the theoretical line was 29.7 GN m^{-2}. The fact that the theoretical line was parallel to that obtained from the results for the slotted specimen was taken as an added confirmation of this value.

3.6 Determination of Moduli

Two separate experimental determinations of the moduli were made. In the first, Cornu's method (JERRARD and McNEIL, 1960) was used, which gave values of both Young's modulus and Poisson's ratio. In the second, which was performed by B.R. McQuillin in this laboratory, a value of Young's modulus was obtained from measurements in three-point bending.

Cornu's method consists of measuring the radii of transverse and longitudinal curvature of a beam subjected to four-point bending. The radii are calculated from the spacing of interference fringes set up between the upper surface of the beam and a flat glass plate placed on this surface. Poisson's ratio is given by the ratio of the two radii, and Young's modulus is proportional to the longitudinal radius which, in turn, varies with the moment of inertia of the beam and the applied bending moment. In practice, photographs were taken of the fringe pattern for several values of the applied load, and the radii obtained from the photographs were used to calculate average values of Young's modulus, E, and Poisson's ratio, ν. From these, assuming isotropic elasticity, the shear modulus, μ, could be calculated using the relation

$$E = 2\mu(1+\nu) \qquad (3.13)$$

Further values of the moduli were obtained from the manufacturer of the glass and these, together with the experimentally determined values, are shown in table 3.2.

Table 3.2

Values of the moduli

	Cornu's method	three-point bend	manufacturer's data
$E \times 10^{-10}$ N m^{-2}	7.12	7.04	7.59
$\mu \times 10^{-10}$ N m^{-2}	2.97	-	2.97
ν	0.20	-	0.22

No significant difference was found between the 32 oz sheet and the Float glass in the experiments, so the values given in the first column of table 3.2 were used in all the calculations in this thesis.

3.7 Crack Propagation Measurements in Air

The crack propagation measurements in air were conducted with the objective of discovering the pattern of variation of crack speed with G_c, the crack driving force, or K_c, the crack tip stress intensity factor, over as wide a range of crack speeds as possible. The approximate range of crack speeds covered was from 10^{-10} m s^{-1} to 10^{-1} m s^{-1}, the limit at the lower end being set by the length of time necessary to achieve a measurable increase in crack length. At 10^{-10} m s^{-1} a crack takes approximately twelve days to cover a distance of the order of 10^{-4} m, which was the minimum increment of crack length that could be conveniently measured. The higher limit of 10^{-1} m s^{-1} was set by the difficulty of timing fast running cracks with the available equipment.

The distance between the crack tip and the line of the loading points was measured using a cathetometer which was fitted with both a vernier and a micrometer. The latter enabled very small increments of crack length to be measured more accurately than was possible using the vernier alone. For timing at the higher crack propagation rates a Griffin and George 'Centisecond' timer was used, which, as its name implies, could measure times to within one-hundreth of a second. For the lower rates a stop watch or a calender was used.

In addition to the calibration measurements described previously,

some preliminary trials were conducted to see how quickly the system responded to a change of load, and whether the previous loading history affected the crack propagation rate at a given load. No effects, either due to changing the load or due to the previous pattern of loading, could be detected. Accelerations and decelerations of the crack took place over very short periods of time, and there was no apparent overshoot. The same crack speed was obtained at a given load irrespective of whether the previous load was larger or smaller than the given one.

In the experimental measurements, at least six values of crack length, and corresponding times, were measured at each value of load. This was not possible at the highest crack speeds, at which only a single determination could be made in any one specimen of the time taken for the crack to traverse a known distance. The quality of the scribed diamond line, used to guide the crack, was found to affect the crack speed, particularly at the lower end of the speed range. Care was taken, especially at low loads, to measure the crack speeds in regions where there was no visible surface damage associated with the diamond line. Nevertheless, a larger scatter in the measured speeds was always found at the lower speeds.

3.8 Crack Propagation Measurements in Liquid Environments

Four liquids were chosen which, it was hoped, would provide as broad a spread of information as possible on environmental effects on crack propagation rates. The liquids were deionised water, dry liquid paraffin* and dry dimethyl sulphoxide (DMSO)**, all at room

* BDH 29436, wt per ml at 20°C 0.870 - 0.890 g
** BDH 28216, wt per ml at 20°C 1.099 - 1.101 g

temperature, and liquid nitrogen. The liquid nitrogen experiments are described separately in the next section. Deionised water and dry paraffin, as well as air, were used by GUNASEKERA (1970) in this laboratory in a parallel study of the effects of these environments on the time-dependence of the hardness of Float glass.

The three liquids tested at room temperature were contained in metal-framed, glass-lined tanks which were tall enough to cover about 80 per cent of the specimen. The tanks were glazed using a putty based on chalk, linseed oil and zinc soap, so prior to use the inside joints were sealed with epoxy resin (Araldite MY 753/HY 951). The paraffin was dried over sodium wire and fresh pieces of wire were added at regular intervals, and the liquid stirred, in order to minimise the effects of absorption of atmospheric water vapour at the open top of the container. Similar precautions were taken with the DMSO, which was dried over molecular sieve (Union Carbide, Type 4A).

Attempts were made to estimate the water content of the liquid paraffin using both electrical conductivity measurements and infra-red spectroscopy. No water could be detected in paraffin dried over sodium wire with either method. DMSO when pure, crystallises in the range 18° - 19°C, and the presence of only very small amounts of water is sufficient to prevent any crystallisation occurring (DRINKARD and KIVELSON, 1968). Thus, if the DMSO would crystallise in this range it was considered to be dry.

The experimental procedure for the tests in liquids followed that for the tests in air. No difficulty was encountered in locating the crack tip in a specimen immersed in liquid, even though the

refractive index of DMSO, for example, was very close to that of glass. On several occasions it was observed that the crack would apparently leave the liquid environment behind at high crack speeds.

3.9 Experiments in Liquid Nitrogen

A special dewar, which was silvered, apart from two 25 mm wide windows which were diametrically opposite each other and ran down the length of the vessel, was used for the measurements in liquid nitrogen. The dewar had a capacity of some 14 l (1.4×10^{-3} m^3) and was supported in a thermally insulated box. The specimen rested on ballotini, as before, which lay on a platform suspended in the dewar and which was supported on the box. The arrangement is illustrated diagrammatically in figure 3.12.

When cooling the specimen to the temperature of liquid nitrogen, care had to be taken to avoid premature failure. In addition to the straightforward precautions of cooling slowly to prevent the specimen spalling, and of ensuring that there was sufficient clearance between the specimen and the machine to allow for their different thermal contraction rates, it was also found necessary to cool the specimen in a dry environment. This was to prevent the condensing and freezing of atmospheric water vapour in the slot or pre-existing crack, since it was found that sufficient pressure was exerted by the water on freezing to propagate the crack in the cleavage mode. The dry environment was achieved by enclosing the upper half of the specimen in a polyethylene bag which was flushed with nitrogen gas dried over P_2O_5. The addition of a liquid nitrogen cold-trap in the gas line also aided the cooling of the specimen.

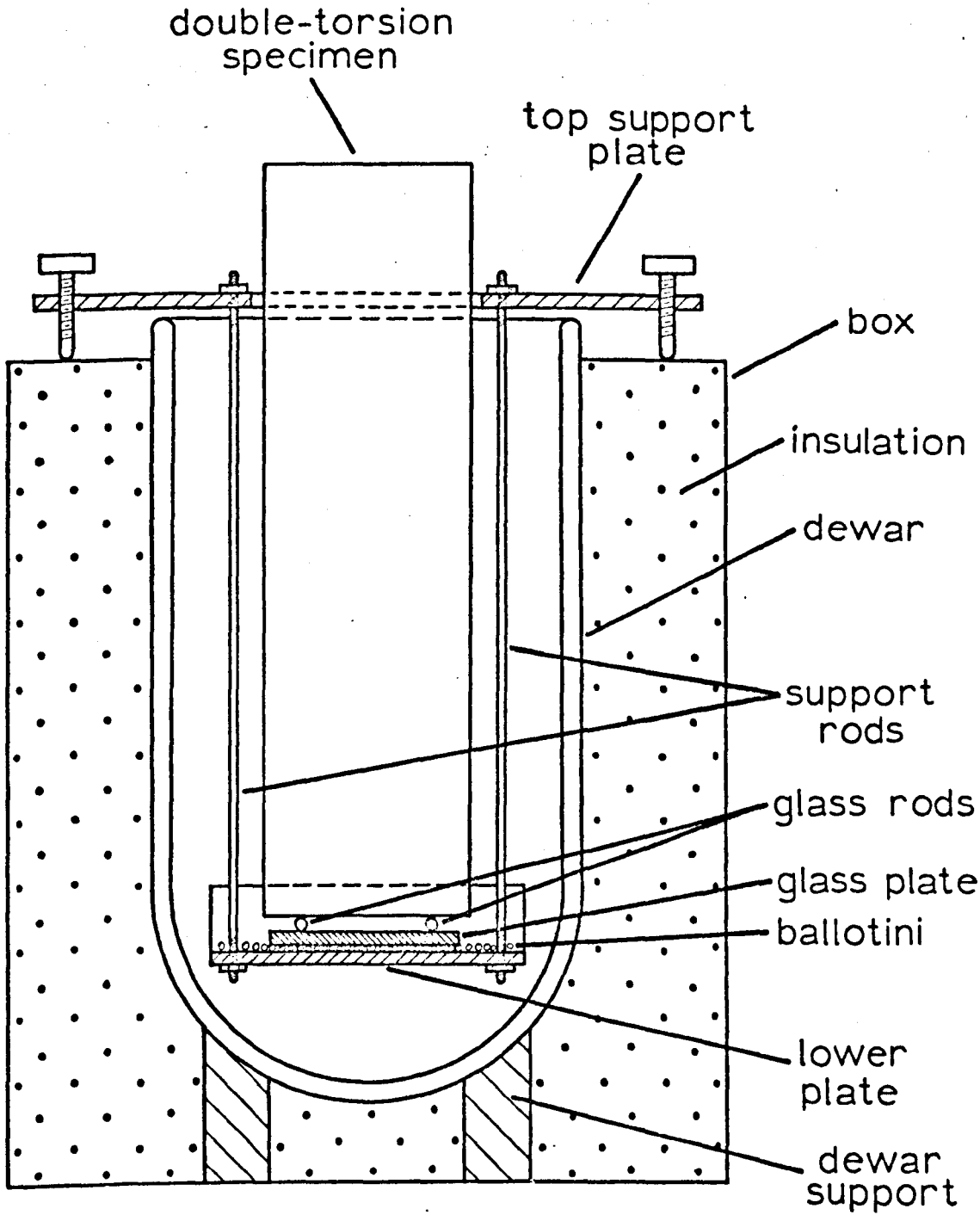

Figure 3.12 Diagram of dewar and specimen support system used for tests in liquid nitrogen

Initially, difficulties were experienced with starting the crack from the slot in liquid nitrogen, or, if precracked specimens were used, with the cracks running out to one side of the specimen as the liquid nitrogen level approached the crack tip when the dewar was being filled. It was eventually found that the highest success rate, in terms of growing a controlled crack in liquid nitrogen, was achieved using a precracked specimen and ensuring that the upper portion of the specimen was cooled to as low a temperature as possible whilst the liquid nitrogen was being added. The success rate was still not very high and only a limited number of measurements was obtained. Readings of deflection were taken in addition to those of load and crack length so that the effect of any variation of the shear modulus with temperature could be eliminated.

CHAPTER 4

RESULTS AND PRELIMINARY ANALYSIS

4.1 Introduction

In this chapter the results of the measurements in the five different environments are presented and are discussed qualitatively. The results of previous investigations into the variation of crack speed with applied stress in glass are reviewed and are compared with the results obtained in this work. All the results are shown in the form of graphs of log (crack speed) versus the strain energy release rate, G_c. The choice of G_c as the fracture mechanics parameter was not made on any fundamental grounds, but rather because it made the comparison of the results of this work with those of other investigators more straightforward.

For the results of this work, G_c was calculated in one of two ways. For tests in which simultaneous measurements of load and deflection were taken, G_c was calculated from

$$G_c = [G_c(f)\, G_c(\theta)]^{\frac{1}{2}} \qquad (4.1)$$

In practice, the applied load, F, was measured, and, for a pulley of radius R

$$FR = f\,m \qquad (4.2)$$

Evaluating equation (4.1) and combining with equation (4.2) leads to

$$G_c = \frac{FR\theta}{2bL} \qquad (4.3)$$

When only the load was measured, G_c was obtained from

$$G_c = G_c(f) - e \qquad (4.4)$$

where $G_c(f)$ was calculated from equation (3.11), substituting FR for fm, and e was the correction factor determined in the compliance calibration tests for the thickness of glass being considered.

4.2 Results in the Different Environments

Figures 4.1 to 4.5 show the results obtained in air, deionised water, dry paraffin, dry DMSO and liquid nitrogen, respectively. For comparison, the line of the air results is shown on the other four plots. The lines drawn through the experimental points are the best fit lines, determined by eye. It is worth noting that the results obtained in air with the final form of the cleavage apparatus were wholly in agreement with those shown in figure 4.1. With the exception of the tests in liquid nitrogen, figure 4.5, all three thicknesses of glass were tested in each of the environments. No systematic variation of crack propagation behaviour with specimen thickness was found.

In the range of crack speeds from 10^{-10} ms^{-1} to 10^{-3} ms^{-1}, each experimental point represents the mean value of at least six consecutive determinations of the crack speed while the crack propagated under constant load. The data were subjected to a small sample statistical analysis to give the mean values, the standard deviations and the 95 per cent confidence intervals for each set of measurements. Typical examples of the 95 per cent confidence intervals are shown in figure 4.1. It can be seen that the uncertainty associated with an experimental point increases with

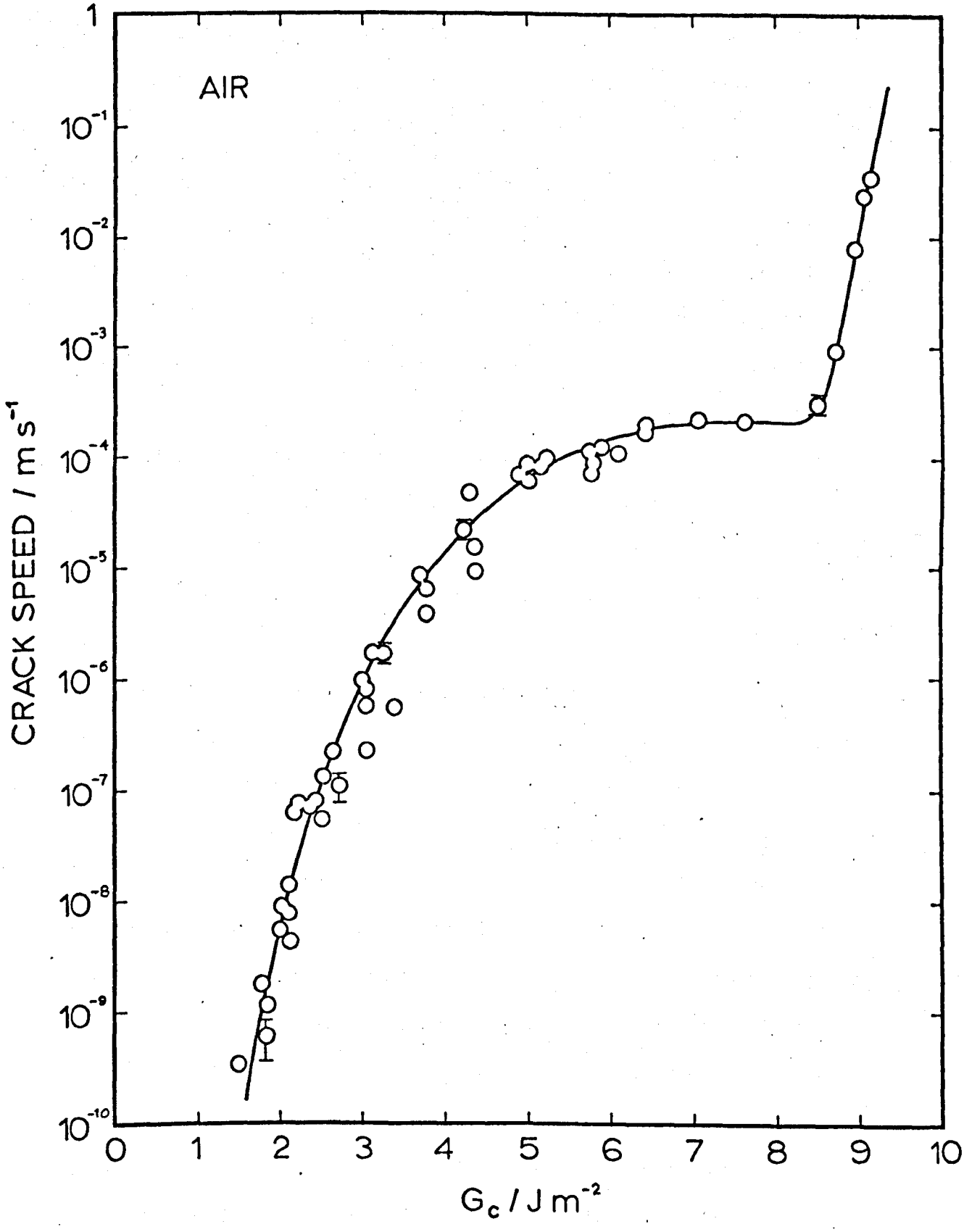

Figure 4.1 Variation of crack speed with G_c in air

decreasing crack speed. This increasing uncertainty was more marked in the air results than in those from other environments, and probably reflected the effect of variations in humidity on measurements which were taken at intervals of several days. The tests in air were performed in the ambient laboratory environment, with no special control of temperature or humidity. The temperature was normally between 20°C and 23°C and the relative humidity was normally in the range between about 50 and 70 per cent. Such a humidity variation would also account for the larger scatter of experimental points obtained in air compared to those from the other environments. As noted in Chapter 3, it was not found possible to perform successive measurements of the crack speed at speeds in excess of about 10^{-2} ms^{-1}. These speeds were determined from single measurements of the time taken for a crack to traverse a predetermined length in a specimen.

At high values of G_c, the results from air, dry paraffin and DMSO appear to lie on the same straight line. Although no such line is apparent in the results from deionised water, some evidence was obtained for its existence at values of G_c in excess of about 9.5 J m^{-2}. An attempt to measure the crack speed in water at a load corresponding to this value of G_c was unsuccessful since the crack speed was too great, implying that there is a sharp increase in the slope of the log (crack speed) versus G_c curve in this region. If the linear dependence of log (crack speed) on G_c at high values of G_c is common to all four room temperature environments, it may be plausibly argued that this represents environment-independent crack growth in glass.*

At the lowest values of G_c, the curve for water (figure 4.2) is falling more steeply and is at a lower value of G_c than that for air (figure 4.1). This suggests that the lowest results in water are

* This is consistent with the environment-independence of G_c at crack-branching found by J.W. Johnson in this laboratory.

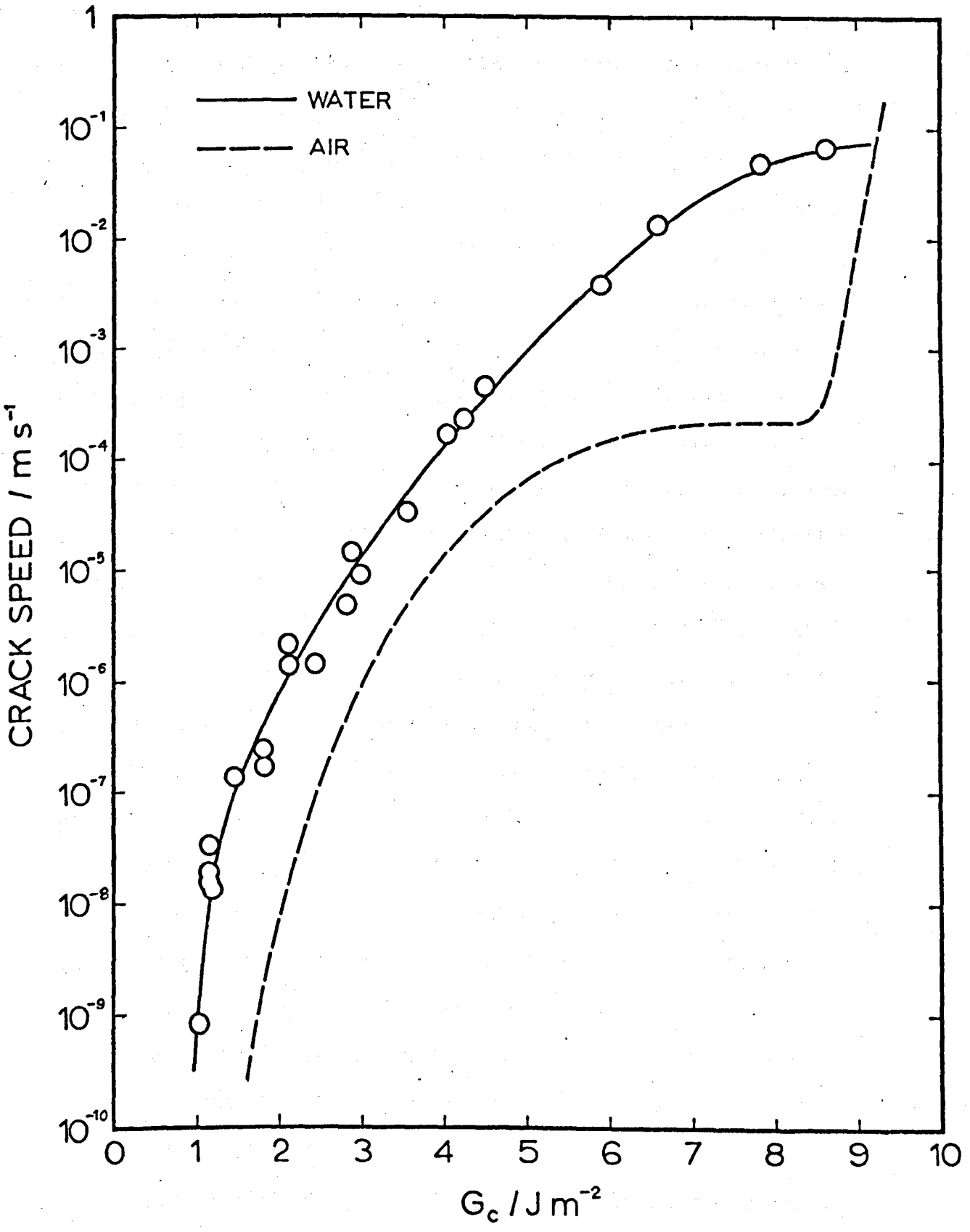

Figure 4.2 Variation of crack speed with G_c in deionised water

closer than those in air to the minimum value of G_c, below which no crack growth would occur. However, it would appear from figures 4.1 and 4.2 that the minimum values in the two environments, towards which the curves are tending, are not very different, and may be estimated to be about 1 J m^{-2}. It is interesting that this is very close to the value which GRIFFITH (1920) used for the surface energy of glass. The static fatigue limit for glass, or the stress below which no failure will occur, irrespective of time under load, is usually taken to be approximately one-third of the instantaneous breaking stress (HOLLAND and TURNER, 1940; MOULD, 1961). From figure 4.1, the value of G_c at which the crack speed becomes a very rapidly increasing function of G_c, is about 9 J m^{-2}. Since G_c is proportional to the square of the applied stress, the ratio of the stress below which no crack growth occurs to the stress at G_c = 9 J m^{-2}, which may be taken to correspond to the instantaneous breaking stress, is in good agreement with that obtained from static fatigue data.

The drastic effect of water on the propagation of cracks in glass can be seen by comparing figure 4.2 with figures 4.1 and 4.3. At all values of G_c for which data were obtained, the crack speed in water is between one and two orders of magnitude higher than it is in air, and is up to six orders of magnitude higher than it is in dry paraffin. The reaction between glass and water is a highly complex one, the details of which are still not well understood. RANA and DOUGLAS (1961) found that, although the initial rate of the reaction varied with the square root of time, their results could not be explained by a simple diffusion-controlled mechanism. The reaction would appear to involve both the exchange of H^+ ions for the alkali or alkaline earth ions in the glass, and the exchange

of OH^- ions for silicate ions formed either by the breakdown of the primary silica network of the glass, or at existing terminations of the network (CHARLES, 1958a; HOLLAND, 1964). Since it is known that the viscosity of vitreous silica at high temperatures decreases markedly with increasing 'water' content (HETHERINGTON and JACK, 1962), it might be expected that rupture of the silica network by the action of water at room temperature would produce a mechanically softer glass. If there is plasticity associated with crack propagation in glass, then the effect of water on the fracture behaviour could be explained in terms of its effect on the flow stress of such a mechanically softened region at the crack tip. This mechanism is explored more fully in a later chapter.

It is uncertain whether the shape of the curve for paraffin (figure 4.3) below a G_c of 7 J m^{-2} represents the genuine environment-independent behaviour of glass, or an interaction between paraffin, or an impurity, and glass, or whether it is due to the effect of residual water in the paraffin. A comparison of figure 4.3 with the results of WIEDERHORN (1967), which are discussed later in this chapter, suggests that, if the 'knee' of figure 4.3 were due to the effect of residual water, then the concentration of water in the paraffin was the equivalent of a relative humidity <u>in air</u> of about 0.01 per cent (approximately 2×10^{-6} mole fraction). In view of the greatly reduced mobility of water molecules in paraffin compared to that in air, the actual concentration of water in paraffin, required to produce such an effect, would have to be very much higher than this. The alternative explanations are difficult to comment on in any detail. The liquid paraffin hydrocarbons are non-polar, and, in general, do not dissolve ionic or covalent solids.

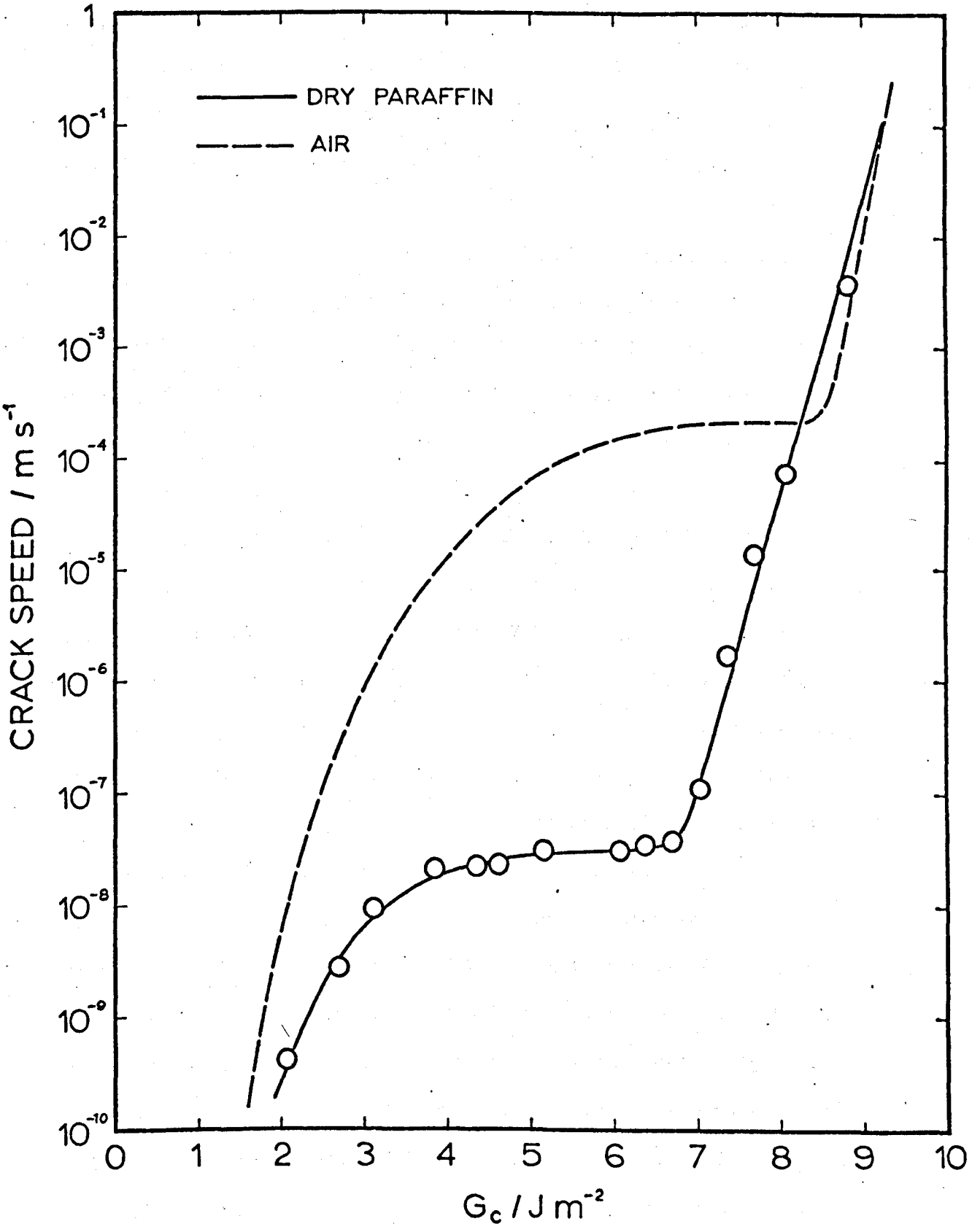

Figure 4.3 Variation of crack speed with G_c in dry liquid paraffin

They are saturated by about 100 ppm of water (approximately 10^{-3} mole fraction). The nature and concentration of any impurities present in the paraffin were not known, but it is thought unlikely that these were significant since the paraffin was a similar grade to that used for medicinal purposes. Although the attempts to measure the water content of the paraffin were not successful, it is estimated that the maximum water content could not have exceeded about 10^{-4} mole fraction (this estimate was kindly corroborated by Messrs. Shaw Moisture Meters, Bradford, Yorks). It is possible that this was a sufficient concentration to cause the observed pattern of results.

As with the liquid paraffin results, it cannot be entirely ruled out that the pattern of variation of crack speed with G_c in DMSO (figure 4.4), for G_c below about 7.5 J m^{-2}, is due to the presence of a small amount of water in the DMSO. However, this seems unlikely. It is thought that water forms a highly associated structure with DMSO (see e.g. PARKER, 1963, 1965) and that the presence of only small amounts of water is sufficient to depress the freezing point significantly. DRINKARD and KIVELSON (1958) found that a mixture of 0.66 mole fraction of water in DMSO would only freeze at the temperature of liquid nitrogen (-196°C). Since the freezing point of the DMSO used in this work remained between 18°C and 19°C, its water content must have been exceedingly low. Some of the tests were carried out with the top of the tank closed with a polyethylene bag, which fitted between the top of the specimen and the loading pins. The bag was flushed with nitrogen gas dried over P_2O_5. No significant difference was detected between the results of these tests and those performed with the tank open to

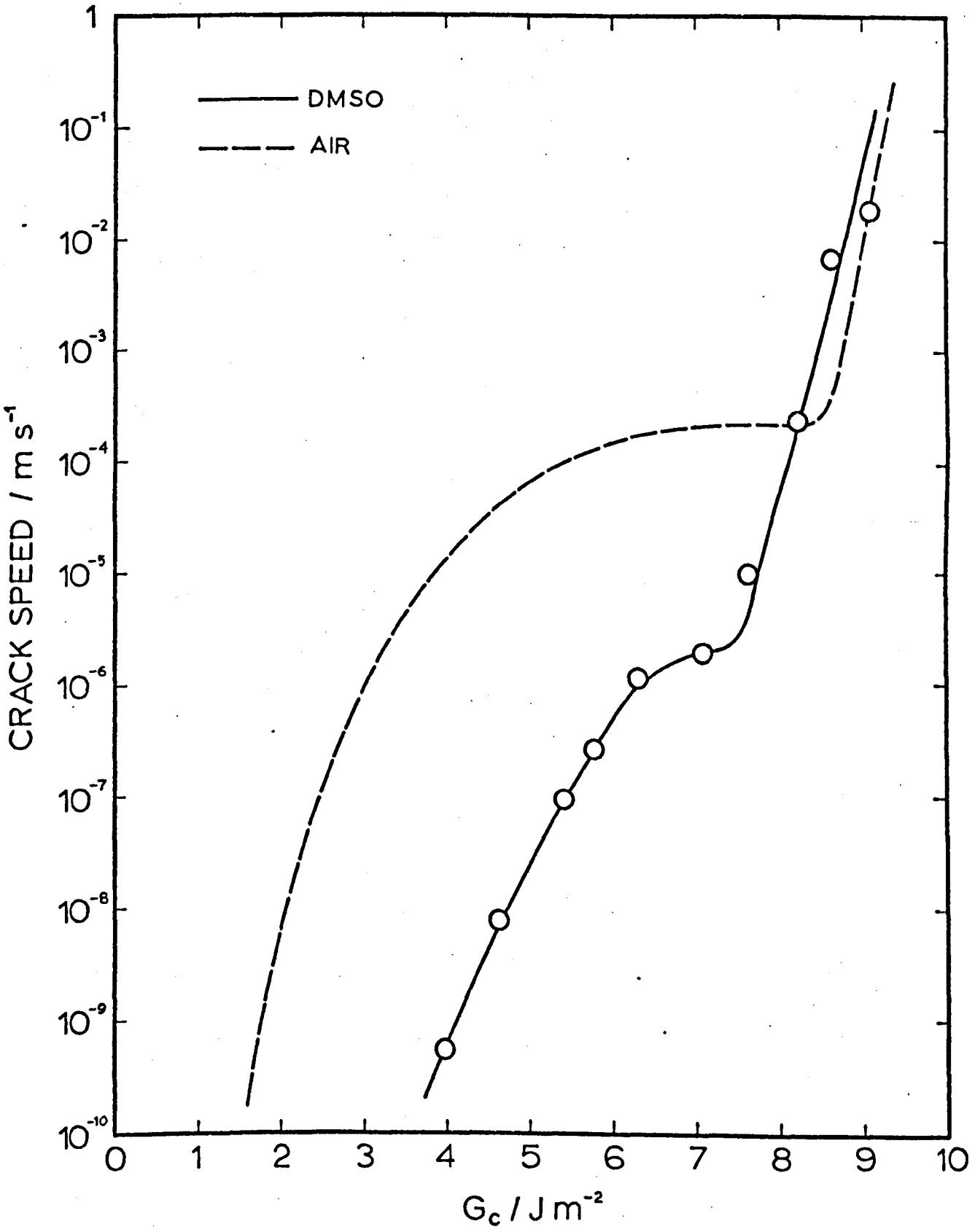

Figure 4.4 Variation of crack speed with G_c in dry dimethyl sulphoxide

the atmosphere. It seems reasonable, therefore, to suppose that the pattern of crack propagation behaviour shown in figure 4.4 reflects a reaction between DMSO and glass at lower crack speeds.

Dimethyl sulphoxide (DMSO) is one of a class of compounds known as dipolar, aprotic solvents. These are solvents with high dipole moments and dielectric constants but, unlike water, although they may contain hydrogen atoms, cannot donate suitable labile hydrogen to form strong hydrogen bonds with an appropriate chemical species (PARKER, 1963). Some of the physical properties of DMSO are compared with those of water in table 4.1, in which the data for DMSO are taken from SCHLÄFER and SCHAFFERNICHT (1960).

Table 4.1

Some physical properties of DMSO and water at 20°C

	DMSO	water
density, kg m^{-3}	1.1×10^{3}	10^{3}
molar volume, m^{3} $mole^{-1}$	0.071	0.018
dipole moment, C m	14.3×10^{-30}	6.12×10^{-30}
dielectric constant	45	80
surface tension, N m^{-1}	0.046	0.072
viscosity, N s m^{-2}	2.47×10^{-3}	1.00×10^{-3}
specific conductance, S m^{-1}	3×10^{3}	7×10^{4}

No reports of a reaction between DMSO and glass have been found in the literature. However, it has been reported that DMSO dissolves epoxy resins (see e.g. PARKER, 1965). In view of the fact that the tank used to contain the DMSO was sealed with epoxy resin over a putty (see 3.8), it is possible that the DMSO became

contaminated with either dissolved epoxide or leached-out constituents of the putty. SMIT and STEIN (1972) found that, in the presence of low concentrations of electrolyte in DMSO, both crystalline and vitreous calcium silicate would dissolve, the vitreous form dissolving to a greater extent. The process was thought to include the dissolution of SiO_4^{4-} groups. The presence of ionic species, leached-out from the putty, in the DMSO used in this work, could mean that a similar solution process occurred.

As noted previously, there were considerable difficulties associated with the measurements of crack propagation rates in liquid nitrogen. Although WIEDERHORN (1966a) observed slow crack growth prior to failure in tension at constant load in this environment, the results shown here (figure 4.5) are the first reported measurements of the dependence on G_c of crack speed in glass in liquid nitrogen. The rate of increase of log (crack speed) with G_c in liquid nitrogen does not differ significantly from those of the environment-independent regions found in air, paraffin and DMSO. The value of G_c at a given crack speed is about 10 per cent higher in liquid nitrogen than in the room temperature environments. This difference, which is probably significant, is qualitatively consistent with the variation of G_c with temperature found by SCHÖNERT, UMHAUER and KLEMM (1969), whose results in vacuo at 23°C and 100°C are shown in figure 4.5. However, the results of this work suggest a much lower temperature dependence of G_c than found by Schönert et al. The fracture energies in liquid nitrogen measured by LINGER (1967) and WIEDERHORN (1969) (see table 1.1) correspond to values of G_c of 8.2 J m^{-2} and 9.2 J m^{-2}. Arguably, neither of these results is inconsistent with the results of this

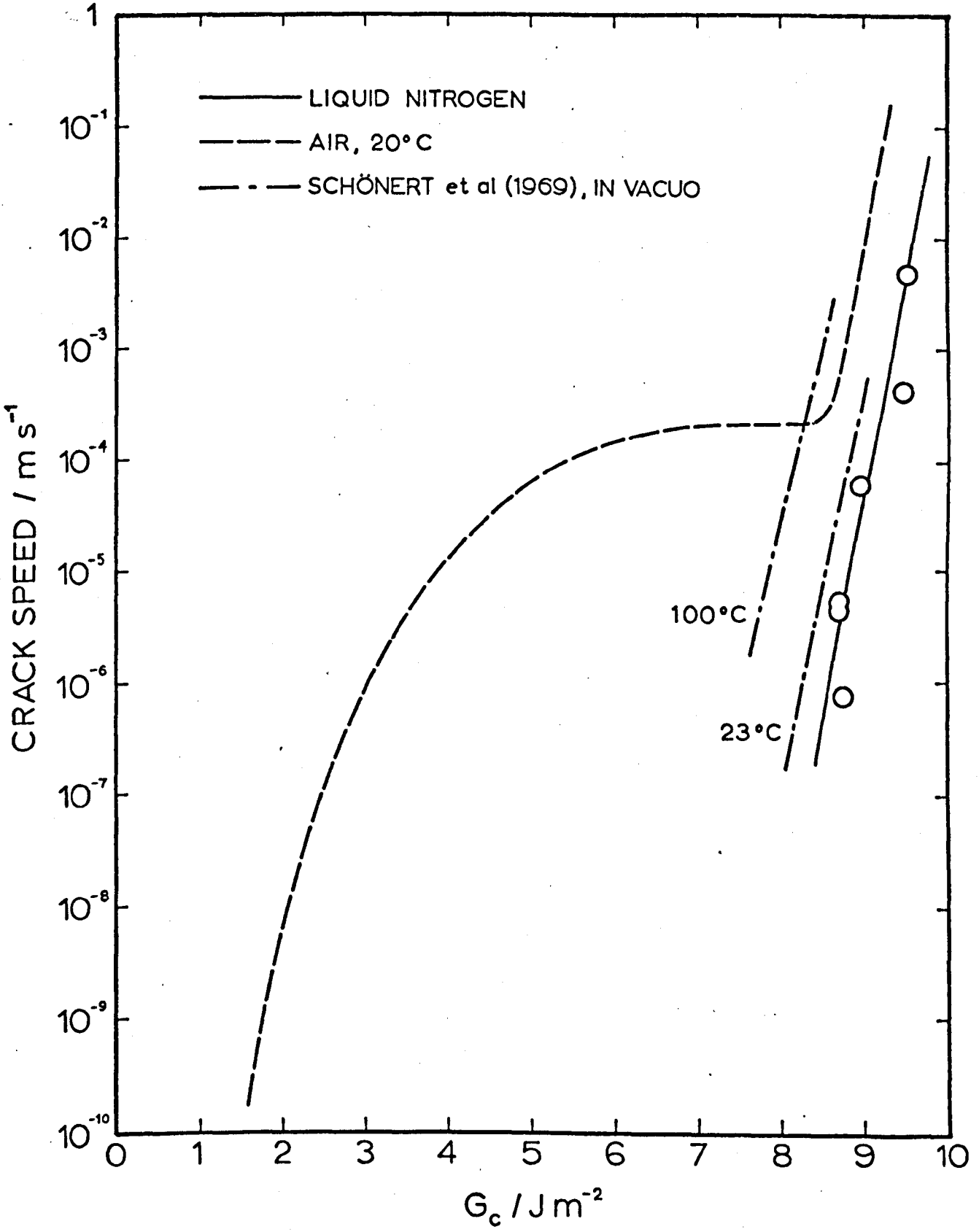

Figure 4.5 Variation of crack speed with G_c in liquid nitrogen

work, the disagreement between them probably arising out of the different loading conditions employed which produced different apparent initiation points of fast fracture. The high rate of increase of log (crack speed) with G_c, both in liquid nitrogen and in the environment-independent regions at room temperature , provides an explanation for the apparent lack of static fatigue under these conditions (e.g. Chapter 1 of this work; BAKER and PRESTON, 1946).

4.3 Previous Work

Certain of the earlier observations of crack growth in glass were discussed at the end of Chapter 1. Discussion of the later work, which contained measurements of the variation of crack speed with some function of applied load, has been left to this chapter so that it may be compared more readily with the experimental results of this thesis.

The earliest measurements were those of OUTWATER and GERRY (1966) and of IRWIN (1966). Novel techniques were used in both of these works, which had in common that a constant G was produced by a constant applied load. Outwater and Gerry introduced the double-torsion configuration which has formed the basis of the bulk of the experimental work of this thesis. They used a method involving direct dead-weight loading of the glass specimen, and calculated G_c from the IRWIN and KIES (1954) expression

$$G_c = \frac{F^2}{2b} \cdot \frac{\partial C}{\partial L} \qquad (4.5)$$

in which $\partial C/\partial L$ was evaluated in a separate compliance calibration experiment. Their experiments were performed in laboratory air and they plotted their results in the form of log (crack speed) vs.

log G_c. IRWIN (1966) modified the tapered cleavage technique introduced by MOSTOVOY and RIPLING (1966) to obtain not only the sensibly constant G with constant applied load characteristic of this configuration, but also crack propagation perpendicular to the line of loading without recourse to side grooves or surface scratches. It was claimed that this was achieved by increasing the angle of the taper to 90° so that the crack propagated along the diagonal of a square, although the direction of crack propagation may have owed more to the proximity of the free end of the specimen than to the angle of the taper. Measurements were taken in dry, wet and normal air environments, although consistent results were only obtained from the tests in normal air.

There have been three more recent investigations. WIEDERHORN (1967, 1971) used the same testing arrangement as he had previously used for his fracture energy measurements on microscope slides (WIEDERHORN, 1969). This involved measuring crack lengths as a function of time in parallel cleavage specimens subjected to a constant load. Measurements were taken at room temperature in nitrogen gas whose relative humidity varied from 0.0017 per cent to 100 per cent. KIES and CLARK (1969) used the identical experimental arrangement to that of OUTWATER and GERRY (1966). They investigated the variation of crack speed with G_c in room temperature air at different relative humidities ranging from 0.2 per cent to 100 per cent. The third of these investigations, that of SCHÖNERT, UMHAUER and KLEMM (1969), has produced the most complete set of results, both in terms of the range of G_c, and of the variety of environments which they covered. They measured crack speeds in microscope slides under constant load in tension at different

temperatures in air, in water and in vacuo.

4.4 Comparison of Results

In figures 4.6, 4.7 and 4.8, the results obtained in this work are compared with the results obtained by the investigators discussed in the previous section. The figures show, respectively, the results in air of approximately 50 per cent relative humidity, in dry or evacuated environments, and in water. It can be seen that, with the exception of the results in water, there are large differences between different people's results.

Considering, first of all, the results in air (figure 4.6); the three sets of measurements in most serious disagreement with those of this work are those of SHAND (1961), OUTWATER and GERRY (1966) and IRWIN (1966). Shand's work was discussed in Chapter 1, where it was shown that the procedure adopted to infer crack speeds from times to failure contained some puzzling inconsistencies. Irwin derived an analytical expression for G_c for the configuration he used, but subsequently found that this was in error by about 15 per cent when compared with the results of a compliance calibration measurement. However, it would require a correction of about double this amount before the slope of Irwin's curve was in reasonable agreement with that of this work. It is possible that the proximity of the free end of the specimen affected his results. The work of Outwater and Gerry cannot be commented on in any detail since the authors do not provide any detail. Both their work and Irwin's were preliminary reports on new techniques, and neither have ever been published in any form other than as internal research reports. This is, perhaps, an added justification for not placing too much

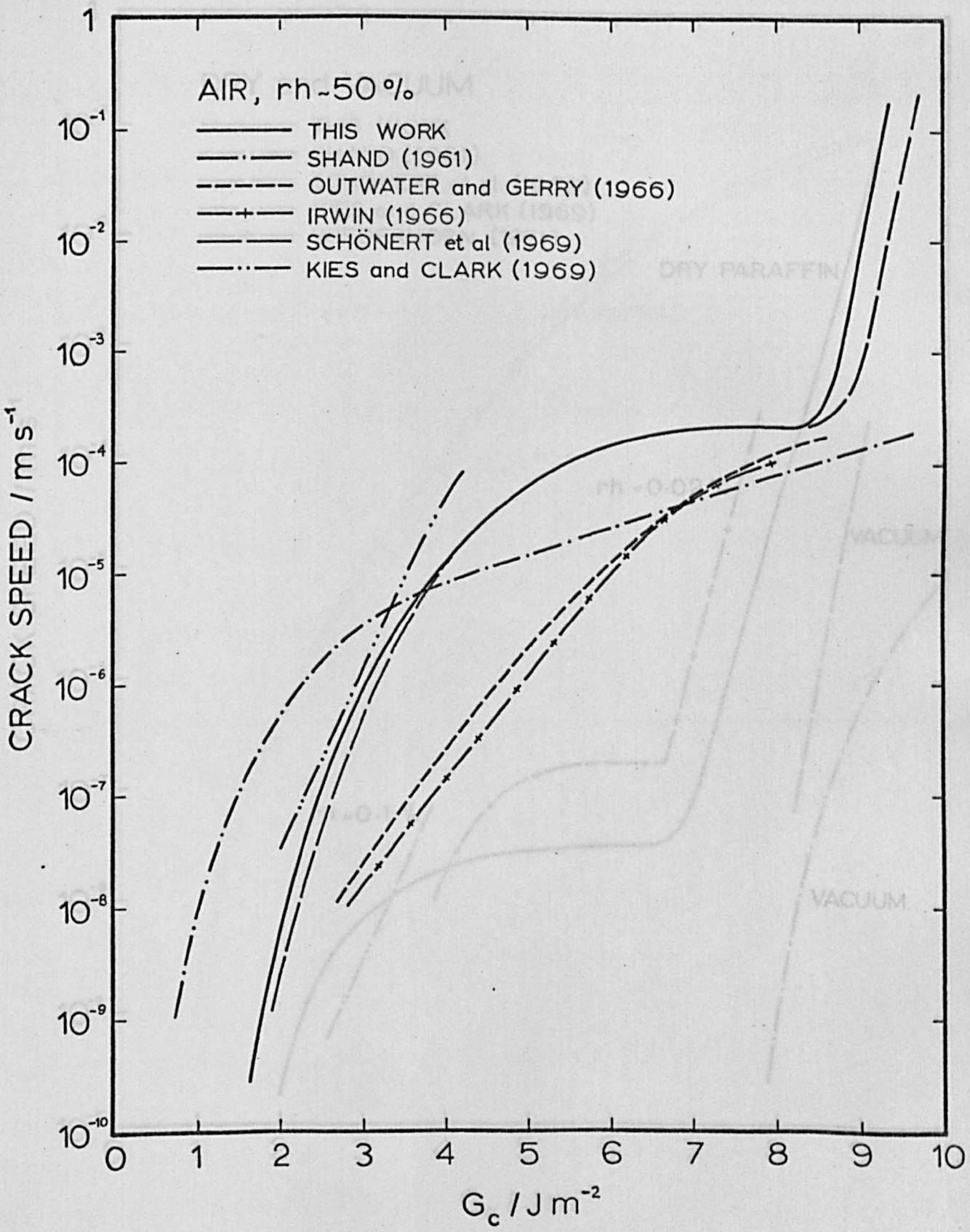

Figure 4.6 Comparison of the results in air of different investigators

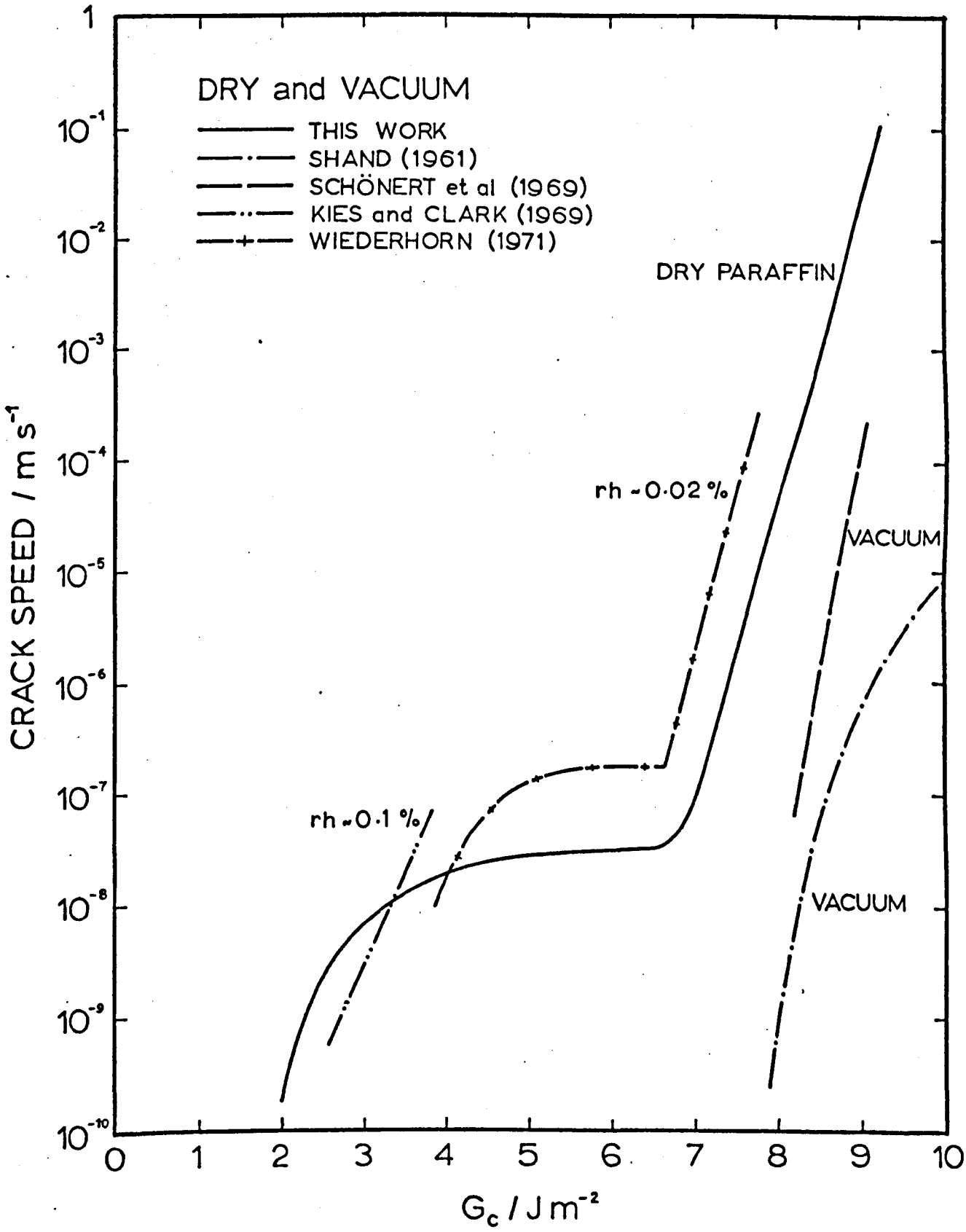

Figure 4.7 Comparison of the results in a dry environment of different investigators

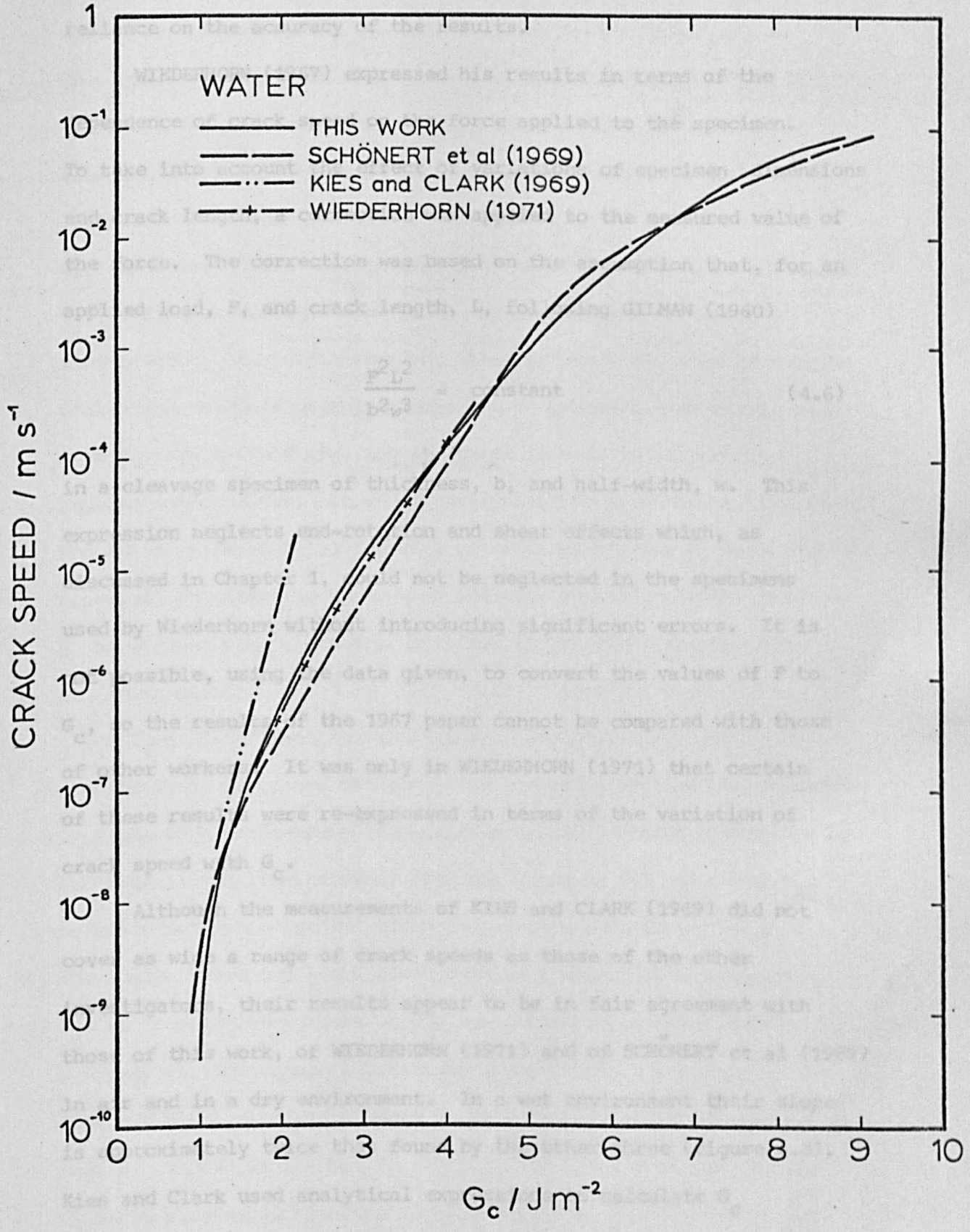

Figure 4.8 Comparison of the results in water of different investigators

reliance on the accuracy of the results.

WIEDERHORN (1967) expressed his results in terms of the dependence of crack speed on the force applied to the specimen. To take into account the effect of variations of specimen dimensions and crack length, a correction was applied to the measured value of the force. The correction was based on the assumption that, for an applied load, F, and crack length, L, following GILMAN (1960)

$$\frac{F^2L^2}{b^2w^3} = \text{constant} \qquad (4.6)$$

in a cleavage specimen of thickness, b, and half-width, w. This expression neglects end-rotation and shear effects which, as discussed in Chapter 1, could not be neglected in the specimens used by Wiederhorn without introducing significant errors. It is not possible, using the data given, to convert the values of F to G_c, so the results of the 1967 paper cannot be compared with those of other workers. It was only in WIEDERHORN (1971) that certain of these results were re-expressed in terms of the variation of crack speed with G_c.

Although the measurements of KIES and CLARK (1969) did not cover as wide a range of crack speeds as those of the other investigators, their results appear to be in fair agreement with those of this work, of WIEDERHORN (1971) and of SCHÖNERT et al (1969) in air and in a dry environment. In a wet environment their slope is approximately twice that found by the other three (figure 4.8). Kies and Clark used analytical expressions to calculate G_c corresponding to equations (3.11) and (3.12) in this work. Apart from omitting the $(1 - 0.63\ ^{b}/_{w})$ correction factor, their equations

differ from equations (3.11) and (3.12) by factors of $^1/_4$ and 4 respectively. This makes the extent of the agreement in figures 4.6 and 4.7 rather surprising. Unlike the results of this work, Kies and Clark found that G_c at a given crack speed in humid air depended on the specimen thickness. In $^1/_8$ in (3 mm) glass G_c was approximately 50 per cent greater than it was in $^1/_4$ in (6 mm) glass.

If the results of work which appears subject to error or inconsistency can be disregarded, there are only two sets of results with which the work of this thesis can be compared. As can be seen from figures 4.6 and 4.8, the agreement is good in air and in aqueous environments. In a dry environment or in a vacuum (figure 4.7), the rates of exponential increase of crack speed with G_c are in close agreement but there is up to a 15 per cent variation in the value of G_c at a given speed. Such a variation is not found for the other two environments.

Both SCHÖNERT et al (1969) and WIEDERHORN (1967, 1971) qualitatively explained the form of the results in humid environments in terms of a change-over from crack propagation being controlled by the rate of reaction between water and glass at low values of G_c, to environment-independent crack propagation at high values of G_c. The region where the crack speed remains constant with increasing G_c, at intermediate values of G_c, was explained as resulting from a transport-limited availability of water at the crack tip. Schönert et al observed changes in the crack front in this transition region. VARNER and FRÉCHETTE (1970, 1971) found that very faint, hitherto undetected fracture surface markings, were either convex or concave to the fracture origin depending on whether the crack was accelerating or decelerating through the transition region.

These markings were formed only in the transition region, and were thought to result from discontinuous propagation of the crack in the interior of the material as sufficient water alternately became available and was then used up. A transition region of this kind might be expected to occur, for a given relative humidity, at different crack speeds depending on the thickness of the specimen and the geometry of the crack. The agreement between the observed constant crack speed regions in this work, which used 3 mm to 6 mm glass loaded in double-torsion, in the work of Schönert et al, who used tensile loading of 0.5 mm microscope slides, and the single result quoted by Varner and Fréchette, who worked with 1 mm and 2 mm glass in tension, does not appear to support the case for a region where crack propagation is controlled by the transport-limited availability of water at the crack tip (the dependence of G_c on specimen thickness found by Kies and Clark was at a lower crack speed than that of the transition region and, in any case, was the inverse of what might be expected from a transport-limited process).

A more detailed examination of the results and possible interpretations are considered in Chapter 6.

CHAPTER 5

APPARENT CRACK HEALING IN GLASS

5.1 Introduction

Earlier in this thesis it has been noted that cracks produced in an ideally brittle material should heal reversibly when unloaded, provided that the freshly fractured surfaces have not been changed by, for example, environmental attack. Glass has often been quoted in the past as almost such an ideal material and, thus, might be expected to exhibit crack healing. However, it now seems certain that some form of inelastic, energy-absorbing process takes place at the tips of cracks in glass, especially in view of the discrepancy between the estimated surface energy and the work required to propagate cracks in glass (MARSH, 1964b; LINGER and HOLLOWAY, 1968; WIEDERHORN, 1969). If this process can be considered to be one of plastic deformation, the plastic displacement can be estimated to be about 5×10^{-10} m and the plastic zone size to be about 10^{-8} m. Plausibly this very limited plastic deformation would only prevent crack healing close to the crack tip. Further away the elastic stress field could bring opposite crack faces sufficiently close together to allow healing to take place. This would not conflict with observations of residual stresses at the roots of unloaded cracks in glass (DALLADAY and TWYMAN, 1921; HOLLAND and TURNER, 1937; MARSH, 1963b). However, as well as environmental action on the fracture surfaces mentioned previously, the presence of debris, or the occurrence of any relative movement of the crack faces in the crack plane would almost certainly prevent a healing process from taking place.

In the next section of this chapter, previously reported observations of apparent crack healing in glass are described. This is followed by an account of some experimental investigations undertaken in the course of this work. The possibility that the observed phenomena could be explained by an interaction between water vapour and cracks in glass, rather than by a genuine healing process, is then examined.

5.2 Previous Observations

In recent years, several investigators have reported apparent crack healing in glass. FINKEL' and KUTKIN (1962a, b) found that cracks propagated in glass plates under static bending loads would disappear when the plates were unloaded. The same cracks could be induced to reopen and close repeatedly by successive loading and unloading. They explained this phenomenon as being due to the relaxing elastic stress field bringing the crack faces closer together than the wavelength of light. FAYET (1969) used double-torsion loading and viewed the crack through crossed polarisers. He observed that the maximum photoelastic stress concentration followed the tip of the reopening and closing crack, implying that the apparently healed region was load-bearing.

LINGER (1967) measured an apparent fracture energy for repropagating a closed crack in a double-cantilever beam specimen in a dry nitrogen environment (< 4% rh). He obtained a consistent value of $\gamma = 0.5$ J m^{-2} ($G_c = 1.0$ J m^{-2}) for a series of constant displacement measurements at different apparent crack lengths. Similar experiments on unbroken glass in the same environment gave

a value for the fracture energy of 3.8 J m^{-2}. WIEDERHORN and TOWNSEND (1970) induced cracks in microscope slides by applying a three-point bending load across one end. The cracks were allowed to close and were then repropagated in dry nitrogen (< 0.04% rh) in the double-cantilever beam configuration. Values obtained for the apparent fracture energy for repropagating the closed crack were 2.3 ± 0.3 J m^{-2} for cracks induced by mechanical shock, and 0.2 ± 0.2 J m^{-2} for cracks induced by slow loading. Both these quoted values and the conclusions drawn by Wiederhorn and Townsend are open to doubt for reasons to be discussed more fully later. Finally, CHEESEMAN and LAWN (1970) found no tendency for cone cracks, formed in glass under a spherical indenter, to heal naturally. They could, however, induce partial healing by subjecting the cracks to either compressive stresses or heat treatment. They suggested that such healing occurs only at localised regions of intimate contact.

5.3 Experimental Observations

Preliminary observations and measurements were performed on the double-torsion specimens of Float and sheet glass used in the investigation of crack propagation which formed the main work of this thesis.

It was noticed that in laboratory air (50-70% rh), the cracks in these specimens tended to close up when the load was removed, but that this did not occur with specimens immersed in water. Once a crack had closed in air it could be induced to reopen and close reversibly by successive application and removal of a very much smaller load than was required to propagate a crack in unbroken glass.

The load required to just reopen a crack corresponded to a value of G_c of 1.2 J m^{-2}, and that to just prevent a crack closing, a G_c of 0.16 J m^{-2}.

An attempt was made to propagate a crack at right-angles to, and across, a closed crack in a Float glass specimen. If successful, this would demonstrate that a substantial degree of healing had taken place. The crack was initiated thermally and then propagated by four-point loading. The sequence of events was as depicted in figure 5.1 (a)-(d). An island opened in the closed crack when the cross-crack was about 2 mm away, the cross-crack ran into this island, and then the remainder of the closed crack opened up. As a test of whether or not genuine crack healing had taken place, the results of this experiment were inconclusive. Unless strength recovery on healing is greater than about 30 per cent it would be expected that this form of crack-stopping mechanism would occur. COOK and GORDON (1964) showed that, if a plane of weakness is present normal to a propagating crack, the crack will preferentially turn into this plane, provided that the cohesion of the interfaces of the plane is less than about 30 per cent of the general strength of the material.

Further experiments were carried out on microscope slides loaded in double-torsion. Cracks were started along diamond lines scribed part way along the centre-line of the specimen and were then propagated until they were well clear of the scribed line. The cracks would close and reopen reversibly beyond the scribed line on unloading and reloading. Examination in a Vickers projection microscope of a slide containing a closed crack failed to reveal any crack line in the surface, even at highest power (~ 600X). However, a line could be seen in such a specimen after it had been immersed

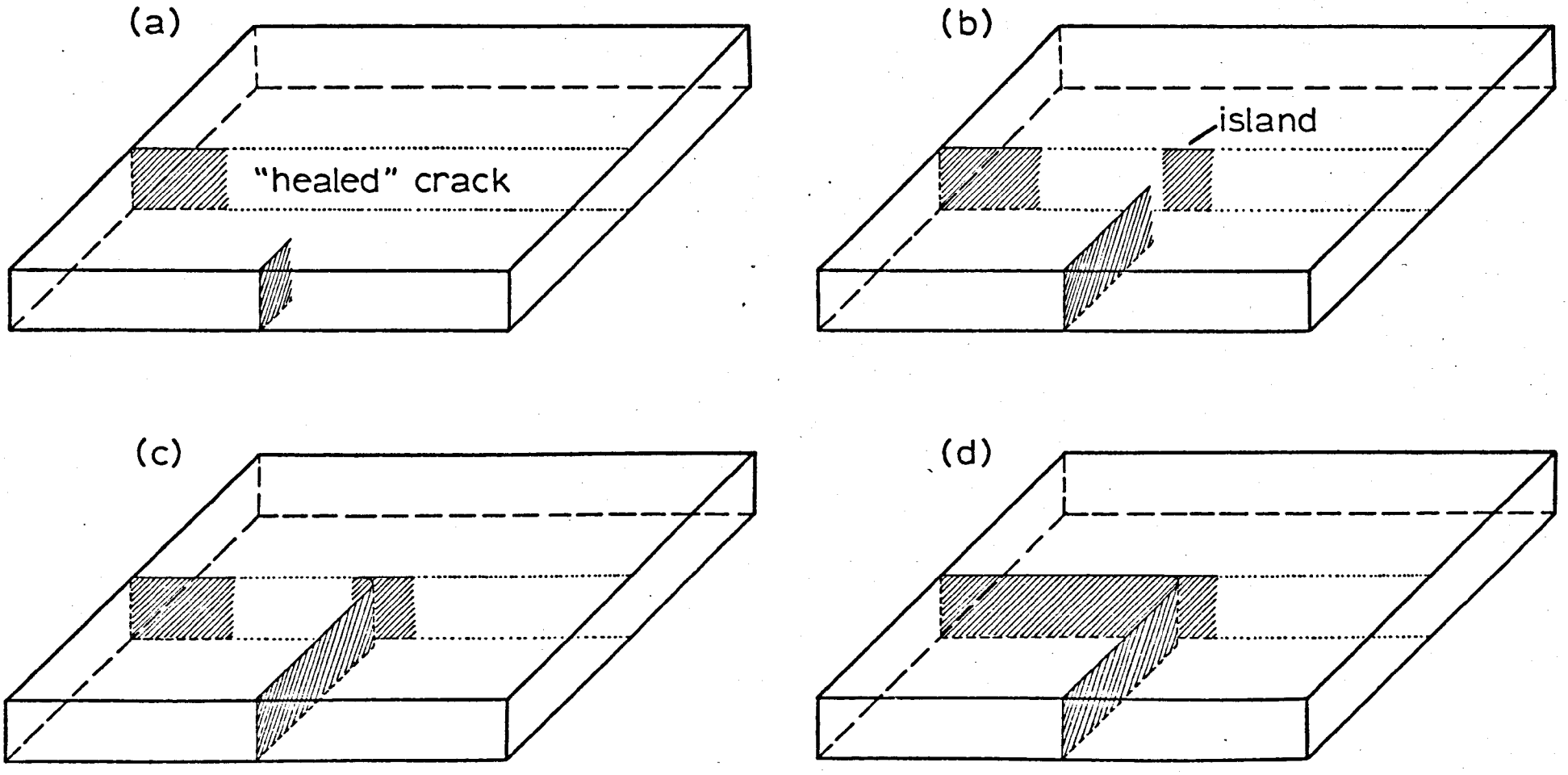

Figure 5.1 (a) - (d) Illustration of sequence of events as a crack propagated at right-angles to the line of a 'healed' crack

in water for less than five seconds. The line became increasingly pronounced with increasing times of immersion, and eventually the crack would become visible to the naked eye. Closed cracks would not reopen on immersion in acetone, nor would they in a vacuum of 10^{-5} torr (1.33×10^{-3} N m^{-2}), even after prolonged periods (three weeks) in vacuo, both at room temperature and at 120°C. Closed cracks, in specimens which had been kept in vacuo for such prolonged periods, would not reopen on immersion in water.

The positions of the opened and closed crack "tips" were marked on specimens containing cracks which had been propagated and allowed to close in air. These specimens were then placed in a vacuum chamber with the cracks held open under load. The chamber was evacuated to 10^{-5} torr and the specimens were unloaded. The cracks were observed to close, but only about half way to their former closed position. When laboratory air at atmospheric pressure was admitted to the chamber, the cracks closed back to the marks which indicated their previous closed positions in air. The cracks remained closed at these marks when the chamber was re-evacuated.

The above experiment was repeated, but with the addition of an extra stage. Instead of unloading the specimens after evacuating the laboratory air, the chamber was first flushed with either dry air or dry argon (both were dried over phosphorus pentoxide, P_2O_5). The dry gas was then pumped out and the specimens were unloaded. The crack were observed to close, but only partially, as in the previous experiment. They remained in this position when dry air, or dry argon, was re-admitted to the chamber. When the dry gas was removed and laboratory air admitted to the chamber, the cracks closed back to the marks, as before. The humidities of the air and argon

were not measured, but MORLEY (1904) quotes a water content of less than 1 mg in 40,000 l, corresponding to a relative humidity of 2×10^{-4} per cent, for air dried over P_2O_5 in this way.

5.4 Discussion

The experimental observations presented in the preceding section show that cracks close more fully in the presence of water vapour than in a vacuum or in a dry gaseous environment. This is the converse of what might be expected from a genuine healing process, since it is known that water reacts with, in particular, the alkali silicate glasses (see e.g. HOLLAND, 1964).

It might be thought that water vapour could not condense in cracks formed in dry environments, such as those used by LINGER (1967) and WIEDERHORN and TOWNSEND (1970). WIEDERHORN (1967) has previously argued that such condensation could not occur in cracks in glass at relative humidities less than 35 per cent. This follows from the substitution of appropriate values into the Kelvin equation (THOMSON, 1871), which relates the vapour pressure, p, over a curved liquid surface to the radius of curvature, r, of the surface. For a liquid of surface tension, s, and molar volume, V, the equation is

$$\ln \left(\frac{p}{p_o}\right) = \frac{2sV}{rRT} \qquad (5.1)$$

where p_o is the vapour pressure of the liquid over a flat surface, R is the gas constant, and T is the absolute temperature. For relative humidities less than 35 per cent equation (5.1) requires meniscus radii comparable to the dimensions of the water molecule for condensation to take place. At this level the problem can no

longer be modelled by a classical liquid. Further, a relative humidity of 99 per cent is needed before condensation of water in a 10^{-7} m gap is predicted, such a gap corresponding to a just sub-visible crack face separation.

Although the Kelvin equation has been verified experimentally for small liquid droplets (LA MER and GRUEN, 1952), increasing doubt has been cast on its validity for small radius, concave surfaces. SHERESHEFSKY and CARTER (1950) found water vapour pressure lowerings between 7 and 80 times greater than predicted by the equation for water in capillaries whose radii ranged from 9×10^{-6} m to 3×10^{-6} m. HORI (1956) reported that the vapour pressure of water between glass plates separated by 1.4×10^{-7} m was effectively equal to zero, in that no evaporation was found in the range of pressure between 10^{-3} and 1 torr (1 torr = 1.33×10^{2} N m^{-2}). The properties of capillary-held water appear to depend on the way in which the capillary material is wetted, and vapour pressure lowerings for water introduced from the vapour phase have been found to be greater than those predicted by the Kelvin equation by factors which ranged from 30 to 500 in capillaries whose diameters ranged from 5×10^{-5} m to 10^{-6} m (EVERETT, HAYNES and McELROY, 1971). In the light of these findings, it becomes plausible to assume that the condensation of water is responsible for the apparent healing of cracks, even at the relative humidity of 0.04 per cent used by WIEDERHORN and TOWNSEND (1970).

There is a further reason to suppose that genuine crack healing did not take place in the work of Wiederhorn and Townsend. The bending stresses used to induce the inital crack in their specimens left a web of unbroken glass along the crack line. This is the same effect as was discussed previously in connection with the double-torsion

specimens. In the subsequent repropagation in cleavage of the "healed" crack this web was fractured. Rib-like markings which appeared on the fracture surface of the web did not carry on into the previously fractured surface (figure 5.2). If a substantial degree of genuine healing had occurred, as implied by the quoted recoveries in strength of up to 80 per cent, then, plausibly, some of these fracture surface markings, which corresponded to positions where the crack was unloaded, would have extended across into the healed region. Wiederhorn and Townsend also found that an initial crack, in general, would not propagate along the centre-line of a specimen. Instead, it curved away from the centre-line towards one side of the specimen. To correct for the effect of this on their measured values of fracture energy, they assumed that a crack, whose tip was a distance x from the centre-line when measurements were taken, was equivalent to one which had run parallel to the centre-line and a distance x from it (figure 5.3). This assumption seems to be of doubtful validity.

Capillary condensation of water in a crack in glass, after initial, partial closure of the crack by the relaxing stress field, would account for the crack closing completely in moist air, but not doing so in a vacuum or in a dry gas, the humidity of which was probably lower than used by previous investigators. Capillary condensation would also account for the closed crack becoming visible on immersion in water since, without an air-water interface there could be no surface tension on the crack faces. It would account for the failure of fracture surface markings on a previously unbroken portion of the crack face to carry over onto the previously broken area. The fact that the load required to just prevent a crack closing corresponds to an apparent fracture energy of very much the same value as the surface energy of water is also consistent with capillary

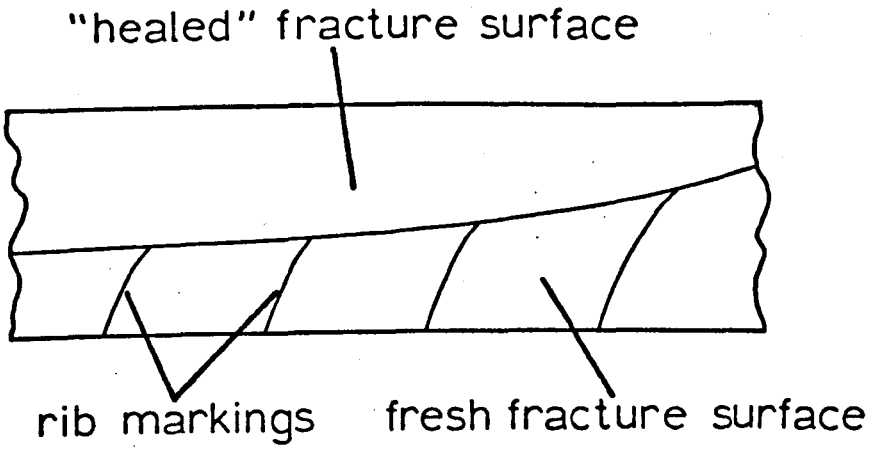

Figure 5.2 Sketch of fracture surface obtained by WIEDERHORN and TOWNSEND (1970)

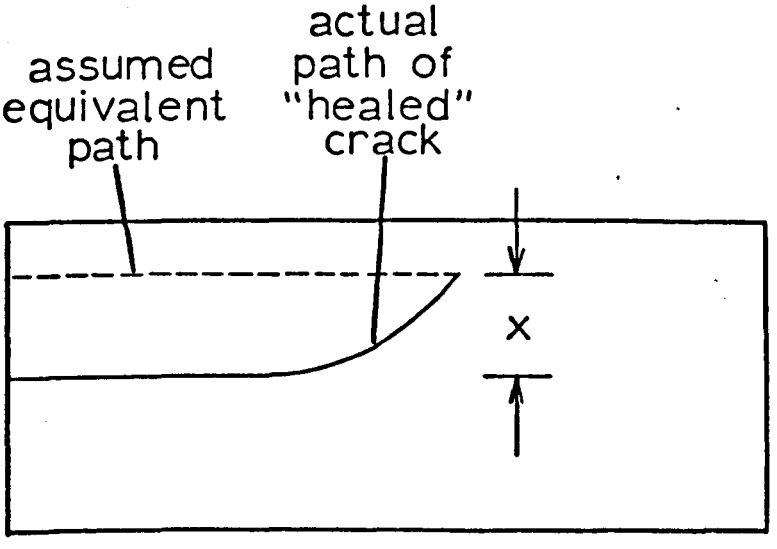

Figure 5.3 Diagram illustrating method of correction for out-of-midplane crack propagation adopted by WIEDERHORN and TOWNSEND (1970)

condensation.

The possibility that genuine crack healing can take place in glass under suitable circumstances cannot, a priori, be ruled out. It is the author's opinion that such healing has not yet been conclusively demonstrated. Although the proposed process of capillary condensation has not provided a complete explanation of the phenomena observed both in this work and in that of other investigators, it is felt that a better account of the known facts is provided by this proposal than by the assumption of crack healing. It is known that water condensed in glass capillaries displays anomalous behaviour (see e.g. HASTED, 1971; EVERETT, HAYNES and McELROY, 1971) and it is to be hoped that elucidation of this behaviour, together with further, detailed work on the apparent healing of cracks in glass, might provide a more complete explanation of the observed phenomena.

CHAPTER 6

A LIMITED PLASTICITY CRITERION FOR FRACTURE

6.1 Introduction

Any complete theory of slow crack propagation in glass must be able to account for the high fracture energies relative to the surface energy, for the dependence of crack speed on environment, in particular the drastic effect of water, and for the environment-independent variation of crack speed with G_c. In this chapter it is hoped to show that a theory based on a limited plasticity fracture criterion, together with a time-dependent flow stress, can, in principle, satisfy these requirements although, in practice, the correlation between theory and experiment is less than perfect.

Before detailing the theoretical approach, other possible sources of energy dissipation are considered, followed by an account of previous attempts to explain slow crack propagation behaviour in glass. The conversion of indentation hardness to flow stress is then discussed and this leads to a consideration of the variation of flow stress with time and an interpretation of the crack propagation results in terms of this and a limited plasticity fracture criterion. The concluding section, both of this chapter and of this thesis, summarises what has been achieved and discusses the need for further work.

6.2 Energy Dissipation in Fracture

As a preliminary to considering possible dissipative processes in the material, dynamic effects need to be examined to see whether

this source could have provided a significant contribution to the increase of G_c with crack speed found in the environment-independent region of crack propagation. The kinetic energy, k_e, of the system is

$$k_e = \tfrac{1}{2}(I + MR^2)\left(\frac{d\theta}{dt}\right)^2 \qquad (6.1)$$

where I is the moment of inertia of the machine plus specimen, M is the load, $d\theta/dt$ is the angular velocity of the pulley of radius R. $d\theta/dt$ may be expressed in terms of the crack speed, v, and crack length, L

$$\frac{d\theta}{dt} = v\frac{d\theta}{dL} \qquad (6.2)$$

By evaluating $d\theta/dL$ from equations (3.3), (3.6) and (3.10), k_e may be written as

$$k_e = \frac{I}{dJ} \cdot \frac{v^2}{v_s^2} \cdot \frac{U}{L} + \tfrac{1}{2}MR^2\left(\frac{d\theta}{dt}\right)^2 \qquad (6.3)$$

where d is the density, J is the polar moment of inertia and U is the strain energy of the specimen, and v_s is the velocity of sound in the material. Substitution of appropriate values into equation (6.3) shows that, even at the highest crack speeds encountered in this work, k_e was less than 0.1 per cent of U, and could, therefore, be neglected in the calculation of G_c.

Possible reasons for the discrepancy between the fracture energy and the surface energy in glass include electrostatic, visco-elastic, and plastic effects. Electrostatic effects, as found in the fracture of mica (OBREIMOFF, 1930), do not seem to play an important part in the fracture of glass since there is no systematic variation

of fracture energy, or of crack speed at a given G_c, with the dielectric constant of the environment. A viscoelastic material is, essentially, one in which the elastic modulus decreases with time under load. Such a material not only has rate-sensitive properties, but also dissipates more strain energy during propagation of a crack than is required to form the new surfaces. BJORKLUND (1948) and HODGDON, STUART and BJORKLUND (1950) used a linear viscoelastic model for glass and the theory of rate processes (GLASSTONE, LAIDLER and EYRING, 1941) in the development of a theoretical explanation of the static fatigue data of GLATHART and PRESTON (1946). Although there was a good correlation between their theory and these results, this was obtained by fitting their spring and dashpot constants to the results, rather than by deriving the constants from viscoelastic data. As far as is known, viscoelastic effects in glass are very small. SCHLAPP (1965), for example, found that the increase in strain was only about 4 per cent of the instantaneous strain in a glass specimen held at 3 per cent strain for 10^6 seconds. It therefore appears unlikely that viscoelastic energy dissipation makes a significant contribution to the fracture energy of glass.

In metals and plastics, limited plasticity in the region of the crack tip is recognised as, in most cases, the dominant energy absorbing process in fracture. In glass, although microplastic effects associated with scratches and indentations are well known, there is no direct evidence of plasticity in tension, either on a macroscopic scale, or at the tips of cracks. Nonetheless, as noted in Chapter 1, MARSH (1963, 1964) showed that the assumption of a limited scale of plasticity accompanying fracture in glass could provide not only an explanation for the high values of fracture energy,

but also, through the variation of the flow stress with time, an explanation of static fatigue.

WIEDERHORN (1969), in his work on fracture energy, thought that plastic deformation at the tip of a crack in glass could account for the high values of fracture energy in water-free environments. In his work on slow crack propagation in glass (WIEDERHORN, 1967, 1971) and its relationship to static fatigue (WIEDERHORN and BOLZ, 1970), however, he interpreted his results in terms of the stress corrosion theory of CHARLES and HILLIG (1961). This interpretation was based on the similarity of the form of the equation which Charles and Hillig derived to one which could be used to describe the stress- and temperature-dependence of crack growth. Also the activation energy he obtained for crack growth was similar to the one which CHARLES (1958a) obtained for the corrosion rate in glass, and which was used by Charles and Hillig. Apart from the criticisms of the Charles and Hillig theory discussed in Chapter 1, this theory cannot account for G_c being higher than the surface energy, even in water. Nor can it account for the dependence of crack speed on G_c in the absence of water, as WIEDERHORN (1967) admits. He explored the possibility of accounting for the crack propagation behaviour under these conditions in terms of a thermal fluctuation theory, such as that put forward by HILLIG (1962), but concluded that far higher stresses were required for crack growth to result from thermal fluctuations than were observed in practice.

SCHÖNERT, UMHAUER and KLEMM (1969) also accepted that the Charles and Hillig theory provided a suitable explanation of their results when water was present. In the absence of water, and in the environment-independent region, they attempted to fit their results

to an equation which GIBBS and CUTLER (1951) derived by the application of the theory of rate processes to bond rupture at the tip of a crack in glass. This fit was based on the similarity in the form of the Gibbs and Cutler equation to an empirical equation which described their results. The Gibbs and Cutler equation used a parameter which was a function of crack length and applied stress and which had the dimensions of energy. Schönert et al assumed that this parameter, whose evaluation depended on detailed knowledge of the atomic bonding energy and its variation with distance and applied stress, could be identified with G_c. Although making this assumption allowed them to calculate an activation energy for crack growth, it also led to a predicted increase in crack length of about 100 bond lengths per ruptured bond. It is difficult to see how this might occur. They concluded that their measurements were insufficiently accurate to check the validity of the modified Gibbs and Cutler equation.

The temperature dependence of crack growth in glass in different environments can equally well be explained in principle by a temperature dependence of plastic flow. As will be seen later, there is insufficient data available to correlate the dependence on temperature of these two processes. It can only be said, therefore, that such an interpretation is consistent with both the crack growth data and the explanation of the fracture of glass in terms of plastic flow.

Plastic work at the tip of a crack would lead to the dissipation of energy as heat, and it is of interest to consider whether such a heating effect could have influenced the results for crack propagation in glass. This problem has been considered by WILLIAMS (1965) and RICE and LEVY (1969). A simple approach is to

argue that for there to be a significant heating effect, the diffusion length, l, of the thermal energy cannot be greater than, say, ten times the plastic zone size in the time, t, that the material in the zone is under load, where

$$l \approx (D\,t)^{\frac{1}{2}} \qquad (6.4)$$

and the thermal diffusivity

$$D = \frac{k}{dc} \qquad (6.5)$$

For glass, the thermal conductivity, $k = 0.72\ W\ m^{-1}\ K^{-1}$, the specific heat, $c = 1.13\ kJ\,kg^{-1}\,K^{-1}$ and the density, $d = 2.5 \times 10^{3}\ kg\ m^{-3}$, thus $D = 2.5 \times 10^{-7}\ m^{2}s^{-1}$. The time, t, can be taken as r_p/v, where r_p is the plastic zone size at fracture and v is the crack speed. Then, putting $l = 10\,r_p \approx 10^{-7}$ m gives a minimum crack speed for significant heating effects of $v \approx 0.25\ m\,s^{-1}$. This is at the upper end of the range of crack speeds measured in this work. By way of comparison, substituting the above values of k, c, d and r_p into the expression derived by WILLIAMS (1965) for a characteristic time for adiabatic heating in a plastic zone

$$t = \frac{dc\,r_p^{2}}{2k} \qquad (6.6)$$

leads to $v \approx 100\,m\,s^{-1}$, which is very much higher than any crack speeds encountered in this work. It therefore seems unlikely that heating effects associated with plastic work can significantly affect crack propagation in glass at crack speeds below $1\,m\,s^{-1}$.

Two attempts, both unsuccessful, were made in the course of this work to obtain some direct evidence for plastic flow at the tips of cracks in glass. The first was an examination of a crack tip in

a very thin specimen of glass by direct transmission electron microscopy. The aim of this was to see whether a plastic extension could be detected and measured. Perhaps not surprisingly, observation was hampered by charging effects in the electron beam, and the crack tip could not be resolved. The second was a search for possible 'shear lips' at the edges of glass fracture surfaces by scanning electron microscopy. Such lips are known to occur in certain metals, and are thought to arise out of the transition from plane strain to plane stress conditions (see Chapter 2). Even at the highest resolution of the microscope (about 0.03 μm), no deviation from a flat fracture surface could be detected in glass specimens. The failure of these attempts does not invalidate the assumption of limited plasticity accompanying fracture in glass. 'Shear lips' are not found in all materials which fail in a brittle manner and, in any case, it can be argued that even if they did exist on glass fracture surfaces, the resolution of the microscope was not high enough for them to be detected since their size would be of the same order as the plastic zone size, or approximately 10^{-8} m.

6.3 Indentation Hardness and Yield Stress

One of the earliest investigations into the indentation hardness of glass using a pyramidal indenter was that of TAYLOR (1949, 1950). He used a Vickers diamond indenter (a square-based pyramid with an included angle of 136°) and found that the hardness, P, defined by

$$P = \frac{2F \sin \theta/2}{\delta^2} \qquad (6.7)$$

was independent of load (F is the applied load, θ is the angle between opposite faces of the indenter and δ is the diagonal length of the indentation). He also found an approximate correspondence between the volume of material displaced by the indentation and that piled-up around the rim of the indentation. AINSWORTH (1954) confirmed the load-independence of P but found that P depended on the time for which the load was applied. Assuming that the indentation resulted from plastic flow, he also attempted to estimate the yield stress, σ_Y, from his results using the relationship observed to hold for the fully work-hardened, softer metals (e.g. TABOR, 1951)

$$P \approx 3\sigma_Y \qquad (6.8)$$

For soda-lime silica glass, equation (6.8) leads to a value of $\sigma_Y \approx 2$ GN m^{-2}, or E/35, which is less than the maximum experimentally determined failure stresses.

DOUGLAS (1958) considered that the deformation mechanism under an indenter in glass was not plastic flow, but cold viscous flow brought about by a reduction in the viscosity of glass under the influence of the high stresses in the vicinity of the indenter. MARSH (1963a, 1964a) pointed out that, whilst this argument was physically reasonable, very much higher stresses than those under an indenter would be required to achieve a sufficient reduction of the viscosity. ERNSBERGER (1968) and NEELY and MACKENZIE (1968) concluded that densification was the primary deformation mechanism in the indenting of glass. Ernsberger obtained quantitative evidence for this in fused silica, the extent of the densified material beneath the indentation, determined by refractive index measurements, corresponding approximately to the volume of material displaced. He

suggested that a similar situation obtained in the soft glasses, such as soda-lime silica, but no quantitative evidence was given to support this. Neither Ernsberger nor Neely and Mackenzie found a piling-up of material around the rim of the indentation such as first reported by TAYLOR (1949) for borosilicate glass and subsequently observed by LINGER (1967) in soda-lime silica glass. Although the experiments of BRIDGMAN and SIMON (1953) and MACKENZIE (1963) showed that densification of glasses occurs under high pressure, they also revealed that such densification is much more marked in vitreous silica than in the metal oxide glasses. In these soft glasses a volume-conserving mode of deformation was shown to dominate. GUNASEKERA (1970) argued that, in view of the lack of detailed information on the flow process in glass, both at atomic and phenomenological levels, there was little point in distinguishing between volume conserving and non-volume conserving flow. Since there is no a priori reason for supposing that there are two separate processes, they should both be regarded as contributions to a permanent deformation which occurs at a critical applied stress, the yield stress.

If indentations in glass are produced by plastic flow, and if the flow stress in this situation is comparable to that under tensile loading (as is the case for metals), then the applicability of equation (6.8) must be suspect since flow stresses calculated with this equation (AINSWORTH, 1954) are much smaller than the maximum experimentally determined breaking stresses. A theoretical basis for equation (6.8) has been provided by consideration of the indentation of a rigid, perfectly plastic solid (HILL, LEE and TUPPER, 1947; LOCKETT, 1963), into which the indenter sinks by cutting and sideward

displacement of the material. However, SAMUELS and MULHEARN (1957) and MULHEARN (1959) showed that, with large angled indenters, the displacement is downward rather than to the side, and that the mode of deformation could be represented by a radial compression. Similar results were obtained by ATKINS and TABOR (1965), who found that the changeover from cutting to radial compression occurred at an indenter angle of about 105° in copper. The change in mode of deformation was attributed to the increasing importance of elastic deformations as the indenter angle increased. MARSH (1963a, 1964a) suggested that materials with high values of σ_Y/E, which remain elastic to large strains, deform in the radial compression mode on indentation, although a third, intermediate mode of deformation was identified by HIRST and HOWSE (1969). The latter occurred when highly elastic materials were indented by acute angled wedges, and was described as a complex elastic-plastic process. It seems unlikely, however, from the results of Hirst and Howse, that this deformation mode applies to glass being indented by a Vickers pyramid.

The radial compression mode of deformation can be likened to the expansion of a spherical cavity under internal pressure in an elastic-plastic material. The solution for P/σ_Y for this situation is given by HILL (1950), and may be written as

$$\frac{P}{\sigma_Y} = \frac{2}{3} + \frac{2}{3} B \ln Z \qquad (6.9)$$

where B and Z are both functions of σ_Y/E and Poisson's ratio, ν. By measuring the compressive yield stress and P for a wide range of fully work-hardened materials, Marsh obtained values of P/σ_Y which could be plotted against $B \ln Z$ (figure 6.1). He found that the results for materials with low σ_Y/E followed equation (6.8), whilst those for

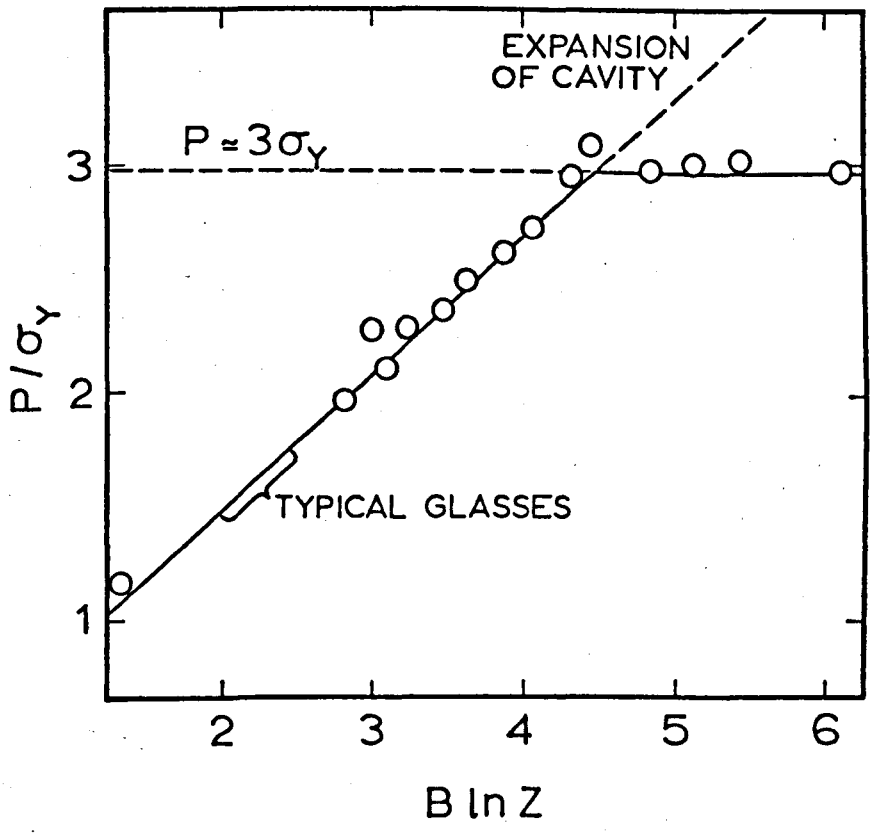

Figure 6.1 P/σ_Y versus B ln Z (after MARSH, 1963a)

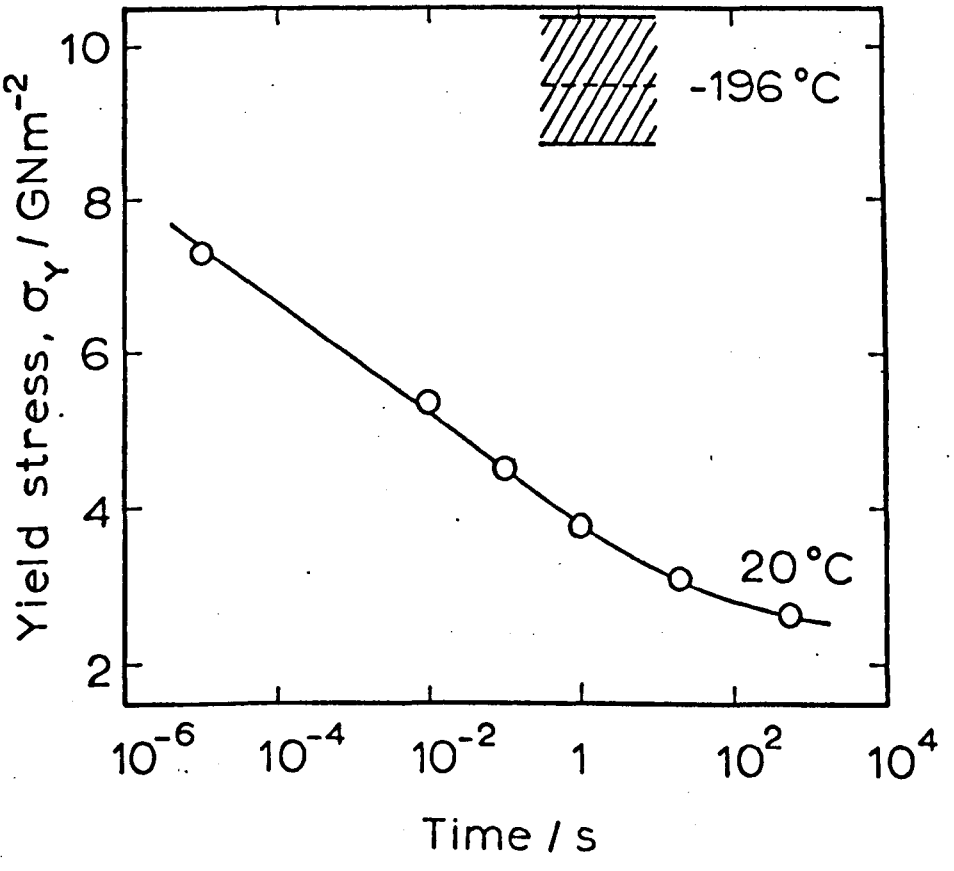

Figure 6.2 Variation of yield stress in air with time (after MARSH, 1964b)

materials with high σ_Y/E could be fitted by a modified form of equation (6.9) in which

$$\frac{P}{\sigma_Y} = 0.28 + 0.60\ B \ln Z \qquad (6.10)$$

Yield stresses calculated from equation (6.10) for a variety of glasses under different conditions were shown to be in good agreement with the tensile failure stresses of flaw-free specimens under similar conditions (MARSH, 1963b, 1964b). Marsh also found that the hardness, and therefore the yield stress, decreased with time under load. His time-dependent yield stress data, obtained in air at 20°C, are shown in figure 6.2. The value of σ_Y at 10^{-5} s has been recalculated from Marsh's result for P at this time since his value of σ_Y does not appear to correspond to that derived from equation (6.10). In liquid nitrogen, Marsh found that the hardness at 0.5 s and 30 s differed by less than 5 per cent, which was his estimated standard deviation of the results. However, at high values of P, σ_Y/E becomes a rapidly increasing function of P/E, and a 5 per cent variation in P produces approximately a 10 per cent variation in σ_Y. Marsh's results in liquid nitrogen are shown in the form of a scatter band in figure 6.2, from which it can be seen that these results neither confirm nor deny the possibility of the yield stress being time-dependent in liquid nitrogen. The values of the yield stress have been calculated using the empirical equation of MALLINDER and PROCTOR (1964) for the decrease in modulus with strain, as discussed in Chapter 1, assuming a strain of 8 per cent under the Vickers indenter.

GUNASEKERA (1970) extended Marsh's work on indentation hardness to include environmental effects. Using much smaller loads than Marsh, he measured the variation of hardness with time of both 'natural'

and freshly cleaved surfaces of Float glass in air, in water and in dry paraffin (all at room temperature). He found that whilst the hardness of the cleaved surfaces was independent of load, that of the 'natural' surfaces increased with load up to a load of about 1.5 kg, after which it equalled the hardness of the cleaved surfaces. Marsh used a load of 3 kg on 'natural' surfaces, and his yield stress results and those of Gunasekera on cleaved surfaces in air are in good agreement, as may be seen in figure 6.3(a). Also shown are Gunasekera's results in water and in dry paraffin. The data used in figures 6.3(a) and 6.3(b) are tabulated in Appendix 1. In figure 6.3(b) the results are replotted in the form of reciprocal yield stress versus ln (time). The lines were calculated by the method of least squares assuming that the short-time and dry paraffin results reflected environment-independent behaviour. Such a linear representation obviously breaks down at both very long and very short times, where the yield stress is expected to reach minimum and maximum values, respectively. In the calculation of the line for water, it was assumed that the two points at the longest times reflected an approach to a minimum value of yield stress, and these were omitted. The value of the slope is decreased by about 10 per cent if they are included in the calculation.

It is recognised that the above assumptions and the selection of the changeover points from environment-independent to environment-dependent behaviour are, to a certain extent, arbitrary. However; it is not proposed that the lines shown in figure 6.3(b) are more than illustrations of the way in which the variation of flow stress with time may be reasonably represented. With only a little more scatter, comparable straight lines may be constructed to represent the data

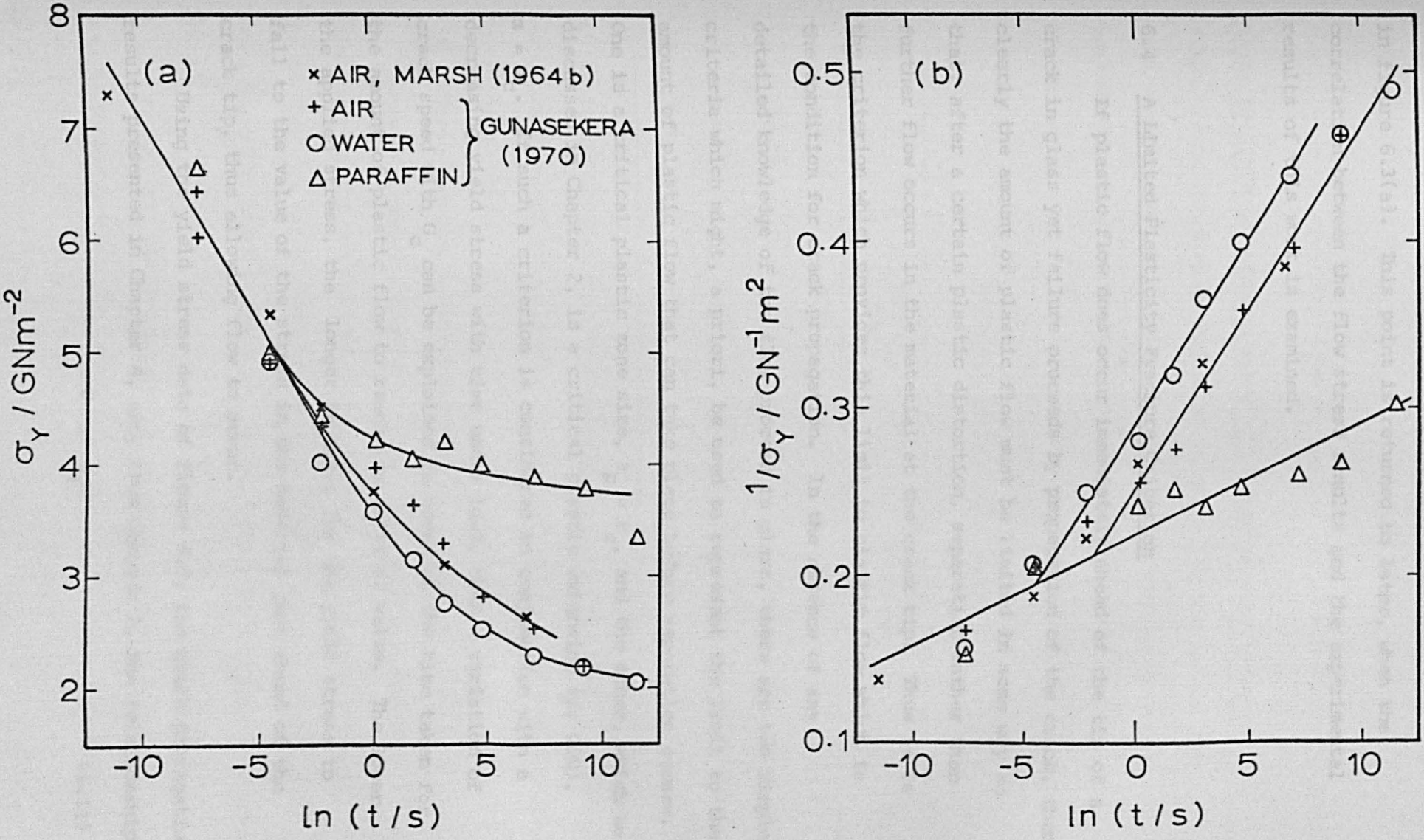

Figure 6.3 Variation of (a) yield stress and (b) reciprocal yield stress in different environments with ln (time) (data from MARSH, 1964b and GUNASEKERA, 1970)

in figure 6.3(a). This point is returned to later, when the correlation between the flow stress results and the experimental results of this work is examined.

6.4 A Limited Plasticity Fracture Criterion

If plastic flow does occur immediately ahead of the tip of a crack in glass yet failure proceeds by propagation of the crack, then clearly the amount of plastic flow must be limited in some way so that, after a certain plastic distortion, separation rather than further flow occurs in the material at the crack tip. Thus it is the criterion which provides this limit to plastic flow which is the condition for crack propagation. In the absence of any detailed knowledge of the flow process in glass, there are two simple criteria which might, a priori, be used to represent the limit to the amount of plastic flow that can take place before separation occurs. One is a critical plastic zone size, $r_p = r_c$, and the other, which was discussed in Chapter 2, is a critical plastic extension (or COD), $\alpha = \alpha_c$. If such a criterion is considered in conjunction with a decreasing yield stress with time under load, then a variation of crack speed with G_c can be explained in terms of the time taken for the amount of plastic flow to reach its critical value. The lower the applied stress, the longer it takes for the yield stress to fall to the value of the stress in the material just ahead of the crack tip, thus allowing flow to occur.

Using the yield stress data of figure 6.3, the crack propagation results presented in Chapter 4, and, from Chapter 2, the relationships

$$G = \sigma_Y \alpha \qquad (6.11)$$

and

$$r_p = \frac{EG}{2\pi\sigma_Y^2} \qquad (6.12)$$

it is possible to estimate α and r_p at four corresponding points. These are at the minimum values of σ_Y and G_c in wet and in dry environments, and at the points of transition from environment-dependent to environment-independent behaviour in air and in water. The values of α and r_p at these points are shown in table 6.1 from

Table 6.1 Values of α and r_p

	dry $t \to \infty$	wet $t \to \infty$	wet → dry	air → dry
σ_Y /GN m^{-2}	3.5	2.0	5.3	4.8
G_c /J m^{-2}	5.0	1.0	9.5	8.4
α /n m	1.5	0.5	1.8	1.7
r_p /n m	4.0	3.6	3.8	4.0

which it can be seen that r_p remains essentially constant and appears to be independent of environment whilst α (wet) is approximately one-third of α (dry).

These results, whilst consistent with either $r_p = r_c$ or $\alpha = \alpha_c$ (α_c being environment-dependent), cannot be said to establish conclusively the validity of either of these as fracture criteria. To do this the correlation between the time-dependence of the yield stress and the crack propagation results needs to be examined in more detail.

By adopting different starting hypotheses, a variety of relationships between the crack speed, v, and either G_c and α_c or

K_c and r_c can be derived. To illustrate the derivation it will be assumed that $\alpha = \alpha_c$ is the fracture criterion, that

$$v = \frac{\delta r_p}{\delta t} \tag{6.13}$$

and that the variation of yield stress with time can be represented by

$$\frac{1}{\sigma_Y} = A \ln B t \tag{6.14}$$

where A and B are constants. If it is further assumed that the time scale for plastic flow at the tip of a crack is identical to that for plastic flow under an indenter then, if $t = t_c$ when α reaches α_c, from equations (6.11) and (6.14), t_c is given by

$$t_c = \exp \{ \frac{\alpha_c}{AG_c} - \ln B \} \tag{6.15}$$

Differentiating equation (6.12) with respect to t,

$$v = \frac{EG_c}{\pi \sigma_Y} \cdot \frac{\delta}{\delta t} (\frac{1}{\sigma_Y})$$

$$= \frac{E\alpha_c}{\pi} \cdot \frac{A}{t_c} \tag{6.16}$$

Thus, from equations (6.15) and (6.16)

$$\ln v = \ln (\frac{EA\alpha_c}{\pi}) + \ln B - \frac{\alpha_c}{AG_c} \tag{6.17}$$

If, instead, $r_p = r_c$ is taken as the fracture criterion, an equation is obtained of the form

$$\ln v = (\text{constant}) - \frac{(2\pi r_c)^{\frac{1}{2}}}{AK_c} \tag{6.18}$$

By representing the variation of yield stress with time by

$$\sigma_Y = C \ln D t \tag{6.19}$$

instead of by equation (6.14), the equations for $\alpha = \alpha_c$ and $r_p = r_c$ become

$$\ln v = (\text{constant}) + \frac{G_c}{C\alpha_c} \qquad (6.20)$$

and

$$\ln v = (\text{constant}) + \frac{K_c}{C(2\pi r_c)^{\frac{1}{2}}} \qquad (6.21)$$

respectively. Other starting hypotheses are possible, for instance that

$$v = \frac{r_p(c)}{t_c} \qquad (6.22)$$

where $r_p = r_p(c)$ when $t = t_c$, but generally these do not affect the slope terms in the above equations for $\ln v$, although the intercepts change. Thus there are four possible parameters with which $\ln v$ might vary linearly, namely G_c, K_c, G_c^{-1} and K_c^{-1}, depending on which fracture criterion and which yield stress equation is applied.

In figures 6.4 to 6.7 the experimental results of this work in air, water and paraffin are shown plotted in these four forms (the data are tabulated in Appendix 2). In addition to the environment-independent lines, regions of linear behaviour can be found for all three environments in each of the figures. As with the flow stress results, the selection of the experimental points to be included in a linear region is, to a certain extent, arbitrary. For example, in figures 6.6 and 6.7, the dashed lines are the least squares lines through all the points in paraffin and in water, whilst the continuous lines are the least squares lines in the selected linear regions.

Calculated values of α_c and r_c from the slopes of the lines in figures 6.4 to 6.7, using the above equations for $\ln v$ and the

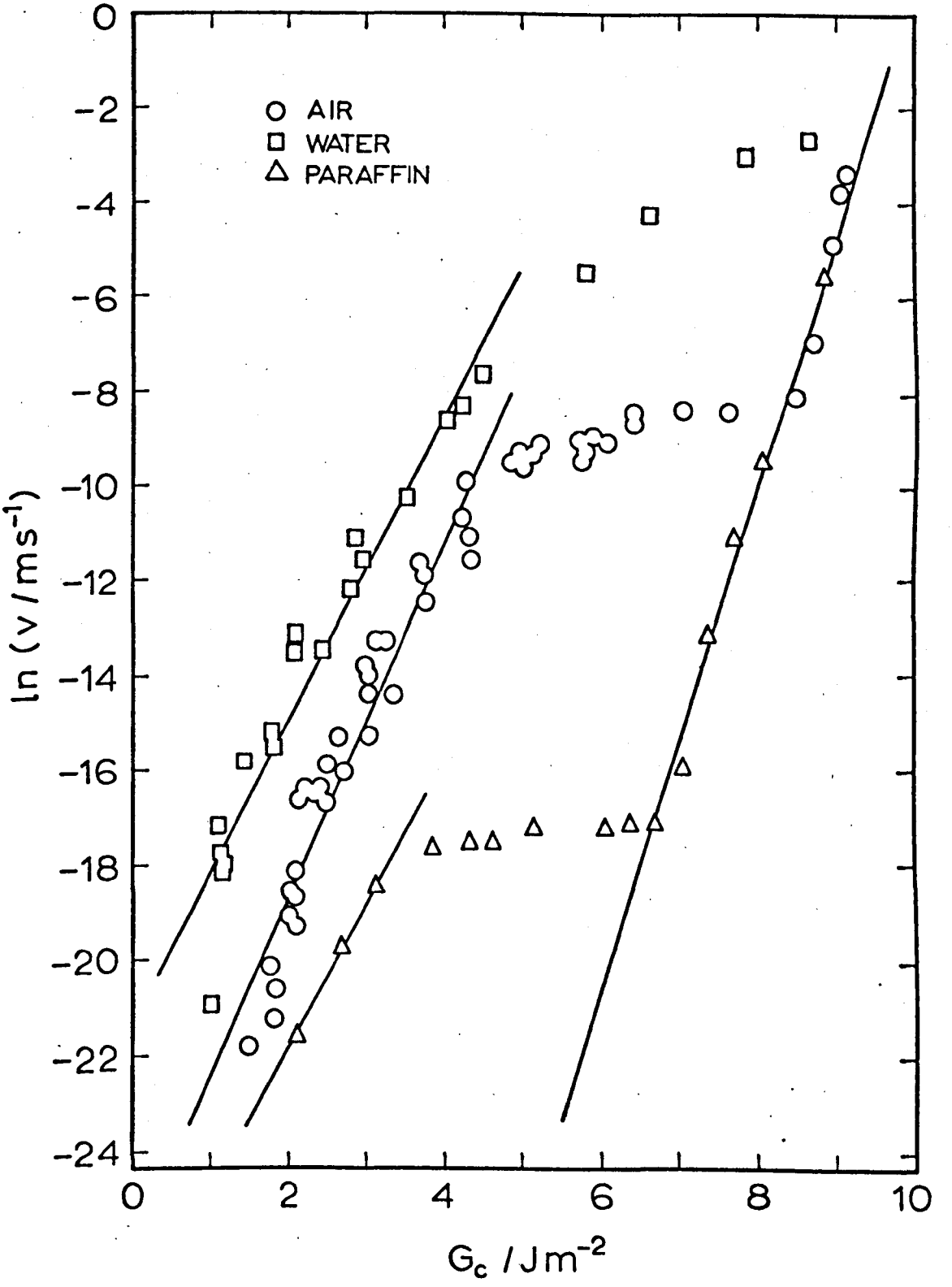

Figure 6.4 Dependence of ln (crack speed) on G_c

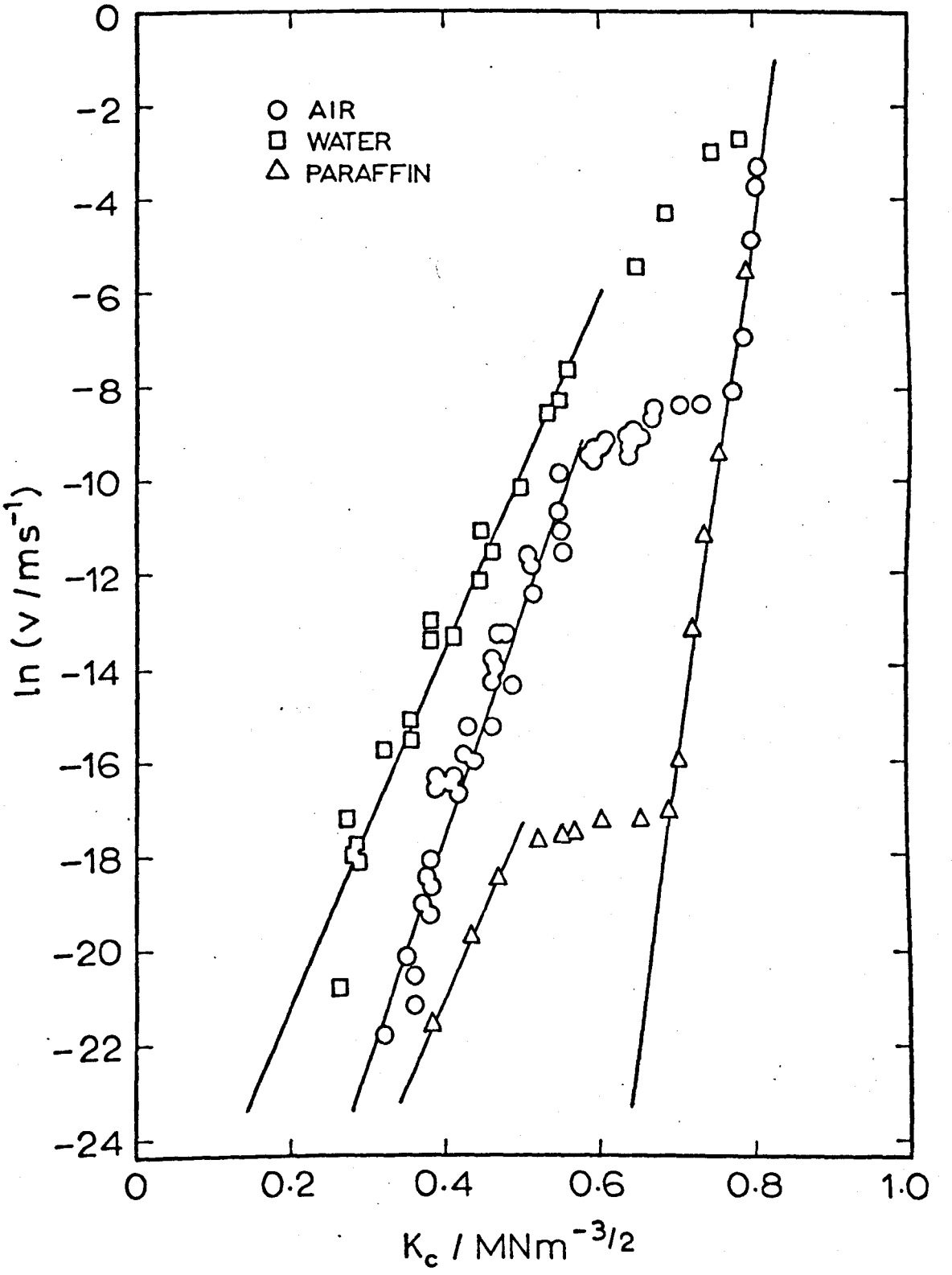

Figure 6.5 Dependence of ln (crack speed) on K_c

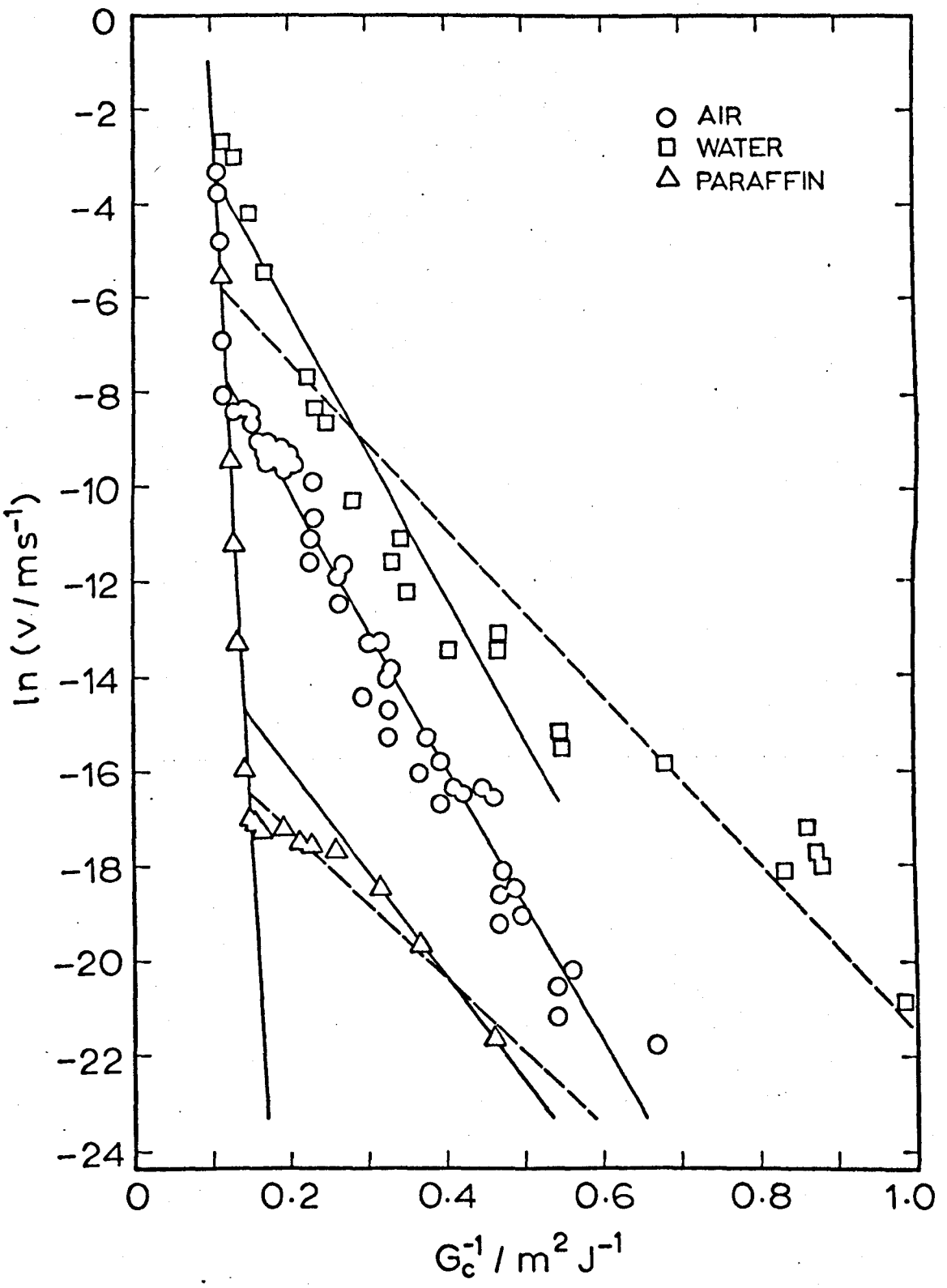

Figure 6.6 Dependence of ln (crack speed) on G_c^{-1}

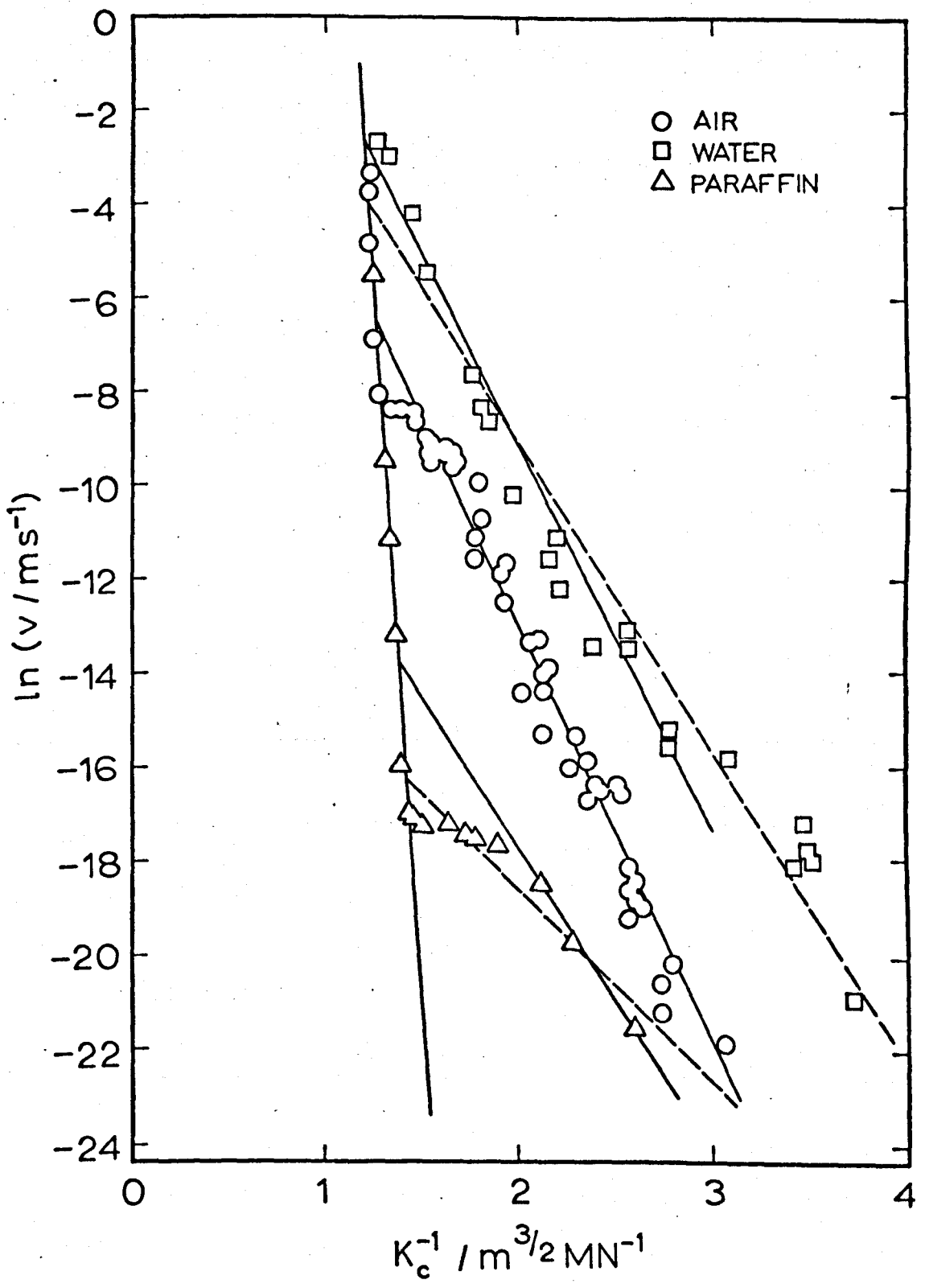

Figure 6.7 Dependence of ln (crack speed) on K_c^{-1}

appropriate form of the variation of yield stress with time, are in reasonable agreement with the values shown in table 6.1, which were estimated on the basis of a simple correlation of corresponding points in the yield stress and crack speed results. The results in paraffin have not been considered here since it has been assumed that the yield stress results in this environment represent the environment-independent, or dry behaviour. The ratios of α_c (wet) to α_c (dry) and of r_c (wet) to r_c (dry) calculated from the slopes in figures 6.4 to 6.7 do, however, differ in some cases from the ratios obtained from table 6.1. In table 6.2 these ratios are shown together with the values of α_c and r_c obtained from the results in water. Both $\ln v = f(G_c^{-1})$ and $\ln v = f(K_c)$ provide values of these ratios which are

Table 6.2 Typical values of α_c and r_c in wet environments, and the ratios of their values in wet and dry environments

equation	α_c (wet) / nm	r_c (wet) / nm	$\frac{\alpha_c(\text{wet})}{\alpha_c(\text{dry})}$	$\frac{r_c(\text{wet})}{r_c(\text{dry})}$
$\ln v = f(G_c)$, (6.20)	1.57		3	
$\ln v = f(K_c)$, (6.21)		3.8		1
$\ln v = f(G_c^{-1})$, (6.17)	0.56		$1/3$	
$\ln v = f(K_c^{-1})$, (6.18)		5.25		$1/5$
from table 6.1	0.50	3.6	$1/3$	1

consistent with those of table 6.1. Since the latter were calculated on the simple assumption that yield stresses measured under different conditions in indentation tests were the same as the yield stresses at the crack tip under identical conditions, they may be used to provide a check on the self-consistency of the different equations for $\ln v$, whose derivation involved additional hypotheses.

A further check of the proposed model for crack propagation in

glass should be provided by the values of α_c or r_c from the intercepts of the straight lines. If these are evaluated, however, it is found that α_c from the intercepts is between 10 and 10^7 times its value from the slopes, whilst the discrepancy in r_c is even worse, ranging from 10^{-10} to 10^{24} of its slope values. Since α_c and r_c appear in the intercepts in the form of $\ln \alpha_c$ and $\ln r_c$ (see e.g. equation 6.17), relatively small changes in the intercept have a drastic effect on the values of α_c and r_c. In view of this and of the arbitrary element in the selection of the linear regions in figures 6.4 to 6.7, some disagreement between the slope and intercept values might be expected. It has not been found possible, though, to select reasonable straight lines through the experimental points which reduce this disagreement to an acceptable figure and still provide values of α_c or r_c which are consistent with those of table 6.1. It seems, therefore, that the assumptions made in developing the equations must be re-examined to see whether these could be responsible for this disagreement.

Accepting that the basic hypothesis is sound, namely that the phenomenon of slow crack growth in glass is explicable in terms of a variation of yield stress with time and a limited plasticity fracture criterion, and bearing in mind that reasonable values of α_c and r_c are obtained from the slopes of the $\ln v$ curves and the variation of either σ_Y or $1/\sigma_Y$ with time, it is possible that the assumed identity of the time scales for plastic flow accompanying indentation and crack propagation is in error. In view of the difference between the size of the region undergoing plastic flow under an indenter and the estimated size of the plastic zone at the tip of a crack in glass, these time scales need not necessarily be identical. A relative

shift in the time scale would not affect A or C, the slopes of equations (6.14) and (6.19) for σ_Y, but would alter the values of the intercepts, $^1/\sigma_o$ and σ_o, which are given by

$$1/\sigma_o = A \ln B \tag{6.23}$$

and

$$\sigma_o = C \ln D \tag{6.24}$$

The shifts that would be required in $^1/\sigma_o$ or σ_o for the slope and intercept values of α_c and r_c to agree can be estimated by substituting the slope values into the intercept expressions of the crack speed equations. For example, from equation (6.17) and the crack speed results in water

$$-0.94 = \ln \left(\frac{EA}{\pi}\right) + \ln B + \ln (5.6 \times 10^{-9}) \tag{6.25}$$

or

$$A \ln B = 0.43\, m^2\, GN^{-1} \tag{6.26}$$

From the yield stress results

$$1/\sigma_o = 0.29\, m^2\, GN^{-1} \tag{6.27}$$

Thus $^1/\sigma_o$ needs to be increased by $0.14\, m^2\, GN^{-1}$ for α_c from the intercept to agree with α_c from the slope. The calculated shifts in $^1/\sigma_o$ for equation (6.17) and in σ_o for equation (6.21), for air, water and dry environments are shown in table 6.3.

Comparing these shifts with figures 6.3(a) and 6.3(b) it is apparent that neither $\Delta(^1/\sigma_o)$ nor $\Delta\sigma_o$ can be reconciled with a simple shift of the time scale, common to all environments. Although there is no a priori reason for supposing that a relative shift in the time

Table 6.3 Shifts in the intercepts of the yield stress results

equation	environment	$\Delta(1/\sigma_o)$ / $m^2\,GN^{-1}$	$\Delta\sigma_o$/GN m^2
$\ln v = f(G_c^{-1})$, (6.17)	air	+0.14	
	water	+0.14	
	dry	-0.05	
$\ln v = f(K_c)$, (6.21)	air		+2.51
	water		+1.32
	dry		+1.94

scales for plastic flow in the two situations should not be environment-dependent, the results of table 6.3 might equally well be taken to indicate that the theoretical development has been based on faulty premises. It has been implicitly assumed so far that the crack speed could be related to G_c or K_c, or their reciprocals. Arguably, however, since the crack speed tends to zero at a minimum, non-zero value of G_c or K_c, the crack speed should more properly be related to $(G_c - G_o)$ or $(K_c - K_o)$, where G_o and K_o are these minimum values of G_c and K_c. If the experimental data are recalculated in terms of these reduced parameters, results similar to those in tables 6.1 and 6.2 are obtained for α_c and r_c from the slopes, together with a similar disagreement in the intercept results. Adopting the same argument concerning the identity of the time scales, the shifts in $1/\sigma_o$ and σ_o can be calculated as before. These shifts are shown in table 6.4 for equation (6.17) and the corresponding equation for $v = r_p(c)/t_c$, and in table 6.5 for the two forms of equation (6.21). The values of G_o and K_o in both air and water have been estimated from figures 6.4 and 6.5 to be approximately 1.0 $J\,m^{-2}$ and 0.25 $MN\,m^{-3/2}$ respectively, whilst under dry or environment-independent conditions

they have been taken to be 5.0 $J m^{-2}$ and 0.60 $MN m^{-3/2}$, which were the values used in table 6.1.

Table 6.4 Shifts in the intercepts of the flow stress results for $\ln v = f[(G_c - G_o)^{-1}]$

v	$G_o / J m^{-2}$	environment	$\Delta(1/\sigma_o) / m^2 GN^{-1}$
$\partial r_p / \partial t$	1.0	air	+0.11
	1.0	water	+0.14
	5.0	dry	-0.01
$r_p(c) / t_c$	1.0	air	+0.08
	1.0	water	+0.11
	5.0	dry	+0.03

Table 6.5 Shifts in the intercepts of the flow stress results for $\ln v = f(K_c - K_o)$

v	$K_o / MN m^{-3/2}$	environment	$\Delta\sigma_o / GN m^{-2}$
$\partial r_p / \partial t$	0.25	air	-0.77
	0.25	water	-0.82
	0.60	dry	-2.75
$r_p(c) / t_c$	0.25	air	-3.74
	0.25	water	-3.35
	0.60	dry	-3.68

In both tables the first sets of data, with $v = \partial r_p / \partial t$, lead to similar conclusions to those of table 6.4 when compared with figures 6.3(a) and 6.3(b). The second set of data in table 6.4 is consistent, however, with a shift of the zero of $\ln t$ in figure 6.3(b) to approximately $\ln t = 5$, implying that plastic flow at the

tip of a crack takes place on a time scale which is about 150 times longer than under an indenter in all environments. In table 6.5, the second set of data implies that the time scales are the same for plastic flow under an indenter and plastic flow at the tip of a crack, but that the values of the yield stress require a similar correction in all environments. These corrected values of σ_o, however, are smaller than the maximum breaking stresses measured at $t = 1\,s$, and, therefore, appear inapplicable.

Additional, although tentative support for the environment-independent shift of time scale may be provided by the results in paraffin. If, in figure 6.3(b), the experimental point at the longest time is considered to represent the beginning of environment-dependent behaviour, and if the slope of the line through this point is assumed to be similar to the slopes in air and water (which is in accordance with the similarity of the slopes found in the crack propagation results), the calculated shift of $1/\sigma_o$ in paraffin is $0.08\,m^2\,GN^{-1}$, in good agreement with those calculated for air and water, and, hence, consistent with a similar shift in time scale.

To summarise this section, it has been shown that, if the crack speed follows a linear relationship between $\ln v$ and $(G_c - G_o)^{-1}$, it is possible to obtain a consistent correlation between the variation of yield stress with time and the variation of crack speed with $(G_c - G_o)^{-1}$ by assuming that there is a shift in the time scale of plastic flow which is independent of environment, and by taking $\alpha = \alpha_c$. The values of α_c under wet and dry conditions correspond to those estimated from simple considerations. Although this correlation does not provide conclusive evidence for the hypothesis that crack growth in glass is controlled by the fall in yield stress

with time, and even less that the fracture criterion is $\alpha = \alpha_c$, it does indicate, at least in principle, that a theory couched in these terms can be constructed which will account for the phenomenology of slow crack propagation in glass.

Such a theory could also be extended to include the effects of temperature. The results of WESTBROOK (1960) for the variation of indentation hardness of soda-lime silica glass with temperature, when recalculated in terms of the yield stress, show that there is an approximately linear dependence between the yield stress and temperature. Thus the yield stress might be represented by an equation of the form

$$\frac{1}{\sigma_Y} = A \ln Bt - \frac{A'}{T} \qquad (6.28)$$

where A' is a constant. Equation (6.17) would then become

$$\ln v = \ln\left(\frac{EA\alpha_c}{\pi}\right) + \ln B - \frac{A'}{AT} - \frac{\alpha_c}{AG_c} \qquad (6.29)$$

which is consistent with the variation of crack speed with temperature found in practice. Westbrook's work, unfortunately,did not include any measurements of the change in σ_Y with time at different temperatures, and in the absence of such data it is not possible to attempt a quantitative correlation with the crack speed results, especially since it might be expected that A is temperature dependent.

6.5 Concluding Discussion

The experimental results of this thesis have shown that the variations of crack speed with G_c in glass under different environmental

conditions, measured using the double torsion technique (and the cleavage technique in air), are the same as those measured in simple tension by other workers. In effect, these measurements are measurements of static fatigue, since the times to failure in static fatigue are controlled by the rates of slow crack growth, and it is therefore significant that slow crack growth was measured in liquid nitrogen. The very high sensitivity of the crack speed to G_c in this environment is consistent with the observations of delayed failure rather than static fatigue.

The interpretation of the experimental results which has been put forward in terms of the time dependence of the yield stress and a limited plasticity fracture criterion is able to account for the high values of the fracture energy of glass, found in previous work, and also for the observed dependence of crack speed on G_c, both when crack propagation is affected by the presence of water and under conditions when it is independent of the environment. A feature of the proposed mechanism of crack growth is that its validation depends on the correlation between two independent sets of data, from indentation hardness measurements and from the crack propagation measurements of this work. To establish this correlation two subsidiary hypotheses were required, that the time scales for plastic flow were different at the tip of a crack and under an indenter, and that the crack speed was related to $(G_c - G_o)$ or $(K_c - K_o)$ rather than to G_c or K_c.

Although both of these hypotheses are reasonable, the theory based on their use requires further experimental verification before it can be claimed that its validity has been demonstrated. All that can really be claimed at present is that it has been shown that the

theory is consistent with the experimental results. It is interesting, though, to note that the form of the equations developed on the basis of this theory is similar to some of the empirical equations which have been fitted to static fatigue data (see Chapter 1). More measurements are required, both of the variation of indentation hardness with time and of crack propagation rates, in environments of different humidities and at different temperatures, to see whether the correlation established in the previous section can be confirmed. In particular, indentation measurements in paraffin should be made at times greater than 10^5 s to investigate the possible change to environment-dependent behaviour at these times, and the indentation measurements in liquid nitrogen should be repeated over a greater range of times in an attempt to detect any change in hardness with time.

There are four questions whose answers would help to fill some of the gaps in our knowledge of fracture phenomena in glass. In view of the currency of stress corrosion theories, such as that of Charles and Hillig, as explanations of the effect of water on the fracture of glass, can an enhanced corrosion rate of glass under stress in the presence of water be measured directly? Is the static fatigue rate, in terms of the reduced parameters of the universal fatigue curve, composition dependent, or different in pristine and abraded specimens, or both? Can static fatigue of glass in liquid nitrogen be detected if experiments are conducted over sufficiently long times? Finally, does the reduction of elastic modulus of soda-lime silica glass with increasing strain in liquid nitrogen, as measured by Mallinder and Proctor, apply at room temperature? The answer to this last question could affect the conversion of indentation

hardness to yield stress, especially since the two are not linearly related.

If the foregoing account of slow crack propagation in glass, in terms of the crack speed being controlled by a time-dependent yield stress and a limited plasticity fracture criterion, is substantially correct, then it would be desirable to be able to relate this plasticity to the structure of glass. Some comments on this were made at the end of the introductory chapter of this thesis, but it must also be borne in mind that the plastic zone model discussed in Chapter 2 may be regarded as a vehicle for producing characteristic parameters, and need not represent physical reality. It is quite possible that the shape of the plastic zone is unlike that assumed in the model, or even that the plastic flow takes place in a series of small, discrete zones in a region around the crack tip such as is known to occur with the crazing around the tip of a crack in poly(methyl methacrylate). Hopefully, the increasing sophistication of microscopy techniques will allow this, and other outstanding problems of glass structure, to be resolved.

APPENDIX 1

TABULATED RESULTS OF VARIATION OF FLOW STRESS WITH TIME IN AIR, WATER AND DRY PARAFFIN

Table A1.1 Results in air of MARSH (1964b)

σ_Y/GN m^{-2}	t/s	ln(t/s)	σ_Y^{-1}/m^2 GN^{-1}
7.29	10^{-5}	-11.513	0.137
5.34	10^{-2}	- 4.605	0.187
4.50	10^{-1}	- 2.303	0.222
3.76	1	0	0.266
3.08	20	2.996	0.325
2.61	720	6.579	0.383

Table A1.2 Results in air of GUNASEKERA (1970)

σ_Y/GN m^{-2}	t/s	ln(t/s)	σ_Y^{-1}/m^2 GN^{-1}
6.02	5×10^{-4}	-7.601	0.166
4.91	10^{-2}	-4.605	0.204
4.33	10^{-1}	-2.303	0.231
3.98	1	0	0.251
3.64	5	1.609	0.275
3.21	20	2.996	0.312
2.80	110	4.701	0.357
2.53	1010	6.918	0.395
2.17	10^4	9.210	0.461

Table A1.3 Results in water of GUNASEKERA (1970)

σ_Y/GN m^{-2}	t/s	ln(t/s)	σ_Y^{-1}/m^2 GN^{-1}
6.44	5×10^{-4}	-7.601	0.155
4.91	10^{-2}	-4.605	0.204
4.03	10^{-1}	-2.303	0.248
3.59	1	0	0.279
3.15	5	1.609	0.318
2.75	20	2.996	0.364
2.51	110	4.701	0.398
2.29	1010	6.918	0.438
2.17	10^4	9.210	0.461
2.05	10^5	11.513	0.488

Table A1.4 Results in dry paraffin of GUNASEKERA (1970)

σ_Y/GN m^{-2}	t/s	ln(t/s)	σ_Y^{-1}/m^2 GN^{-1}
6.64	5×10^{-4}	-7.601	0.151
4.97	10^{-2}	-4.605	0.201
4.44	10^{-1}	-2.303	0.225
4.20	1	0	0.238
4.03	5	1.609	0.248
4.20	20	2.996	0.238
3.98	110	4.701	0.251
3.88	1010	6.918	0.258
3.76	10^4	9.210	0.266
3.34	10^5	11.513	0.300

APPENDIX 2

TABULATED RESULTS OF CRACK PROPAGATION MEASUREMENTS IN AIR, WATER AND DRY PARAFFIN

Table A2.1 Results in air

$\ln(v/ms^{-1})$	$G_c/J\,m^{-2}$	$G_c^{-1}/m^2\,J^{-1}$	$K_c/MN\,m^{-3/2}$	$K_c^{-1}/m^{3/2}\,MN^{-1}$
-21.82	1.49	0.670	0.326	3.07
-21.24	1.85	0.542	0.363	2.76
-20.62	1.85	0.542	0.363	2.76
-20.18	1.78	0.562	0.356	2.81
-19.28	2.12	0.472	0.389	2.57
-19.07	2.00	0.500	0.377	2.65
-18.67	2.11	0.473	0.388	2.58
-18.55	2.03	0.492	0.381	2.63
-18.13	2.10	0.476	0.387	2.59
-16.72	2.51	0.398	0.423	2.36
-16.61	2.16	0.463	0.392	2.55
-16.50	2.36	0.424	0.410	2.44
-16.39	2.21	0.452	0.397	2.52
-16.36	2.43	0.412	0.416	2.41
-16.03	2.73	0.367	0.441	2.27
-15.87	2.53	0.395	0.425	2.36
-15.32	2.64	0.379	0.434	2.31
-15.31	3.05	0.328	0.466	2.15
-14.43	3.39	0.295	0.491	2.04
-14.37	3.05	0.328	0.466	2.15
-14.07	3.06	0.327	0.467	2.14
-13.87	3.01	0.332	0.463	2.16
-13.32	3.13	0.320	0.472	2.12
-13.33	3.25	0.307	0.481	2.08
-12.50	3.78	0.265	0.519	1.93

Table A2.1 Results in air (continued)

$\ln(v/ms^{-1})$	$G_c/J\,m^{-2}$	$G_c^{-1}/m^2\,J^{-1}$	$K_c/MN\,m^{-3/2}$	$K_c^{-1}/m^{3/2}\,MN^{-1}$
-11.97	3.79	0.264	0.519	1.93
-11.64	3.69	0.271	0.513	1.95
-11.61	4.38	0.228	0.558	1.79
-11.11	4.35	0.230	0.556	1.80
-10.73	4.24	0.236	0.549	1.82
- 9.96	4.30	0.233	0.533	1.81
- 9.68	5.03	0.199	0.598	1.67
- 9.58	4.91	0.204	0.591	1.69
- 9.44	5.16	0.194	0.606	1.65
- 9.38	4.99	0.200	0.596	1.68
- 9.23	5.23	0.191	0.610	1.64
- 9.56	5.79	0.173	0.642	1.56
- 9.34	5.82	0.172	0.644	1.55
- 9.10	5.75	0.174	0.640	1.56
- 9.03	5.89	0.170	0.648	1.54
- 9.14	6.09	0.164	0.659	1.52
- 8.70	6.42	0.156	0.676	1.48
- 8.53	6.45	0.155	0.678	1.48
- 8.43	7.07	0.142	0.709	1.41
- 8.44	7.61	0.131	0.736	1.36
- 8.09	8.50	0.118	0.778	1.29
- 6.95	8.71	0.115	0.788	1.27
- 4.85	8.96	0.112	0.799	1.25
- 3.75	9.07	0.110	0.804	1.25
- 3.36	9.15	0.109	0.807	1.24

Table A2.2 Results in water

$\ln(v/ms^{-1})$	$G_c/J\,m^{-2}$	$G_c^{-1}/m^2\,J^{-1}$	$K_c/MN\,m^{-3/2}$	$K_c^{-1}/m^{3/2}\,MN^{-1}$
-20.88	1.01	0.987	0.269	3.72
-18.14	1.19	0.838	0.291	3.43
-18.02	1.13	0.882	0.284	3.52
-17.80	1.14	0.877	0.285	3.51
-17.24	1.16	0.862	0.287	3.48
-15.81	1.47	0.682	0.323	3.09
-15.57	1.82	0.549	0.360	2.78
-15.22	1.81	0.551	0.359	2.78
-13.47	2.12	0.472	0.389	2.57
-13.46	2.46	0.407	0.419	2.39
-13.10	2.12	0.472	0.389	2.57
-12.25	2.81	0.355	0.448	2.23
-11.63	2.99	0.334	0.462	2.17
-11.17	2.88	0.347	0.453	2.21
-10.29	3.55	0.281	0.503	1.99
- 8.68	4.05	0.247	0.537	1.86
- 8.36	4.24	0.236	0.549	1.82
- 7.70	4.49	0.223	0.565	1.77
- 5.53	5.91	0.169	0.649	1.54
- 4.28	6.59	0.152	0.685	1.46
- 3.01	7.83	0.128	0.747	1.34
- 2.69	8.62	0.116	0.783	1.28

Table A2.3 Results in dry paraffin

$\ln(v/ms^{-1})$	$G_c/J\,m^{-2}$	$G_c^{-1}/m^2\,J^{-1}$	$K_c/MN\,m^{-3/2}$	$K_c^{-1}/m^{3/2}\,MN^{-1}$
-21.63	2.07	0.484	0.384	2.61
-19.73	2.69	0.371	0.438	2.28
-18.52	3.11	0.321	0.471	2.12
-17.71	3.85	0.160	0.524	1.91
-17.64	4.37	0.229	0.558	1.79
-17.59	4.62	0.216	0.574	1.74
-17.31	5.16	0.194	0.606	1.65
-17.30	6.07	0.165	0.657	1.52
-17.18	6.40	0.156	0.675	1.48
-17.13	6.71	0.149	0.691	1.45
-16.02	7.05	0.142	0.708	1.41
-13.28	7.39	0.135	0.725	1.38
-11.19	7.70	0.130	0.740	1.35
- 9.50	8.08	0.124	0.759	1.32
- 5.60	8.81	0.113	0.792	1.26

REFERENCES

AINSWORTH, L. (1954) J. Soc. Glass Technol. 38 479T.

ANDRADE, E.N. da C. and TSIEN, L.C. (1937) Proc. R. Soc. A 159 346.

ATKINS, A.G. and TABOR, D. (1965) J. Mech. Phys. Solids 13 149.

BAKER, T.C. and PRESTON, F.W. (1946) J. appl. Phys. 17 170.

BENBOW, J.J. and ROESLER, F.C. (1947) Proc. phys. Soc. B 70 201.

BERDENNIKOV, W.P. (1933) Sov. Phys. Z. 4 397.
(1934) Zh. fiz. Khim. 5 358.

BERRY, J.P. (1963) J. appl. Phys. 34 62.

BILBY, B.A., COTTRELL, A.H. and SWINDEN, K.H. (1963) Proc. R. Soc. A 272 304.

BJORKLUND, F.E. (1948) MSc Thesis, University of Utah.

BRIDGMAN, P.W. and SIMON, I. (1953) J. appl. Phys. 24 405.

BURDEKIN, F.M. and STONE, D.E.W. (1966) J. Strain Anal. 1 145.

CHARLES, R.J. (1958a) J. appl. Phys. 29 1549.
(1958b) ibid 29 1554.
(1961) Progress in Ceramic Science, Vol. 1, J.E. Burke, ed., Pergamon (New York), p.1.

CHARLES, R.J. and HILLIG, W.B. (1961) Symposium sur la Résistance Mécanique du Verre et les Moyens de l'Améliorer, Florence 1961, Union Continentale Scientifique du Verre (Charleroi, Belgium), 1962, p. 511.

CHEESEMAN, G.L. and LAWN, B.R. (1970) phys. stat. sol. A 3 951.

CLARKE, F.J.P., TATTERSALL, H.G. and TAPPIN, G. (1966) Proc. Br. Ceram. Soc. 6 163.

CONDON, E.U. (1954) Am. J. Phys. 22 224.

COOK, J. and GORDON, J.E. (1964) Proc. R. Soc. A 282 508.

CULF, C.J. (1957) J. Soc. Glass Technol. 41 157 T.

DALLADAY, A.J. and TWYMAN, F. (1921) Trans. opt. Soc. 23 165.

DANFORD, M. and LEVY, H. (1962) J. Am. chem. Soc. 84 3695.

DAVIDGE, R.W. and TAPPIN, G. (1968) J. Mater. Sci. 3 165.

DEMISHEV, G.K. and BARTENEV, G.M. (1966a) Silikattechnik 17 215.
(1966b) ibid 17 344.

DOUGLAS, R.W. (1958) J. Soc. Glass Technol. 42 145 T.

DRINKARD, W. and KIVELSON, D. (1958) J. phys. Chem. 62 1494.

DUGDALE, D.S. (1960) J. Mech. Phys. Solids 8 100.

ELLIOTT, H.A. (1958) J. appl. Phys. 29 224.

ERNSBERGER, F.M. (1960) Proc. R. Soc. A 257 213.
(1968) J. Am. Ceram. Soc. 51 545.

EVERETT, D.H., HAYNES, J.M. and McELROY, P.J. (1971) Sci. Prog. (Oxf), 59 279.

FAYET, A. (1969) private communication.

FINKEL', V.M. and KUTKIN, I.A. (1962a) Soviet Phys. Dokl. 7 231.
(1962b) Soviet Phys. solid St. 4 1038.

GIBBS, P. and CUTLER, I.B. (1951) J. Am. Ceram. Soc. 34 200.

GILLIS, P.P. and GILMAN, J.J. (1964) J. appl. Phys. 35 647.

GILMAN, J.J. (1960) J. appl. Phys. 31 2208.
(1968a) Comments solid St. Phys. 1 122.
(1968b) Proceedings of the Batelle Conference on Dislocation Dynamics, McGraw-Hill (New York), p.3.

GLASSTONE, S., LAIDLER, K.J. and EYRING, H. (1941) The Theory of Rate Processes, McGraw-Hill (New York).

GLATHART, J.L. and PRESTON, F.W. (1946) J. appl. Phys. 17 189.

GORDON, J.E., MARSH, D.M. and PARRATT, M.E.M.L. (1959) Proc. R. Soc. A 249 65.

GRENET, L. (1899) Bull. Soc. Encourag. Ind. natn. (Paris) Ser. 5 4 838.

GRIFFITH, A.A. (1920) Phil. Trans. R. Soc. A 221 163.
(1924) Proceedings, First International Congress of Applied Mechanics, Delft, p. 55.

GRIFFITHS, R. (1968) MSc Thesis, University of Keele.

GUNASEKERA, S.P. (1970) MSc Thesis, University of Keele.

GURNEY, C. and PEARSON, S. (1949) Proc. phys. Soc. B 62 469.

HASTED, J.B. (1971) Contemp. Phys. 12 133.

HAYES, D.J. (1970) PhD Thesis, University of London.

HETHERINGTON, G. and JACK, K.H. (1962) Physics Chem. Glasses 3 129.

HILL, R. (1950) The Mathematical Theory of Plasticity , Oxford, Clarendon Press.

HILL, R., LEE, E.H. and TUPPER, S.J. (1947) Proc. R. Soc. A 188 273.

HILLIG, W.B. (1961) J. appl. Phys. 32 741.

(1962) Modern Aspects of the Vitreous State, Vol. 2, J.D. Mackenzie, ed., Butterworth (London), p. 152.

HIRST, W. and HOWSE, M.G.J.W. (1969) Proc. R. Soc. A 311 429.

HODGDON, F.B., STUART, D.A. and BJORKLUND, F.E. (1950) J. appl. Phys. 21 1156.

HOLLAND, A.J. and TURNER, W.E.S. (1937) J. Soc. Glass Technol. 21 383 T.
(1940) ibid 24 46 T.

HOLLAND, L. (1964) The Properties of Glass Surfaces, Chapman and Hall (London).

HOLLOWAY, D.G. (1959) Phil. Mag. 4 1101.

HORI, T. (1956) Low Temp. Sci. A 15 34. (Translation 62, U.S. Army Snow, Ice and Permafrost Establishment, Wilmette, Ill).

INGLIS, C.E. (1913) Trans. Inst. Naval Architects 55 219.

IRWIN, G.R. (1947) American Society of Metals Symposium on Fracturing of Metals, Cleveland, Ohio

(1956) Proceedings, Ninth International Congress of Applied Mechanics, Brussels, paper 11-101.

(1957) J. appl. Mech. 24 361.

(1958) Handbuch der Physik, Vol. 6, Springer-Verlag (Berlin), p. 551.

(1960) Proceedings, Seventh Sagamore Ordnance Materials Conference, Syracuse University, p. IV-63.

IRWIN, G.R. (1966) N.R.L. Memorandum Report no. 1678.

IRWIN, G.R. and KIES, J.A. (1952) Weld. J.,Lond.,Res. Suppl. 17 95 s.
(1954) ibid 33 193 s.

JERRARD, H.G. and McNEIL, D.B. (1960) Theoretical and Experimental Physics, Chapman and Hall (London), p. 131.

JOHNSON, O.W. (1966) J. appl. Phys. 37 2521.

KIES, J.A. and CLARK, A.B.J. (1969) Proceedings, Second International Conference on Fracture, Brighton 1969, Chapman and Hall (London) 1970, p. 483.

KROPSCHOT, R.H. and MIKESELL, R.P. (1957) J. appl. Phys. 28 610.

LA MER, V.K. and GRUEN, R. (1952) Trans. Faraday Soc. 48 410.

LINGER, K.R. (1967) PhD Thesis, University of Keele.

LINGER, K.R. and HOLLOWAY, D.G. (1968) Phil. Mag. 18 1269.

LOCKETT, F.J. (1963) J. Mech. Phys. Solids 11 345.

McCORMICK, J. (1936) Bull. Am. Ceram. Soc. 15 268.

MACKENZIE, J.D. (1960) Modern Aspects of the Vitreous State, Vol. 1, J.D. Mackenzie, ed., Butterworth (London), p.1.
(1963) J. Am. Ceram. Soc. 46 461.

MACMILLAN, N.H. (1969) PhD Thesis, University of Cambridge.
(1972) J. Mater. Sci. 7 239.

MALLINDER, F.P. and PROCTOR, B.A. (1964) Physics Chem. Glasses 5 91.

MARSH, D.M. (1963a) Tube Investments Research Laboratories, Technical Report no. 159.
(1963b) ibid no. 161.
(1963c) Fracture of Solids, D.C. Drucker and J.J. Gilman, eds., Gordon and Breach (New York), p. 143.
(1964a) Proc. R. Soc. A 279 420.
(1964b) ibid 282 33.

MILIGAN, L.H. (1929) J. Soc. Glass Technol. 13 351 T.

MORLEY, E.W. (1904) J. Am. chem. Soc. 26 1171.

MOSTOVOY, S. and RIPLING, E.J. (1966) J. appl. Polym. Sci. 10 1351.

MOULD, R.E. (1960) J. Am. Ceram. Soc. 43 160.
(1961) ibid 44 481.

MOULD, R.E. and SOUTHWICK, R.D. (1959a) J. Am. Ceram. Soc. 42 542.
(1959b) ibid 42 582.

MULHEARN, T.O. (1959) J. Mech. Phys. Solids 7 85.

MURGATROYD, J.B. (1942) J. Soc. Glass Technol. 26 155 T.
(1944) ibid 28 406 T.

NAKAYAMA, J. (1964) Jap. J. appl. Phys. 3 422.
(1965) J. Am. Ceram. Soc. 48 583.

NÁRAY-SZABÓ, I. and LADIK, J. (1960) Nature 188 226.

NEELY, J.E. and MACKENZIE, J.D. (1968) J. Mater. Sci. 3 603.

NORTHWOOD, D.O. and PORTER, L.J. (1970) J. Am. Ceram. Soc. 53 359.

OBREIMOFF, J.W. (1930) Proc. R. Soc. A 127 290.

ORD, P.R. (1957) J. Soc. Glass Technol. 41 245 T.

OROWAN, E. (1934) Z. Krist. A 89 327.
(1944) Nature 154 341.
(1945-6) Trans. Inst. Engrs Shipbuilders Scotland 89 165.
(1948-9) Rep. Prog. Phys. 12 185.
(1955) Weld. J., Lond.,Res. Suppl. 34 157 s.

OTTO, W.H. (1955) J. Am. Ceram. Soc. 38 122.

OUTWATER, J.O. and GERRY, D.J. (1966) Report on Contract NONR 3219 (01) (X), Office of Naval Research, Washington, D.C.
(1967) Mod. Plast. 45 156.

PARIS, P.C. and SIH, G.C. (1964) Symposium on Fracture Toughness Testing and its Applications, Chicago 1964, ASTM STP 381, 1965, p. 30.

PARKER, A.J. (1963) Quart. Rev. chem. Soc. 16 163.
(1965) Advances in Organic Chemistry, Vol. 5, Interscience, (New York), p. 1.

PETER, K.W. (1970) J. non-cryst. Solids 5 103.

POLANYI, M. (1921) Z. Phys. 7 323.

PROCTOR, B.A. (1961) Symposium sur la Résistance Mécanique du Verre et les Moyens de l'Améliorer, Florence 1961, Union Continentale Scientifique du Verre (Charleroi, Belgium), 1962, p. 447.

PROCTOR, B.A., WHITNEY, I. and JOHNSON, J.W. (1967) Proc. R. Soc. A 297 534.

RANA, M.A. and DOUGLAS, R.W. (1961) Physics Chem. Glasses 2 179.

RANDALL, J.T., ROOKSBY, H.P. and COOPER, B.S. (1930) Z. Krist. 75 196.

RICE, J.R. and LEVY, N. (1969) Physics of Strength and Plasticity, A.S. Argon, ed., M.I.T. Press (Cambridge, Mass.), p. 277.

RITTER, J.E. (1969) J. appl. Phys. 40 340.
(1970) Physics Chem. Glasses 11 16.

RITTER, J.E. and SHERBURNE, C.L. (1971) J. Am. Ceram. Soc. 54 601.

ROESLER, F.C. (1956) Proc. phys. Soc. B 69 981.

SAMUELS, L.E. and MULHEARN, T.O. (1957) J. Mech. Phys. Solids 5 125.

SCHLÄFER, H.L. and SCHAFFERNICHT, W. (1960) Angew. Chem. 72 618.

SCHLAPP, D.M. (1965) Physics Chem. Glasses 6 168.

SCHÖNERT, K., UMHAUER, H. and KLEMM, W. (1969) Proceedings, Second International Conference on Fracture, Brighton 1969, Chapman and Hall (London), 1970, p. 474.

SHAND, E.B. (1954) J. Am. Ceram. Soc. 37 559.
(1961) ibid 44 21.

SHERESHEFSKY, J.L. and CARTER, C.P. (1950) J. Am. chem. Soc. 72 3682.

SIMON, I. (1960) Modern Aspects of the Vitreous State, Vol. 1, J.D. Mackenzie, ed., Butterworth (London), p. 120.

SMIT, W. and STEIN, H.N. (1972) J. electroanal. Chem. 37 119.

SNEDDON, I.N. (1946) Proc. R. Soc. A 187 229.
(1961) Report on Contract NONR 486 (06), File no. ERD-126/1, Office of Naval Research (Washington, D.C.), p. 13.

SRAWLEY, J.E. and BROWN, W.F. (1964) NASA Technical Memorandum TM X-52030.

SRAWLEY, J.E. and GROSS, B. (1967) Mater. Res. Stds 7 155.

STUART, D.A. and ANDERSON, O.L. (1953) J. Am. Ceram. Soc. 36 416.

TABOR, D. (1951) The Hardness of Metals, Oxford, Clarendon Press.

TAYLOR, E.W. (1949) Nature 163 323.
(1950) J. Soc. Glass Technol. 34 69 T.

THOMAS, W.F. (1960) Physics Chem. Glasses 1 4.

THOMSON, W. (1871) Phil. Mag. Ser. 4 42 448.

TIMOSHENKO, S.P. (1953) History of the Strength of Materials, McGraw-Hill (New York).

TIMOSHENKO, S.P. and GOODIER, J.N. (1970) Theory of Elasticity, 3rd editon, McGraw-Hill (New York), p. 309.

VALENKOV, N. and PORAI-KOSHITS, E.A. (1936) Z. Krist. 95 195.

VARNER, J.R. and FRÉCHETTE, V.D. (1970) Proceedings, Third International Conference on the Physics of Non-Crystalline Solids, Sheffield 1970, Wiley-Interscience (London), 1972, p. 507.
(1971) J. appl. Phys. 42 1983.

VONNEGUT, B. and GLATHART, J.L. (1946) J. appl. Phys. 17 1082.

WARREN, B.E. (1933) Z. Krist. 86 349.
(1937) J. appl. Phys. 8 645.

WELLS, A.A. (1963) Br. Weld. J. 10 563.

WESTBROOK, J.H. (1960) Physics Chem. Glasses 1 32.

WESTERGAARD, H.M. (1939) J. appl. Mech. 6 A 49.

WESTWOOD, A.R.C. and HITCH, T.T. (1963) J. appl. Phys. 34 3085.

WIEDERHORN, S.M. (1966a) Mater. Sci. Res. 3 503.
(1966b) Environment-Sensitive Mechanical Behaviour of Materials, A.R.C. Westwood and N. Stoloff, eds., Gordon and Breach (New York), p. 293.
(1967) J. Am. Ceram. Soc. 50 407.
(1969) ibid 52 99.
(1971) International Conference on Corrosion Fatigue, Storrs, Conn. 1971, paper 40.

WIEDERHORN, S.M. and BOLZ, L.H. (1970) J. Am. Ceram. Soc. 53 543.

WIEDERHORN, S.M., SHORB, A.M. and MOSES, R.L. (1968) J. appl. Phys. 39 1569.

WIEDERHORN, S.M. and TOWNSEND, P.R. (1970) J. Am. Ceram. Soc. 53 486.

WILLIAMS, J.G. (1965) Appl. Mater. Res. 4 104.

ZACHARIASEN, W.H. (1932) J. Am. chem. Soc. 54 3841.

ZARZYCKI, J. and MEZARD, R. (1962) Physics Chem. Glasses 3 163.

ZIJLSTRA, A. (1961) Symposium sur la Résistance Mécanique du Verre et les Moyens de l'Améliorer, Florence 1961, Union Continentale Scientifique du Verre (Charleroi, Belgium), 1962, p. 135.